

THE GEOMETRY OF TUBULAR BRAIDED STRUCTURES

A THESIS

Presented to

The Faculty of the Division of Graduate

Studies and Research

by

James Richard Goff

In Partial Fulfillment

of the Requirements for the Degree

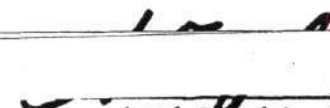
Master of Science in Textiles


Georgia Institute of Technology

June, 1976

THE GEOMETRY OF TUBULAR BRAIDED STRUCTURES

Approved:


Amad Tayebi, Chairman


W. Denny Freeston, Jr.


Milos Konopasek

Date approved by Chairman: 6/3/76

To Gwen

ACKNOWLEDGMENTS

The author wishes to thank his thesis advisor, Dr. Amad Tayebi, for his guidance, flexibility and patience.

He wishes to thank Dr. Milos Konopasek for his friendship and insightful criticism.

Thanks are also expressed to the faculty of the School of Textile Engineering, especially Dr. W. Denney Freeston Jr., Director, for cheerfully providing the facilities and resources for the project.

The author also wishes to thank Bentley-Harris Mfg. Co. for their help in making the test samples.

Permission was given by the Graduate Division to vary figure captions from the Thesis Manual requirements in order that this thesis might be prepared for publication.

TABLE OF CONTENTS

	Page
ACKNOWLEDGMENTS	iii
LIST OF TABLES	v
LIST OF ILLUSTRATIONS	vi
SUMMARY	viii
Chapter	
I. INTRODUCTION	1
Background	
Review of the Literature	
II. THEORY	17
Arc-length Theory	
List of Notation	
Jamming Theory	
III. THEORETICAL RESULTS AND DISCUSSION	53
IV. EXPERIMENT	92
Procedure	
Experimental Results	
Discussion of Results	
V. CONCLUSIONS AND RECOMMENDATIONS	119
APPENDIX	122
BIBLIOGRAPHY	134

LIST OF TABLES

Table	Page
1. Between-Jam Deformation of Diamond Braid	42
2. Between-Jam Deformation of R.H. and L.H. Regular Braid	49
3. Tensile Jamming Analysis of L.H. Regular Unit Cell	70
4. Compressive Jamming Analysis of L.H. Regular Unit Cell	72
5. Mid-Point Jamming Analysis of L.H. Regular Unit Cell	74
6. Tensile Jamming Analysis of R.H. Regular Unit Cell	76
7. Compressive Jamming Analysis of R.H. Regular Unit Cell	78
8. Mid-Point Jamming Analysis of R.H. Regular Unit Cell	80
9. Tensile Jamming Analysis of Diamond Unit Cell	84
10. Compressive Jamming Analysis of Diamond Unit Cell	86
11. Mid-Point Jamming Analysis of Diamond Unit Cell	88
12. Summary of Experiments	97
13. Between-Jam Deformation of Braid with Multifilament Strands	118
14. Array of Experimental Data (Diamond)	124
15. Array of Experimental Data (Regular)	126

LIST OF ILLUSTRATIONS

Figure	Page
1. Extended and Compressed Helix and Unwrapped Helix-Triangle	4
2. Crimped Model of Circular Braid and Photograph	6
3. Idealized Stress-Strain Curve of a Typical Braid	8
4. Flat-Cell Model	13
5. Projection of Circular 1/1 Diamond Braid	27
6. Projection of Circular 2/2 Regular Braid	28
7. Non-Planar Diamond Unit Cell and Lattice Structure	31
8. Test Geometry for Extensive Jamming	33
9. Fabric-Wall Sections of a Strand Intersection at Different (θ) (Compressive Jamming Test)	38
10. Derivation of Orientation Angle (ϕ_c) of the Projected Ellipse Major Axis	39
11. R.H. Regular Braid Lattice Structure of One Full Pattern Repeat	46
12. Procedure for Determining a Set of Jamming Values (SUBROUTINE JAM)	43
13. Typical Diamond Jamming Envelope	41
14. Right- and Left-Handed Jamming Envelopes	48
15. Unit-Cell Strand Length vs. Unit-Cell Width (TYPE=1, n=4)	55
16. Unit-Cell Strand Length vs. Unit-Cell Width (TYPE=1, n=24)	56

LIST OF ILLUSTRATIONS (Continued)

Figure	Page
17. Unit-Cell Strand Length vs. Unit-Cell Width (TYPE=1, n=60)	57
18. Unit-Cell Strand Length vs. Unit-Cell Width (Flat-Cell Model)	59
19. Unit-Cell Strand Length vs. Unit-Cell Width (Helix-Triangle)	60
20. Strand Length at $Q_1=45$ for Different Strand Number, n	62
21. Crimp-Effect vs. Cell Width (TYPE=1, n=4)	63
22. Crimp-Effect vs. Cell Width (TYPE=1, n=24)	64
23. Crimp-Effect vs. Cell Width (TYPE=1, n=60)	65
24. Braid Deformation Curves and Jamming Envelope (TYPE=1, n=24)	67
25. Braid Deformation Curves and Jamming Envelopes (TYPE=2, n=24)	68
26. Distribution of Local Helix Angles for an Alternating Right Trellis Leg (TYPE=1, n=16)	91
27-35. Test Data for Braid Samples (Diamond).	98-106
36-43. Test Data for Braid Samples (Regular).	107-114
44. Structure of Multi-Purpose Braids Computer Program	132

SUMMARY

A theoretical and experimental investigation of the structure of tubular braids is carried out. Relationships are established between braid parameters (i.e. strand number, strand diameter, strand pattern of braiding) and variable braid dimensions (i.e. braid diameter, braid pitch, tensile and compressive jamming configurations).

The theoretical part consists of the building of a geometrical model describing the path of strand axes, and a vector analysis of intersecting strand segments to determine the geometry of jamming. A helix with a sinusoidally varying radius to simulate interlacing crimp was used as a basis for the model. The curved length of the strand was determined by numerical integration with the aid of a digital computer. The prediction of jamming positions was also accomplished by an iterative technique which calculated the relative positions and distances of interlacing strands. The complete analysis, the results of which are displayed in computer plotted graphs, provides a comprehensive description of the potential braid structural deformation between and up to its jamming points.

Tests were performed on "diamond" and "regular" braided polyester monofilament to verify the theoretical predictions. Close agreement was found between theory and

experiment.

CHAPTER I

INTRODUCTION

Background

A modern investigation into the nature of braided structures has been long overdue. Braids have been overshadowed in textile structural mechanics by the more commercially important fibrous assemblies such as woven, non-woven, knitted, and twisted structures. Still the braid is a fundamental textile formation with distinctive structural properties worthy of scientific attention.

A braid is a linear fibrous assembly composed of two major sets of interlacing strands both of which lie on the bias relative to the longitudinal axis of the structure. It can take on a variety of closely related forms: narrow fabric, tubular fabric, cord, and thread. This thesis concentrates on tubular braids, also referred to as "round" or "circular" braids. It is a fibrous cylindrical shell of small diameter consisting of clockwise and counter-clockwise sets of mutually interlacing, spiralling strands. Such an assembly exhibits a special mode of structural deformation when axially extended or compressed. When extended the structure is capable of substantial accommodation of strain since the initially inclined elements are free to pivot to a

position more parallel to the direction of the stress. As the tubular braid extends its diameter decreases until the fabric reaches a point of maximum packing density, called the tensile or extensive jamming point. Conversely, a braid forced to contract in length will have its structural elements re-aligning more perpendicular to the direction of compressive stress increasing its diameter up to a compressive jam point. The extensive and compressive jamming are simple observances of the physical law of non-penetration of solids.

The braid jamming mechanism can be elucidated by comparison to the packing process of twisted multi-filament yarn. In both cases filaments obliquely cross the cross-sectional plane of the structure such that round filaments manifest quasi-elliptical cross-sections. ("Quasi-" since a true ellipse would only be generated by sectioning a straight cylindrical filament; the curvature of the filament axes in question makes the cross-sections differ from true elliptical.) The aspect-ratio of the "ellipses" is a function of the filaments local helix angles, only a fixed number of them can be accommodated in a ring of a given circumference. In yarn packing when a certain layer is filled there can be overflow of an individual strand to an outer layer. Due to the interlacing in tubular braids, the strands are captive members of a particular cross-sectional ring. The braided structure

though allows an additional degree of freedom, namely, the diameter of the whole ring can vary. The net effect is a type of mass migration where all the strands move in or out together.

An extending braid changes its dimensions in accordance with the well-known "helix-effect" introduced by Hamburger[1]. As shown in Figure 1, a triangle formed from an unwrapped helix can be used to illustrate the inter-relationship between the different parameters of the braid. In this representation the length of the hypotenuse of a given geometry is regarded as the independent variable, remaining constant while the other dimensions change.

The jamming mechanism in tubular braids can be conceptualized as a combination of the helix-effect and the obliquity-effect (i.e. strands obliquely crossing the cross-sectional plane of the structure manifesting quasi-elliptical strand cross-sections.) When a braid is axially compressed, the higher aspect-ratio ellipses require and are given more room by an increasing circumference. The compressive jamming geometry in a tubular braid is defined as the point at which the demand for larger cross-sectional area made by the obliquity-effect exceeds the ability of the helix-effect to provide it. Alternately, the extensive jam mechanism can be characterized as a shrinking circumference chasing ellipses of decreasing aspect-ratio. The circumference catching the

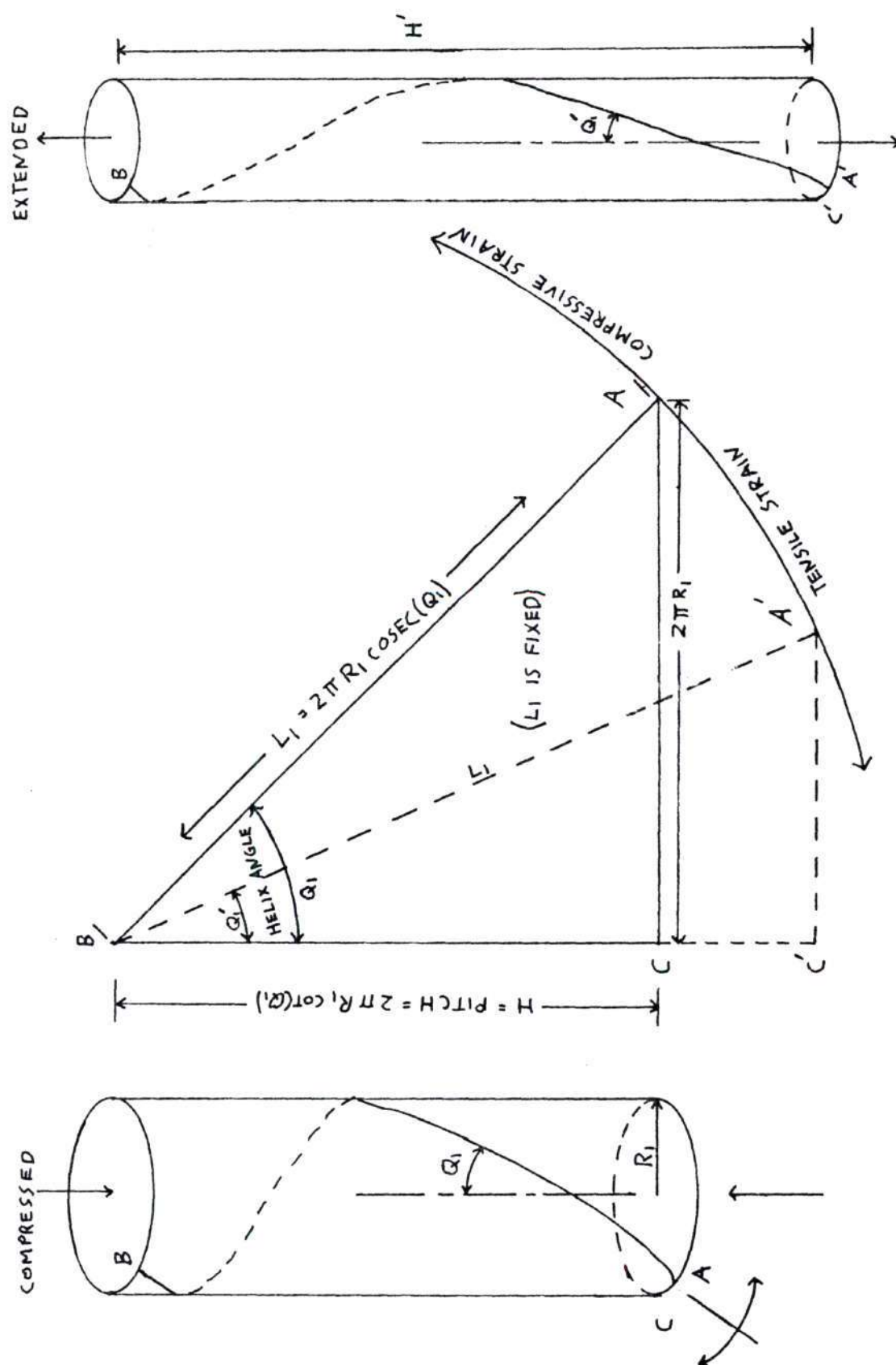
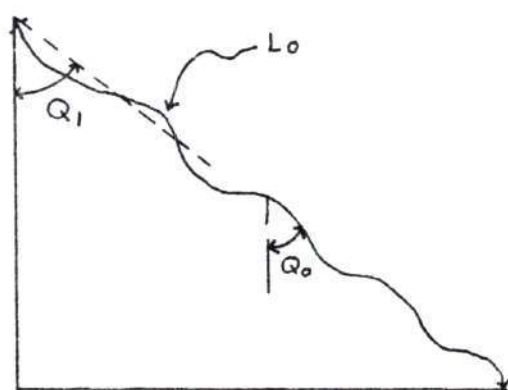


FIGURE 1. EXTENDED AND COMPRESSED HELIX AND UNWRAPPED HELIX-TRIANGLE.

ellipses constitutes the extensive jam point. A mathematical formulation of the jamming phenomena is presented in the following chapter.

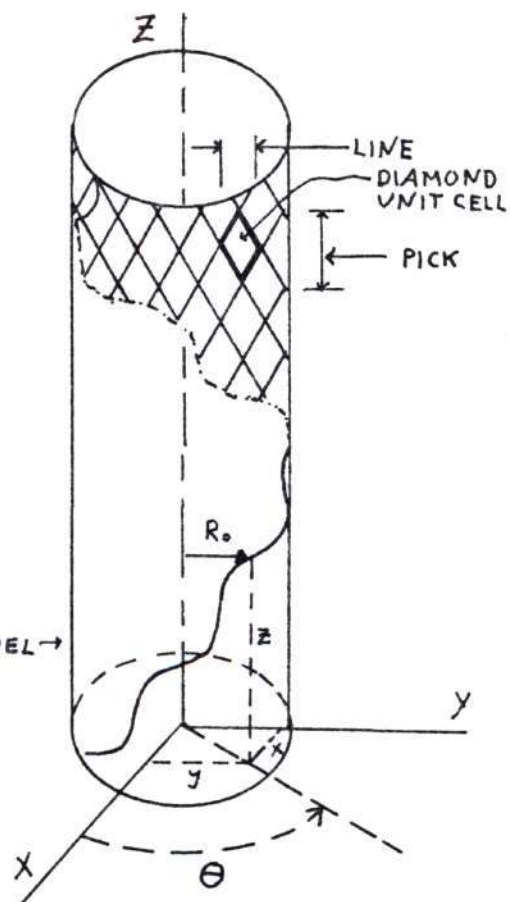
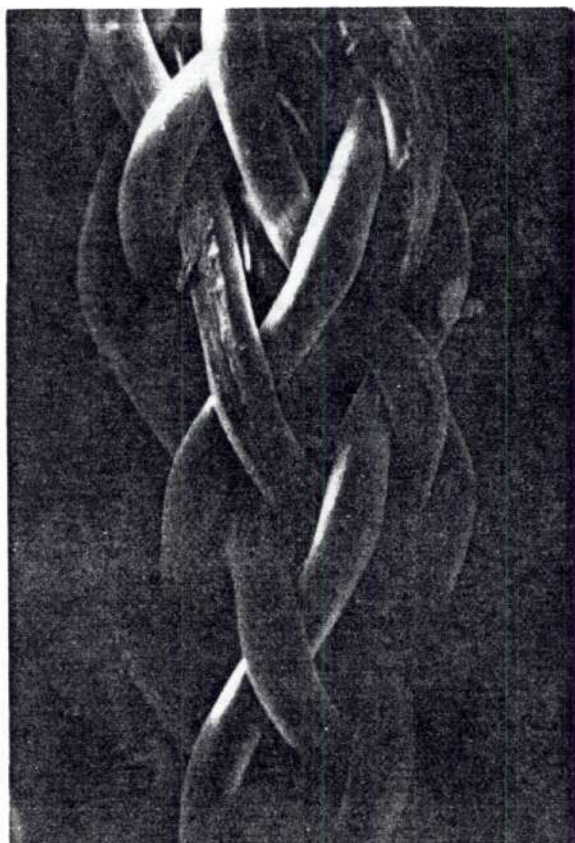
If it were not for such mitigating factors as interlacing crimp, strand cross-section flattening, and strand bending rigidity, a tubular braid could be trivially represented by the helix-triangle. Of these factors, interlacing crimp is probably the first and major cause of the departure of the real from the ideal. It is a necessary ingredient for any model of braid jamming. With this in mind, the braiding strand is postulated as following the general path of a helix with small, regular fluctuations in the helical radius to represent interlacing crimp. A more realistic braid-helix-triangle resembles the schematic in Figure 2. A novel approach to representing the geometry of a crimped strand following a helical path is presented in this thesis.

Friction, a traditional irritant in the building of mechanical models of textile assemblies, has surprisingly small bearing on the braids problem, even though at first glance the large degree of movement present in braid deformation seems to make it an issue. Closer examination shows that the pivoting of structural elements occurs at minimal loads only. Without sizable stress, there are no substantial normal forces and no significant frictional effect. The region of high structural extension under



CRIMPED HELIX- TRIANGLE

CRIMPED HELICAL MODEL →



DIAMOND TUBULAR BRAID
WITH 10 mil. POLYESTER
MONOFILAMENT STRANDS
(12 CARRIER BRAIDER)
SCANNING ELECTRON MICROGRAPH - 30X

FIGURE 2. CRIMPED MODEL OF CIRCULAR BRAID AND PHOTOGRAPH.

negligible load is shown in the stress-strain diagram (Figure 3) as "A". This thesis focuses primarily on the deformation of the braid that occurs within this region.

In order to discuss braids it is first necessary to become familiar with the rudiments of braid anatomy. The hierarchy of structural components of a typical braid is: 1) fiber or filament, 2) yarn or thread, 3) strand, and 4) braid. As the order suggests a strand may consist of several yarns or threads that interlace as a unit. The resulting braid pattern is one analogous to a basket-weave. This thesis deals exclusively with the relationship of single-element strands to braid structure.

As mentioned, a tubular braid consists of two sets of helical strands of opposite sense that interlace with each other. Member strands of the same set travel in concurrent paths. Intersections only occur with members of the opposite set. The two sets of intersecting strands form a lattice of diamond-shaped units. A column of such units is called a "line", while a row is loosely called a "pick" (See Figure 2). The fundamental diamond-shaped unit cell (sometimes called "diamond trellis" or "plait") has been traditionally used as the unit for structural analysis of the braid [3]. For the dimensional analysis of diamond braid only one quadrant of the diamond trellis need be considered, the other being repetitive. Cell dimensions, H_c , W_c , and l_o , used in this thesis (see Figure 7) reflect

A - STRUCTURAL ACCOMMODATION
OF BRAID UNDER NEGLIGIBLE
LOAD

B - EXTENSION DUE TO STRAINING
OF THE STRANDS

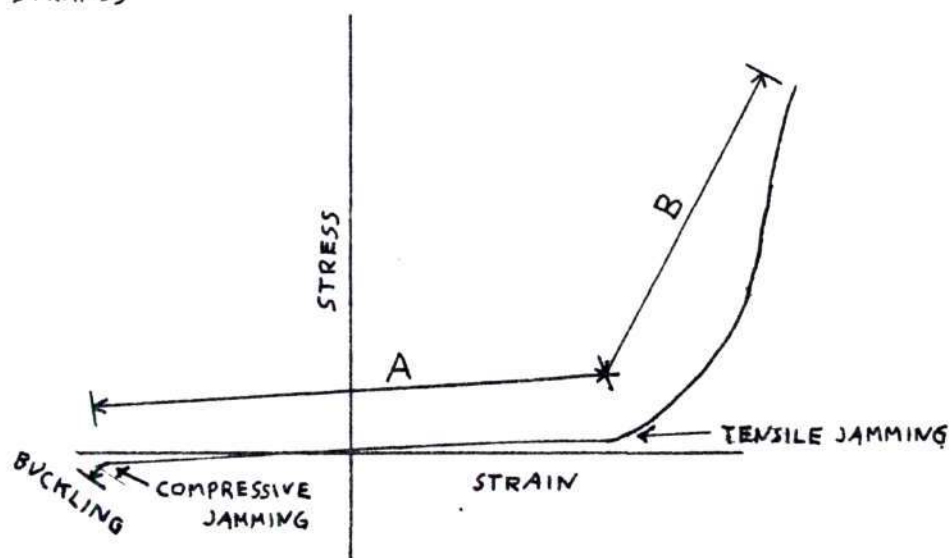


FIGURE 3. IDEALIZED STRESS-STRAIN CURVE OF A TYPICAL BRAID.

this consideration. The pitch of a circular braid is the axial distance along the braid structure required for one strand to make a complete spiral. Pitch in conjunction with the invariant number-of-strands-per-helical-set gives the fabric density in number of stitches or picks per inch.

As in woven structures, there are several patterns of interlacing commonly used. The equivalent form of 1/1 plain weave is called 1/1 or "diamond" braid. A 2/2 braid which is called a "regular" braid is the analog of a 2/2 woven twill. Several yarns braiding together as one, or "basket-weave" variations of each of these basic patterns are common. Commercially, "basket" variants of regular braids predominate. Scientifically speaking, the regular braid poses a more difficult geometric analysis. Accordingly investigation into 1/1 diamond geometry is commonly used as a spring-board into the braid problem. Of the few articles on braid geometry in the literature, none have advanced to the point of considering regular braid structure. This paper begins with 1/1 geometry and extends it to the case of 2/2.

Literature Review

There is scarce mention of either braid geometry or mechanics in past literature. Hamburger [1] (1942) introduces the topic with a practical, primarily empirical look at the strength of shroud lines for parachutes. Next

Brunnschweiler (1954), the principal contributor in the braid area, presents a comprehensive treatment of braid technology history [2] and an analysis of planar, diamond braid geometry [3]. Popper [4] (1970) in an unpublished lecture reviews Brunnschweiler's pioneering efforts and draws on classical yarn mechanics to arrive at a mathematical expression for post-jamming (extensive) braid modulus.

A common use of tubular braids, which is of interest to Hamburger [1] in the context of parachute cord, is as a cover in a sheath/core type composite structure. Such a composite generally consists of a more or less straight bundle of yarns or fibers housed in a hollow tubular braid. Usually the core is the load carrying component while the braid serves to bind it together and provide surface protection. Through proper structural design and/or choice of constituent fibers it is possible to have the cover also contribute tensile support. Hamburger points out that the key to a mechanically efficient composite braid structure lies in rupture elongation balance of core and sheath. The rupture elongations of the two components should correspond since it is usually at the moment of imminent rupture that each supports its maximum load. The present study of between-jam structural deformation of the tubular braid should assist in the future engineering and design of the sheath component. It will provide information concerning

maximum and minimum allowable core diameter as well as the jammed helix angle resulting from a core of any diameter.

Hamburger also discusses the trends relating the details of braid construction to tensile response. He notes that an increase in either cover yarn size or number of picks per inch will cause an increase in the helix angle at tensile jam and a decrease in the braid's ultimate breaking strength.

Brunnschweiler [3] delves into the more theoretical aspects of braids analyzing their structural properties using the approach developed by Peirce [5]. Assuming an idealized geometry for braid and constituent yarns, Brunnschweiler focuses on the diamond trellis as the basic structural unit. He assumes that his yarns are flexible, inextensible, of constant circular cross-section, and non-flattening. The yarns of his model follow elliptical arcs, the lengths of which are determined using an elliptical integral, and straight lines, calculated using trigonometric identities (see Figure 4). His nomenclature is the following

n_y = number of yarns in a strand ("basket")

l = curved length of one leg of diamond element

l_s = straight inclined segment of l

l_t = curved elliptical segment of l

l_u = straight horizontal segment of l

d = yarn diameter (taken as unity to make variables dimensionless)

(α) = angle between yarns

p = perpendicular distance between parallel strands

x = height of diamond trellis

subscript j = jammed dimensions

p_t , (ϕ) , (θ) , q , and z are defined in Figure 4

The diamond, flat-cell model gives the geometric relation for one element of strand as:

$$l = \text{function}(\alpha, x, n_y, d) \quad (\text{I.1})$$

The partitioning of l (see Figure 4) is as follows:

$$l = l_s + l_t + l_u \quad (\text{I.2})$$

Where,

$$l_s = \sqrt{\{(p_t^2 - 3)(\sin^2 \phi + \sec^2 \theta \cos^2 \phi)\}} \quad (\text{I.3})$$

$$\phi = \tan^{-1} p_t - \cos^{-1}(2/\sqrt{1 + p_t^2})$$

$$p_t = x \sin(\alpha/2) - (n_y - 1)$$

$$\theta = 90^\circ - \alpha$$

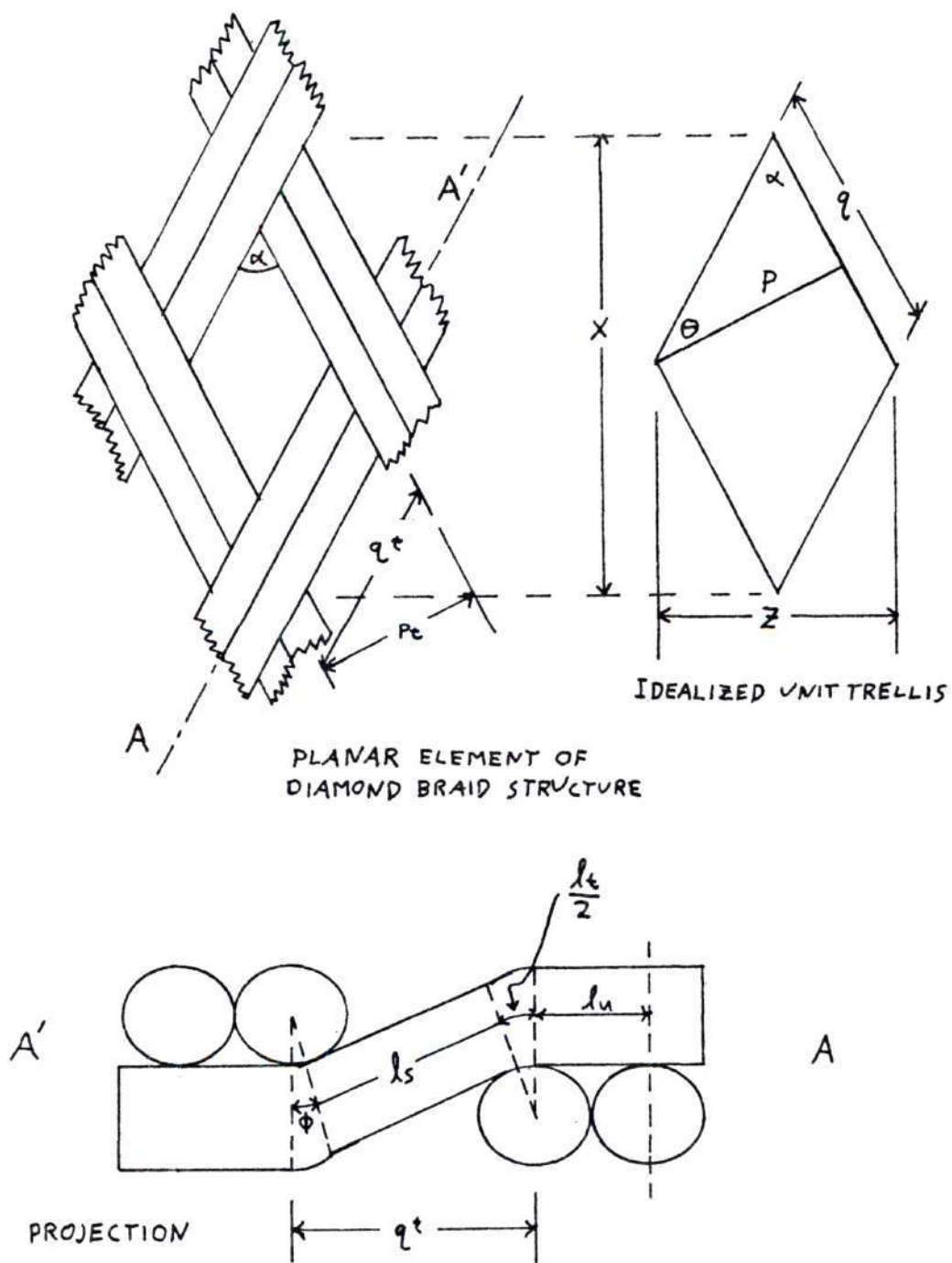


FIGURE 4. FLAT-CELL MODEL ($n_y=2$).

Where,

$$l_t = 2\sec(\theta)E(\theta, \phi) \quad (I.4)$$

$$E(\theta, \phi) = \int_0^\phi \sqrt{1 - \sin^2\theta \sin^2\xi} d\xi$$

And,

$$l_u = (ny - 1)\sec\theta \quad (I.5)$$

Jamming for this planar case as in the circular case is the condition where neighboring strands of the same set are as close as possible while still allowing an interlacing strand to pass between them. Brunnschweiler defines jamming by making the straight inclined length of the interlacing portion of the yarn, l_s , equal to zero (Equation I.2). Therefore the jammed dimensions for the diamond trellis are:

$$p_{tj} = \sqrt{3} \quad ; \quad j = 60^\circ$$

$$x_j = \frac{\sqrt{3} + (ny - 1)}{\sin(\alpha/2)} \quad ; \quad q_j = \frac{\sqrt{3} + (ny - 1)}{\sin\alpha} \quad ; \quad z_j = \frac{\sqrt{3} + (ny - 1)}{\cos(\alpha/2)} \quad (I.6)$$

$$l_j = 2\sec(\theta)E(\theta, 60^\circ) + (n - 1)\sec\theta$$

A key boundary condition used in both Brunnschweiler's flat model and the circular model to be

developed later is that all relative movement of the strands between and during jamming occur within the plane of the fabric. If there was motion normal to the fabric plane it would be the analogue of crimp interchange in woven fabric. Crimp interchange is the outcome of differential loading of warp and filling yarns. Since the two sets of braid strands comprise the same selvage they are always subject to equal loads. Therefore there is no out-of-plane strand displacement meaning the thickness of the braid's fabric wall remains constant throughout the period of structural deformation. Even at jamming, if one assumes incompressibility of yarn cross-section, the fabric thickness remains constant at $2d$.

Brunnschweiler suggests the use of tables and graphs in order to facilitate the use of his complex final equation. However because he finds that there is little to facilitate the extraction of data from his equation for these original graphs and tables, he is very sparing in their presentation. The need for computerized generation and handling of theoretical and experimental data is clearly in evidence.

Throughout his work, Brunnschweiler is investigating circular braids with the use of a planar unit cell. He claims that unless the total number of strands is exceptionally low, less than eight, that the flat diamond cell will be equally applicable to flat and tubular

structures. The validity of this assumption will be critically evaluated.

Using Brunnschweiler's equation, Popper [4] presents in more readily usable graphical form the predicted range of braid dimensions between the jamming limits. Like Brunnschweiler he makes no attempt at experimental verification to see whether the predictions are realistic. This presentation will include the development and utilization of a test procedure to measure the deformation geometry of circular braids.

CHAPTER II

THEORY

Arc-length Theory

The path of a braid strand can be approximated by a simple helix described using an orthogonal coordinate system as follows:

$$f_x(\theta) = R_1 \cos \theta \quad (\text{II.1})$$

$$f_y(\theta) = R_1 \sin \theta$$

$$f_z(\theta) = R_1 \theta \cot Q_1$$

$$F(\theta) = (f_x(\theta), f_y(\theta), f_z(\theta))$$

As the vectorial angle (θ) varies from zero to 2π , a helix with radius R_1 and height (pitch) $2\pi R_1 \cot Q_1$ is swept out (See Figure 1).

The approximate distance between any two close points on the helix is given by the length of the inscribed chord.

$$\text{Chord Length} = ||F(\theta + \Delta\theta) - F(\theta)|| \quad (\text{II.2})$$

Hence if the entire pitch of the helix is partitioned into m such distances the approximate arc-length of the helix would be their sum:

$$\text{Arc-Length} \approx \sum \left\| \frac{F(\theta_k + \Delta\theta_k) - F(\theta_k)}{\Delta\theta} \right\| \Delta\theta_k \quad (\text{II.3})$$

Letting m approach infinity and $(\Delta\theta)$ approach zero permits the summation (II.3) to approach the integral:

$$\text{Arc-Length} = \int_0^\theta \|F'(\theta)\| d\theta \quad (\text{II.4})$$

Substituting (II.1) into (II.4) allows the calculation of arc-length per pitch of the helix.

$$F'(\theta) = (-R_1 \sin\theta, R_1 \cos\theta, R_1 \cot Q_1) \quad (\text{II.5})$$

$$\|F'(\theta)\| = R_1 \csc Q_1 \quad (\text{II.6})$$

$$\int_0^{2\pi} \|F'(\theta)\| d\theta = 2\pi R_1 \csc Q_1 = L_1 \quad (\text{II.7})$$

Appropriately this quantity of arc-length per pitch corresponds to the hypotenuse of the helix triangle in Figure 1.

The effect of interlacing crimp on the strand arc-length can be introduced into the model with the following assumption:

The serpentine path of a strand in a 1/1 tubular braid can be approximated by a sine wave of amplitude equal to the strand's radius r , and frequency equal to one-half the number of strands with which it interlaces, $n/2$, per pitch.*

Note that a strand belonging to the set of "S" helices must interlace with every member of the "Z" helical set. Since there are n strands per set and each cycle of sine wave interlaces with two (over one and under one), $n/2$ cycles are required per pitch. The symbolic form of the crimp wave is:

$$\text{Crimp Wave} = r \sin(n\theta/2) \quad (\text{II.8})$$

Returning to the coordinates of the helix, the new transient

* The author wishes to acknowledge Dr. A. Tayebi for suggesting the "helix with sinusoidally varying radius" as an approach to the braids problem.

helical radius, R_0 , oscillates about nominal helix radius, R_1 , as a function of (θ) . It is given by:

$$R_0 = R_1 + r \sin(n\theta/2) \quad (\text{II.9})$$

And thus the new coordinates of a point on the crimped helix are:

$$g_x(\theta) = R_0 \cos \theta \quad (\text{II.10})$$

$$g_y(\theta) = R_0 \sin \theta$$

$$g_z(\theta) = R_1 \theta \cot Q_1$$

$$G(\theta) = (g_x(\theta), g_y(\theta), g_z(\theta))$$

The assumptions standard for geometric models of textile structures are to be invoked. Strands are circular and non-flattening in cross-section, flexible, and uniform along their length. In contrast to past braid models [3,4], the effect of fabric curvature is not assumed to be negligible. Instead of using alternating straight and elliptical strand segments to approximate the path of the strand axis, we have a sine wave oscillating normal to the cylindrical surface through which it travels.

The notation used is:

L_o = curved strand length* per pitch; arc-length/pitch

L_l = length* of the projection of L_o onto the fabric plane; length of helix triangle hypotenuse

l_o = curved strand length per unit cell; length of leg of unit trellis

l_l = length of the projection of l_o onto the fabric plane

s = any strand arc-length

R_o = transient radius of the crimped model

R_l = nominal helix radius; radius of uncrimped helix triangle

FK = curvature of the braid fabric wall; $1/R_l$

r = strand radius

r_o = transient effective radius of oblique section of inclined strand

a = maximum value of r_o ; major radius of ellipse

d or SD = strand diameter

$D = 2 \times R_l$; braid diameter (nominal)

n or N = number of strands per helical set

$2n$ = total number of strands in braid

Q_o = transient local helix angle for the crimped model

Q_l = nominal helix angle; helix angle for uncrimped model

H = pitch height for crimped and uncrimped models

* Unless otherwise labelled all length dimensions are divided by strand diameter (taken as unity) to make them dimensionless.

H_c = height of unit cell

W_c = width of unit cell

(θ) = internal vectorial angle of helix

W_X, W_Y, W_Z = direction cosines of strand axis, dx/ds ,
 dy/ds , dz/ds

\bar{R} = position vector which generates crimped helix

$\bar{T} = dR/ds$; tangent vector

GC = curvature of strand

GT = geometric torsion of strand

$DIST$ = inter-axial distance between jamming strands

$ELLIP$ = distance required by oblique strand

cross-sections during jamming

JD = jamming distance; $DIST-ELLIP$

(α) = angle between r_o and "a" in ellipse

(ϕ) = angle of rotation of elliptical strand

cross-section

(γ) = angle of inclination of inter-axial chord in jamming

$TYPE = 1$. diamond braid

2. right-hand, regular braid

3. left-hand, regular braid

$MODE = 1$. arc-length calculated according to crimped
 helical model

2. arc-length calculated as simple helix

3. arc-length calculated according to flat-cell model

In order to get the new crimped arc-length, L_0 , apply arc-length formula (II.4) to the crimped helix (II.10):

$$L_0 = \int_0^{2\pi} \sqrt{(g'_x(\theta))^2 + (g'_y(\theta))^2 + (g'_z(\theta))^2} d\theta \quad (\text{II.11})$$

Where the derivatives with respect to (θ) are:

$$f'_x(\theta) = -R_1 \sin \theta + \frac{nrcos(\theta n/2)cos}{2} - \sin(\theta)r\sin(\theta n/2) \quad (\text{II.12})$$

$$f'_y(\theta) = R_1 \cos \theta + \frac{nrcos(\theta n/2)\sin \theta}{2} + \cos(\theta)r\sin(\theta n/2) \quad (\text{II.13})$$

$$f'_z(\theta) = \frac{H}{2\pi} \quad (\text{II.14})$$

The final formula can be summarized by the relation:

$$L_0 = \text{function}(R_1, Q_1, n, r) \quad (\text{II.15})$$

Note that even though Q_0 in a crimped helix oscillates and H remains constant, it is more convenient and clearer to characterize crimped helices by their nominal helix angle,

Q1.

Since the complexity of the arc-length integration does not allow a closed form, analytic solution, the trapezoidal rule and digital computer is employed to provide values of L_0 . Data generated in this manner is presented in the section on theoretical results.

The computer provides great power and flexibility in manipulating the equations and resulting data. It enables the taking of function (II.15) and calculation of sets of R_1 and Q_1 for given r , n , and L_0 . This relationship would not otherwise have been available because of the non-linearity involved. The "false position" algorithm is used to arrive at these values. To have R_1 and Q_1 as dependent variables is important because for a given braid specimen n , r , and L_0 are always fixed and R_1 and Q_1 vary as the braid is deformed. All the deformation-curves for individual braids plotted in this thesis are derived in this manner (e.g. Figure 13).

Discussion Of The Sinusoidal Helix Model

Let us see how the use of the circular model yields a more realistic geometry than the flat-cell approach. If one were to impose curvature on a series of flat cells, the bending would place the underlaps in compression and the overlaps in tension. In actual braid formation, a tubular braid in avoidance of this stress build-up simply requires less strand length for an underlap and more for an overlap.

Unlike the flat-cell model, the cylindrically based sinusoidal model incorporates the longer overlaps and shorter underlaps. This length differentiation is not important in calculating the overall L_0 since the long and short segments compensate for each other, but it is important in jamming. Jamming initiates on the concave side of the bent strand where there is less space for the accommodation of the interlaced strand. To accurately predict jamming it is essential to take the fabric curvature with its longer and shorter strand segments into account.

Another anticipated advantage is that the continuous sine function should more closely approximate a yarn which is a mechanical continuum of small finite bending rigidity. The sinusoidal model does not have the discontinuities in curvature that are present in Brunnschweiler's compound curve.

Regular Braids

Each strand of a regular braid overlaps and underlaps two strands. Regular braids are distinct from basket braids in that each adjacent parallel braiding element interlaces one step out of phase with its neighbor. A regular braid has half the number of interlacings as a diamond braid with the same number of strands.

However, a mere doubling of the wave-length of the sine wave is not the only adjustment required to extend the diamond model to the case of regular braids. In the

previous diamond braid model proper nesting of the strands at interlacing points was achieved by centering the cross-section of the interlaced strand in the sinusoidal trough of the interlacing strand. The result was a fabric wall of thickness $2d$, one of the boundary conditions. This can be seen in Figure 5 where the computer has been used to plot the projection of one pitch of a single braid strand and the cross-sections of the strands with which it interlaces onto the x-y plane. Ellipses are used to approximate the true quasi-elliptical nature of the strand cross-sections mentioned earlier.

If a simple sine wave interlaces two strands neither of them will be centered, the fabric thickness will exceed $2d$, and the configuration will not manifest suitable strand inter-nesting. The corrective necessary, if the sinusoidal character of the model is to be preserved, is to build a compound curve of part sine wave and part constant radius arc in the same manner that straight-lines were pieced together with elliptical arcs. Although this model sacrifices the strand axis curvature continuity, it is hoped that the calculated values will be sufficiently accurate to predict the dimensions of regular braids.

The compound curve is constructed by dividing one interlacing repeat into 4 segments (see Figure 6). The first segment maintains a constant maximum helical radius. The second segment takes the form of one-half of a sine wave

BRAID-TYPE= DIAMOND
 NUMBER OF STRANDS/SET= 16.
 STRAND DIAMETER= 1.

HELIX ANGLE= 21.0
 BRAID DIAM.= 12.2
 STRAND LENGTH/PITCH= 108.6

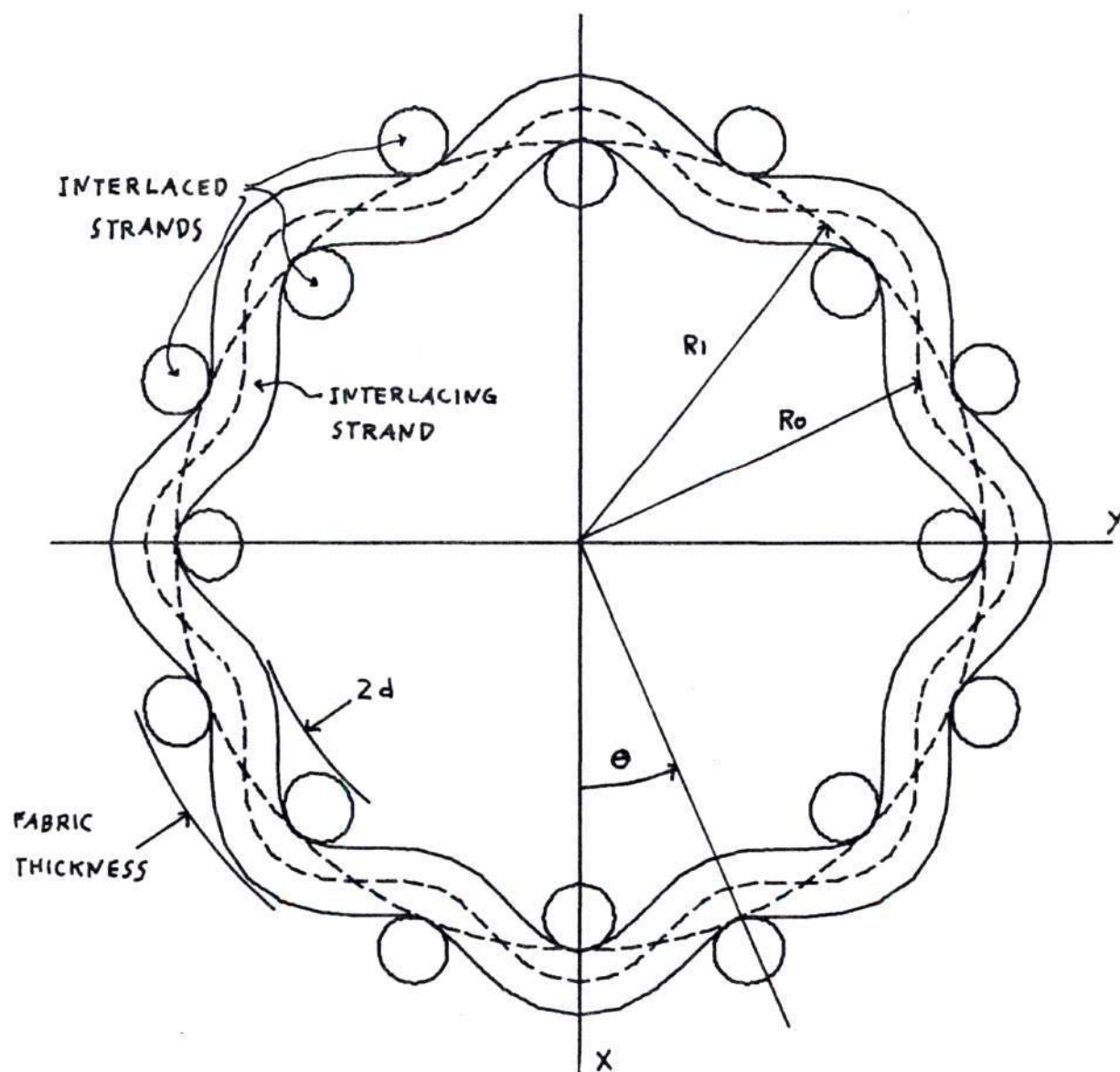


FIGURE 5. PROJECTION OF CIRCULAR 1/1 DIAMOND BRAID.

BRAID-TYPE= REGULAR
 NUMBER OF STRANDS/SET= 16.
 STRAND DIAMETER= 1.

HELIX ANGLE= 21.0
 BRAID DIAM.= 12.2
 STRAND LENGTH/PITCH= 107.9

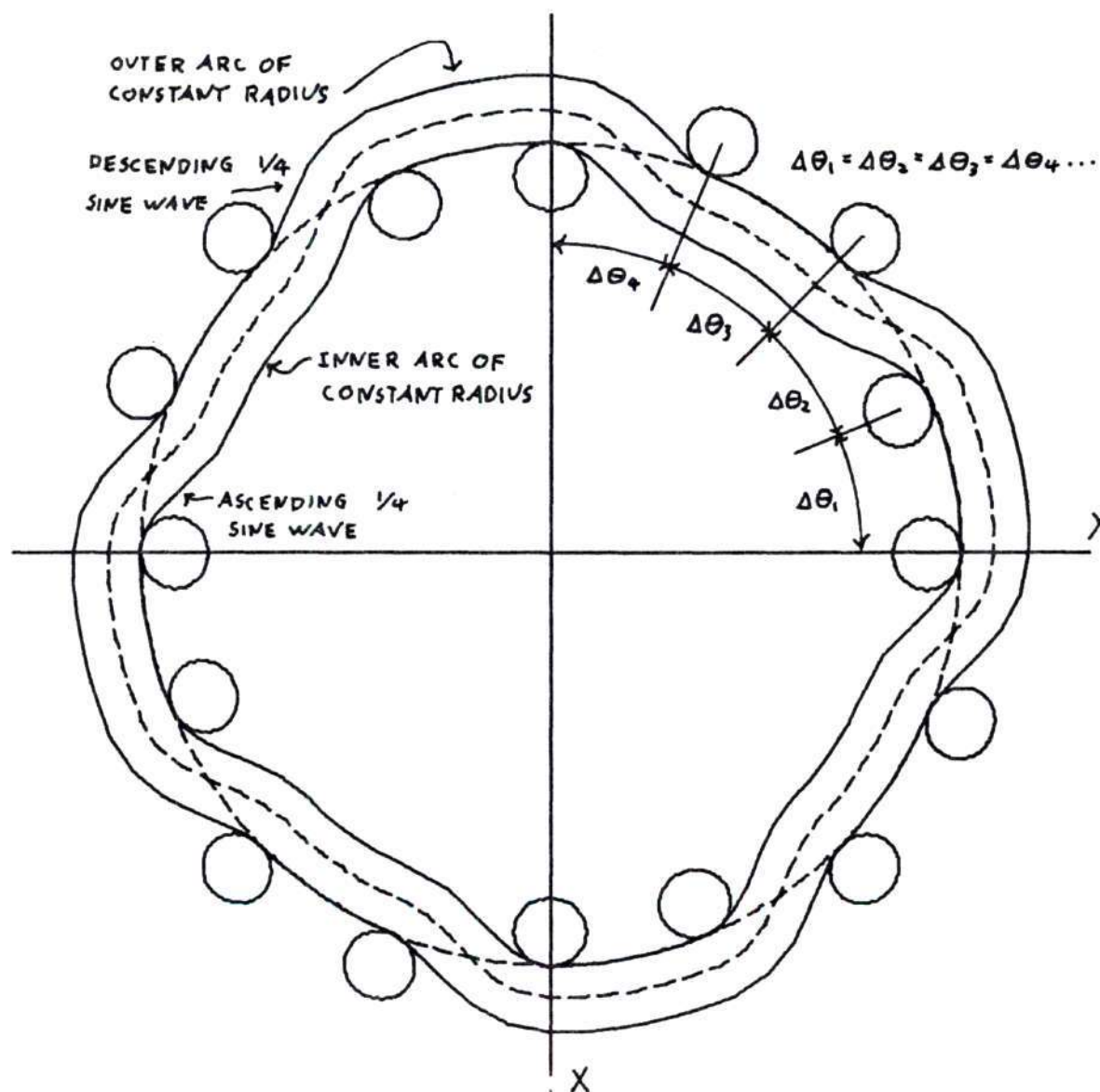


FIGURE 6. PROJECTION OF CIRCULAR 2/2 REGULAR BRAID.

of frequency $n/2$ (the same frequency used in a diamond braid of the same n) which descends from the maximum to minimum radial position, followed by a segment of constant minimum radius. Finally a sinusoidal segment ascends back to the level of maximum helical radius and so on.

Figure 6 illustrates several noteworthy features of the compound curve model of the regular braid. A boundary condition placed on the model is the equidistance of adjacent strands of the same set. Unlike the case of basket braids the two elliptical cross-sections sharing the same overlapping strand do not group together. Such behavior is prevented because of the interlacing phase lag in adjacent strands. Any tendency for a strand to move toward the center of the crimp wave is balanced by a similar tendency in the opposite direction at the strand's next interlacing tier. The equidistant spacing of parallel strands is observable in actual regular braid.

The plot also reveals a drawback in the construction of the inner arcs of constant radius. There is no physical reason for it to have the positive curvature it has unless perhaps the braids is seated on a cylindrical core as it would be in a composite sheath/core construction. The effect on the arc-length calculation of this discrepancy should be negligible.

The arc-length equation for regular braids becomes:

$$L_{O\text{Regular}} = \frac{1}{2}(L_{O\text{Diamond}} + L_1) \quad (\text{II.16})$$

Jamming Theory

Jamming is a condition of high fabric packing density where a position of limiting structural geometry is reached due to the inability of solids to inter-penetrate during braid deformation. In the case of extensive jamming it is the point where extension from the pivoting lattice of diamond trellis units stops and extension due to the straining of the strands begins. For compressive jamming it is where strain from similar structural accommodation stops and the buckling of the tubular braid starts.

A vector analysis of a typical point of interlacing is used as the foundation for the quantification of the jamming phenomenon. Looking at the cylindrical wall of a tubular diamond braid (Figure 7), focus on two contiguous legs (A and B) of a non-planar unit cell and their vertex. There is one point of contact; the "Z" segment starts at the maximum radial position and descends to the minimum while the "S" segment does the opposite. Equation (II.10) gives the coordinates of the "Z" segment. The "S" segment is set out of phase by adding π to the argument of the sine in (II.9) and generated using $-(\theta)$ in (II.10). Jamming is declared if the braid is deformed, i.e. R_1 and Q_1 are

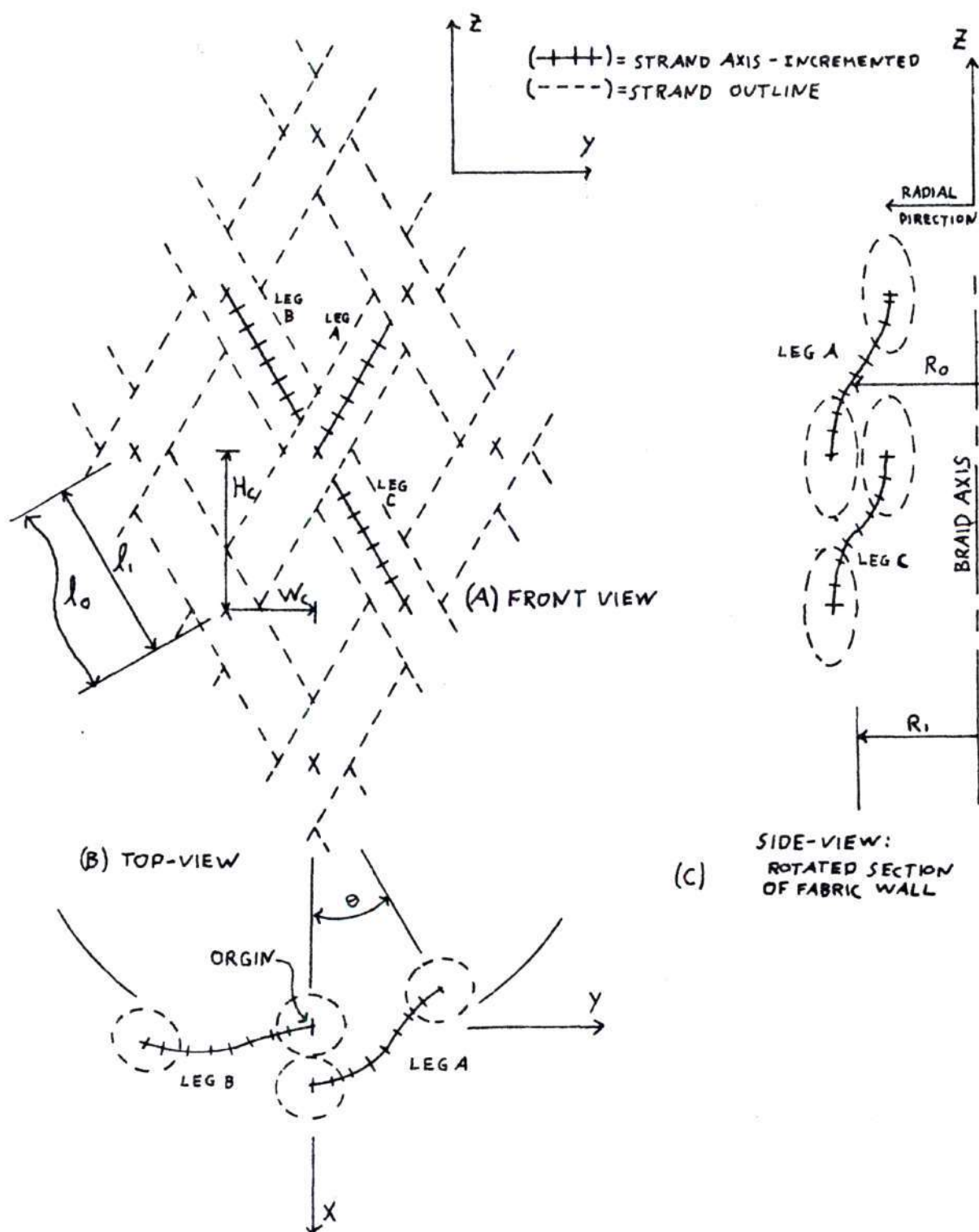


FIGURE 7. NON-PLANAR DIAMOND UNIT CELL AND LATTICE STRUCTURE.

manipulated, so that there is more than the one original point of contact.

The test for jamming consists of using the computer to step up the two legs with as fine an increment as desired and comparing their inter-axial distance, DIST, with the distance required by the thickness of the strands, ELLIP. DIST is readily calculated using the distance formula:

$$\text{DIST} = \sqrt{(x_1 - x'_1)^2 + (y_1 - y'_1)^2 + (z_1 - z'_1)^2} \quad (\text{II.17})$$

The calculation of ELLIP however requires the finding of an effective radius, r_o , for the strand as it cuts the X-Y plane at local helix angle Q_o . The value of r_o is greater than or equal to r due to obliquity. The precise fixing of r_o depends on the relative position of the two strands (see Figure 8). The orientation of the two axes in space found using vector analysis is necessary to calculate values of ELLIP. Using the coordinates for the crimped helix (II.10) as position vector, \bar{R} , and derivatives (II.12-13-14) gives tangent vector \bar{T} :

$$\bar{T} = \frac{d\bar{R}}{ds} = \frac{d\bar{R}}{d\theta} \times \frac{d\theta}{ds} = \frac{(dx/d\theta)\bar{i} + (dy/d\theta)\bar{j} + (dz/d\theta)\bar{k}}{\sqrt{(dx/d\theta)^2 + (dy/d\theta)^2 + (dz/d\theta)^2}} \quad (\text{II.18a})$$

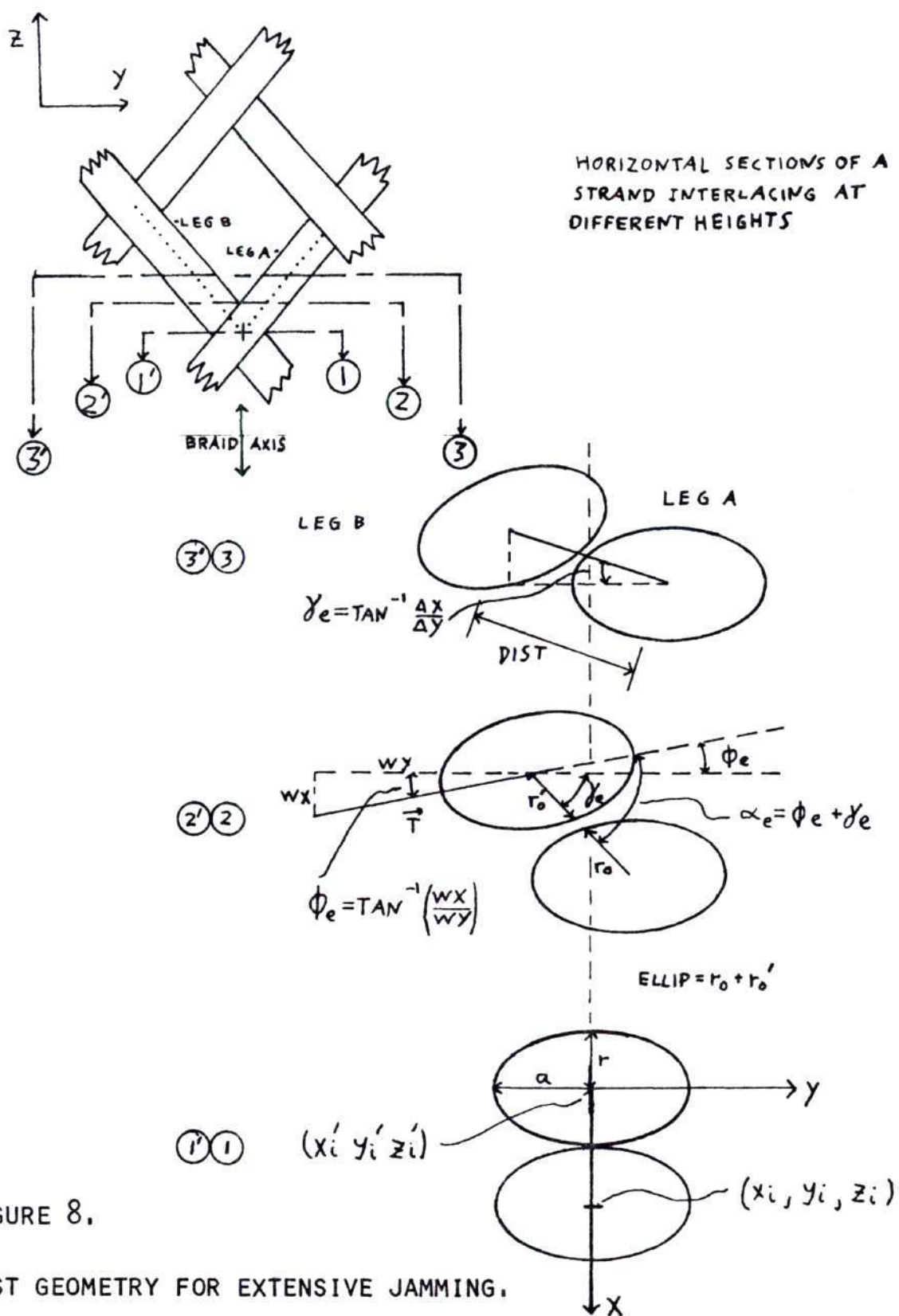


FIGURE 8.

TEST GEOMETRY FOR EXTENSIVE JAMMING.

Rewritten in terms of direction cosines (W_x, W_y, W_z) it is:

$$\bar{T} = W_x \bar{i} + W_y \bar{j} + W_z \bar{k} \quad (\text{II.18b})$$

$$W_x = \frac{1}{\sqrt{\{1 + (dy/dx)^2 + (dz/dx)^2\}}} \quad (\text{II.18c})$$

$$W_y = \frac{1}{\sqrt{\{(dx/dy)^2 + 1 + (dz/dy)^2\}}} \quad (\text{II.18d})$$

$$W_z = \frac{1}{\sqrt{\{(dx/dz)^2 + (dy/dz)^2 + 1\}}} \quad (\text{II.18e})$$

The local helix angle, Q_0 , becomes:

$$Q_0 = \cos^{-1}(dz/ds) = \cos^{-1}(W_z) \quad (\text{II.19})$$

The quasi-elliptical cross-sections of inclined strands are idealized as simple ellipses whose long axis, $2a$, makes an angle (ϕ_e) with the y -axis (see Figure 8):

$$\phi_e = \tan^{-1}(dx/dy) = \tan^{-1}(W_x/W_y) \quad (\text{II.20})$$

The length of the ellipse major radius (transient) is:

$$a_o = r / \cos Q_o \quad (\text{II.21})$$

The effective strand radius can be found using the polar coordinate equation for an ellipse.

$$r_o = \sqrt{\{a_o^2 r^2 / (a_o^2 \sin^2 \alpha + r^2 \cos^2 \alpha)\}} \quad (\text{II.22})$$

Angle (α) is calculated by first finding the angle (γ) formed by the chord between the two strand axes and the x-axis and then rotating the orientation of the elliptical cross-sections (see Figure 8) according to direction cosines, W_x and W_y .

$$\gamma = \tan^{-1}\{(x'_1 - x_1)/(y'_1 - y_1)\} \quad (\text{II.23})$$

$$\alpha = \gamma + \phi \quad (\text{II.24})$$

The final value of ELLIP is the summation of r_o and r_o' from the "S" and "Z" segments. The two quantities are different because the two crimp waves are out of phase. The symmetry that does exist is between the beginning of one segment and the end of the other, not the two beginnings that are being used here. Thus jamming occurs when:

$$0 \geq \text{DIST} - (r'_o + r_o) = \text{DIST} - \text{ELLIP} = \text{JD} \quad (\text{II.25})$$

The above description will hold for the smaller helix angles present in extensive jamming. For larger helix angles in compressive jamming we will have to check two side trellis legs (A and C in Fig. 7) for inter-penetration. Geometry of compressive jamming is slightly different due to the curved nature of the cylindrical surface of the braid. The expressions for DIST (II.18) and the polar equation of an ellipse (II.22) are of course the same, though values of (α) , (γ) , and (ϕ) must be determined according to the radial position of the strands. The inclination of the inter-axial chord (see Figure 9), (γ_c) , is:

$$\gamma_c = \tan^{-1} \left[\frac{\sqrt{(x_1^2 + y_1^2)} - \sqrt{(x_1'^2 + y_1'^2)}}{z_1 - z_1'} \right] \quad (\text{II.26})$$

The angle of rotation of the cross-sectional ellipse (ϕ_c) toward the center of the braid is (see Figures 9 and 10):

$$\phi_c = \tan^{-1} \left[\frac{\sqrt{(W_x^2 + W_y^2)}}{W_z} \sin(\theta - \tan^{-1}(W_x/W_y)) \right] \quad (\text{II.27})$$

Therefore,

$$\alpha_c = \gamma_c + \phi_c \quad (\text{II.28})$$

Angles (α_c) and (α_c') are then inserted into (II.22) to find r_o and r_o' of the right-top and right-bottom strand. The jamming or interpenetration condition occurs according to (II.25).

The information about orientation of the spatial curve formed by the strand axes can be organized in table form (e.g. Table 3). Two additional pieces of information provided by the table are curvature (GC) and geometric torsion (GT). They have been given to complete the description of the helical model with a sinusoidally varying radius. Curvature is indicative of the sharpness of the bends at different stations along the leg of a unit trellis. Geometric torsion is a measure of the curve's departure from

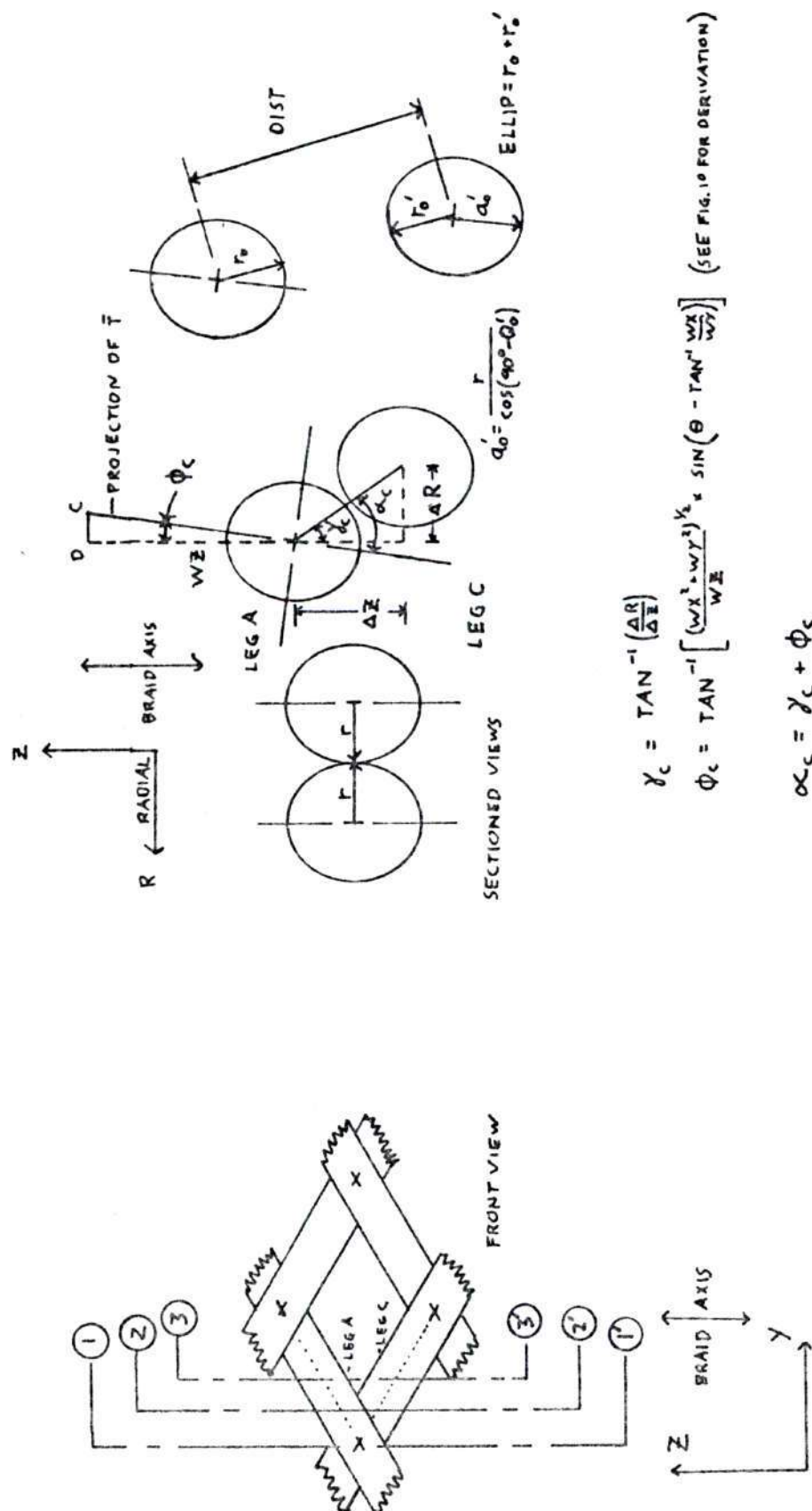


FIGURE 9. FABRIC-WALL SECTIONS OF A STRAND INTERSECTION AT DIFFERENT θ (COMPRESSIVE JAMMING TEST).

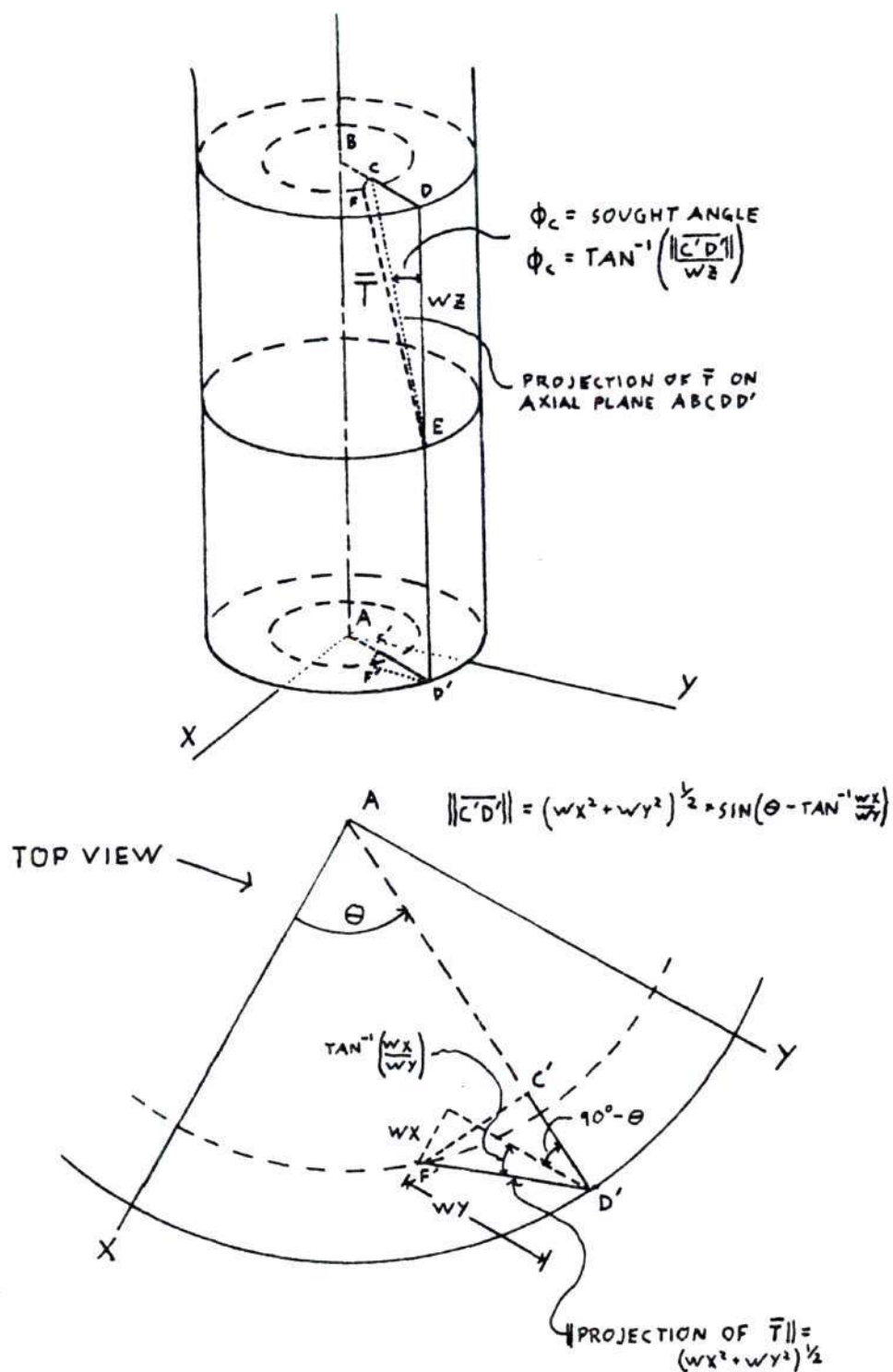


FIGURE 10. DERIVATION OF ORIENTATION ANGLE (ϕ_c) OF THE PROJECTED ELLIPSE MAJOR AXIS.

the plane, its "spatiality". The equations necessary for the calculation of these two quantities are listed in Appendix A. For a more detailed discussion on the textile application of these concepts see [6].

The jamming tests so far described check only for the inter-penetration of one configuration of strand interlacing. For a given braid with braid constants L_0 , n , and d , only one combination of D and Q_1 has been checked. Since it cannot be known apriori which particular combinations to test, the whole range of possible diameters and helix angles must be examined to find one extensive and one compressive jam point. The procedure is made more efficient by using a single set of tests to find jamming values for a whole set of braids with fixed n and d , varying L_0 . The curve formed from this jamming data is called the "jamming envelope" (see Figure 13). The zone to the left of the envelope is an area of theoretically impossible braid formation. The deformation curves of braids with particular L_0 are found on the right-hand side.

The flow of information and the iterative procedures used in the computer program subroutine which generates the jamming envelope is charted in Figure 12. For a given braid pattern with n number of strands per set and a certain strand diameter, d , the subroutine starts with a maximum helix angle and maximum braid diameter. It steps up trellis

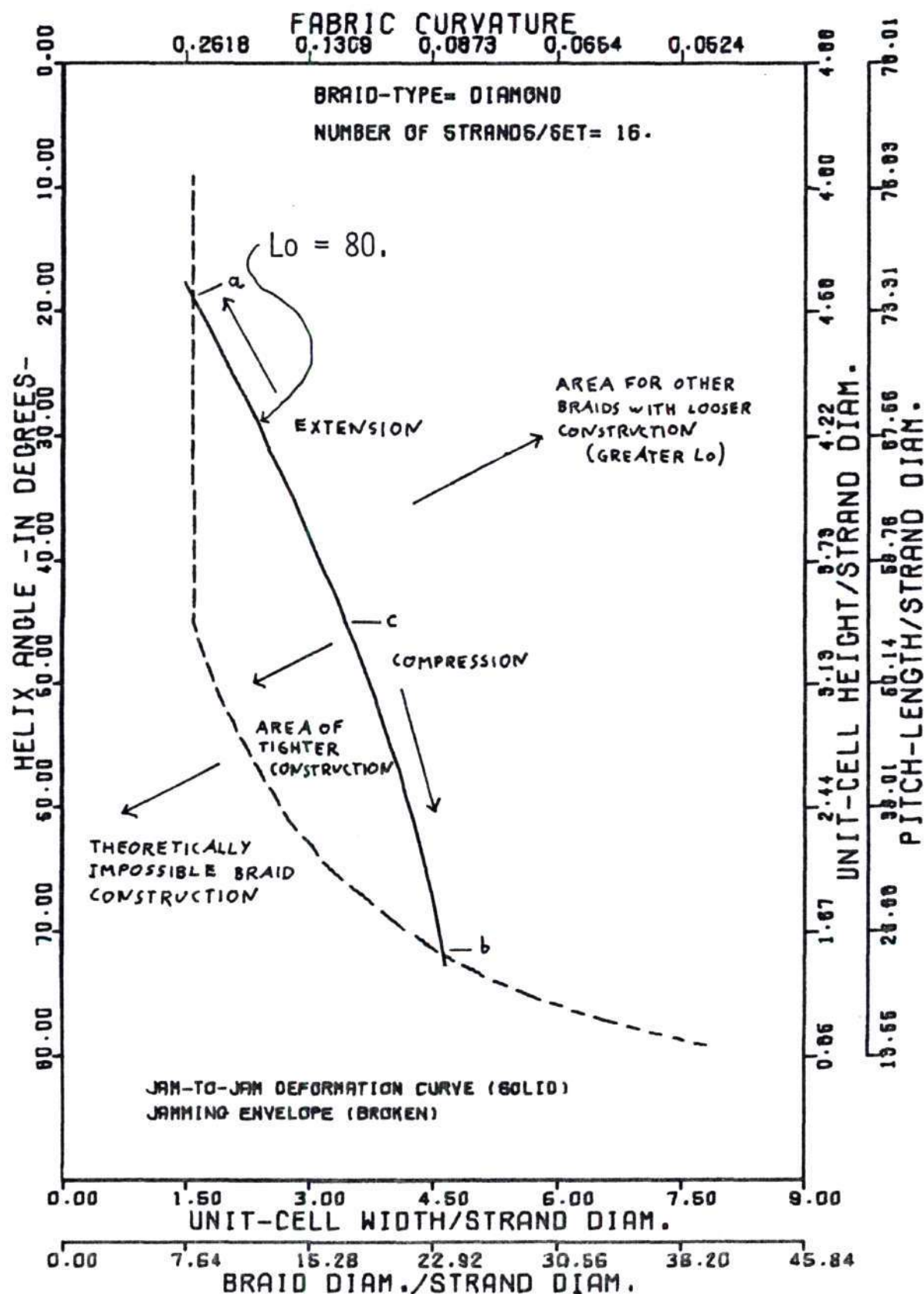
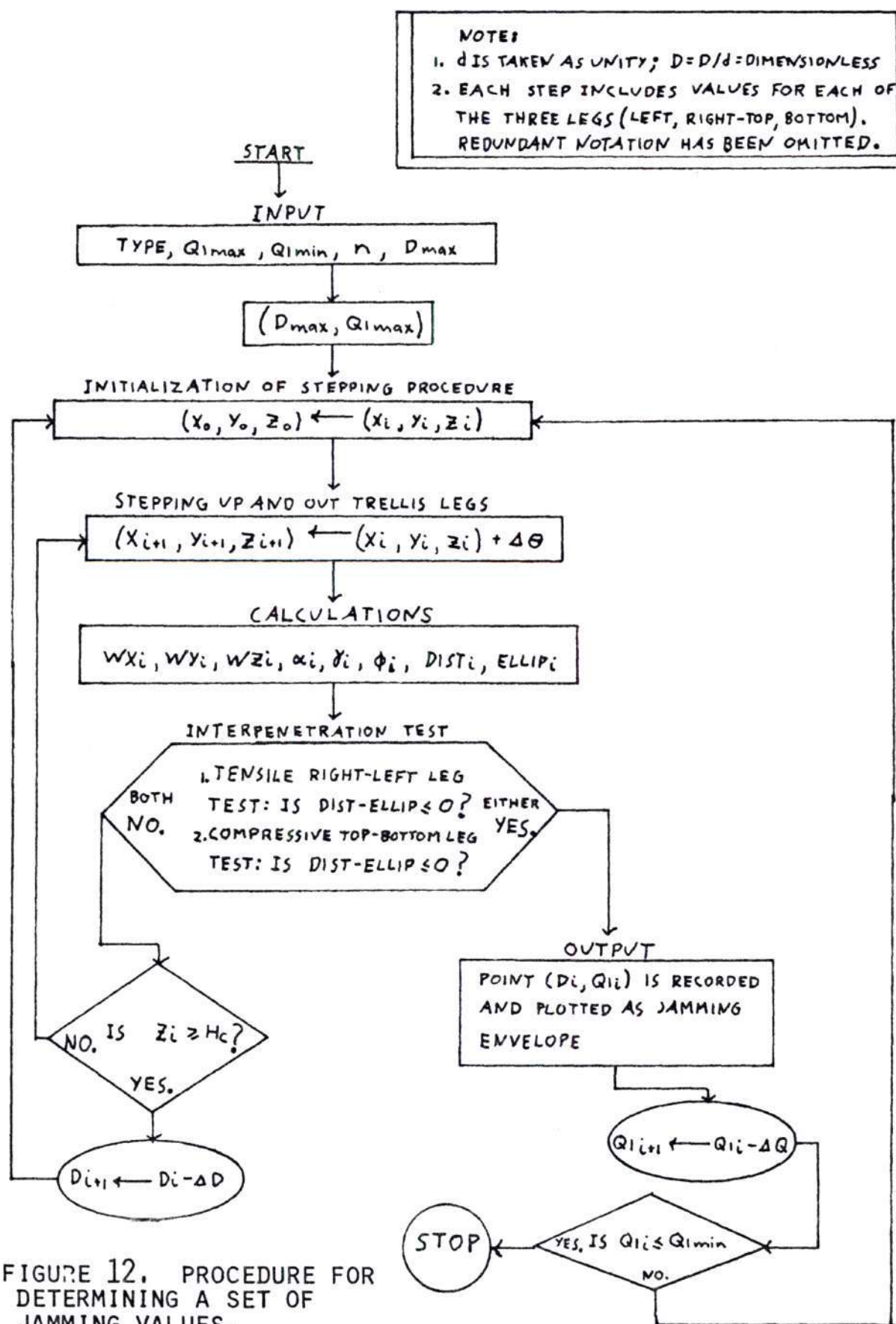


FIGURE 13. TYPICAL DIAMOND JAMMING ENVELOPE.

Table i. Between-Jam Deformation of Diamond Braid.

JAM-TO-JAM BRAID DEFORMATION CURVE										JAM ENVELOPE		CRIMP-EFFECT
TYPE = 1.										MODE = 1		
CONDITION	Q1	H	D	FK	(A ₀)	HC	WC	WC	D	HC	1-L1/L0	
JAMMED	3.0	77.0221	3.4931	.5151	5.0000	4.8139	.7624		7.9915	1.5672	.025222	
JAMMED	11.0	76.5499	4.7364	.4223	5.0000	4.7844	.9300		7.9915	1.5672	.025217	
JAMMED	13.0	75.9844	5.5839	.3582	5.0000	4.7490	1.0964		7.9915	1.5672	.025212	
JAMMED	15.0	75.3283	6.4246	.3113	5.0000	4.7079	1.2615		7.9915	1.5672	.025205	
JAMMED	17.0	74.5766	7.2576	.2756	5.0000	4.6610	1.4250		7.9915	1.5672	.025198	
	19.0	73.7361	8.0817	.2475	5.0000	4.6085	1.5868		7.9915	1.5672	.025190	
	21.0	72.8057	8.8960	.2248	5.0000	4.5504	1.7467		7.9915	1.5672	.025181	
	23.0	71.7887	9.6994	.2062	5.0000	4.4867	1.9045		7.9915	1.5672	.025172	
	25.0	70.6903	10.4911	.1900	5.0000	4.4175	2.0599		7.9915	1.5672	.025162	
	27.0	69.4877	11.2700	.1775	5.0000	4.3430	2.2129		7.9915	1.5672	.025151	
	29.0	68.2106	12.0352	.1662	5.0000	4.2632	2.3631		7.9915	1.5672	.025140	
	31.0	66.8503	12.7858	.1564	5.0000	4.1791	2.5105		7.9915	1.5672	.025128	
	33.0	65.4085	13.5208	.1479	5.0000	4.0890	2.6542		7.9915	1.5672	.025116	
	35.0	63.8971	14.2393	.1405	5.0000	3.9929	2.7959		8.0841	1.5673	.025103	
	37.0	62.2878	14.9406	.1339	5.0000	3.8930	2.9336		8.0841	1.5673	.025090	
	39.0	60.6126	15.6236	.1280	5.0000	3.7893	3.0677		8.0841	1.5673	.025077	
	41.0	58.9835	16.2877	.1229	5.0000	3.6790	3.1981		8.0841	1.5673	.025063	
	43.0	57.3027	16.9319	.1181	5.0000	3.5652	3.3246		8.0841	1.5673	.025050	
	45.0	55.5523	17.5555	.1139	5.0000	3.4470	3.4470		8.0841	1.5673	.025035	
	47.0	53.7446	18.1578	.1101	5.0000	3.3247	3.5653		8.5221	1.6733	.025023	
	49.0	51.8721	18.7379	.1067	5.0000	3.1993	3.6792		9.1412	1.7949	.025009	
	51.0	49.9672	19.2952	.1037	5.0000	3.0690	3.7986		9.7053	1.9056	.024995	
	53.0	48.0424	19.8290	.1009	5.0000	2.9339	3.9334		10.5164	2.0649	.024983	
	55.0	46.0944	20.3387	.0983	5.0000	2.7963	3.9935		11.2700	2.2129	.024969	
	57.0	44.1237	20.8236	.0959	5.0000	2.6552	4.0887		12.1399	2.3637	.024957	
	59.0	42.1292	21.2831	.0940	5.0000	2.5110	4.1789		13.1552	2.5030	.024945	
	61.0	39.1178	21.7167	.0921	5.0000	2.3636	4.2641		14.3560	2.6188	.024933	
	63.0	36.1441	22.1238	.0904	5.0000	2.2134	4.3440		15.4110	2.7259	.024922	
	65.0	32.9672	22.5040	.0889	5.0000	2.0605	4.4187		17.0850	2.8259	.024911	
	67.0	30.4801	22.8568	.0875	5.0000	1.9050	4.4979		18.6004	2.9222	.024900	
	69.0	27.9558	23.1817	.0863	5.0000	1.7472	4.5517		20.4107	3.0076	.024891	
	71.0	25.3974	23.4783	.0852	5.0000	1.5873	4.6100		22.6114	3.0797	.024882	
JAMMED	73.0	22.8079	23.7464	.0842	5.0000	1.4255	4.6626		25.3441	3.1463	.024874	
JAMMED	75.0	20.1906	23.9854	.0834	5.0000	1.2619	4.7095		28.8281	3.2044	.024867	
JAMMED	77.0	17.5487	24.1953	.0827	5.0000	1.0968	4.7507		33.4225	3.2525	.024861	
JAMMED	79.0	14.8853	24.3756	.0820	5.0000	.9303	4.7861		39.7592	3.2967	.024855	
JAMMED	81.0	12.2038	24.5263	.0815	5.0000	.7627	4.8157		49.0606	3.3330	.024851	

ALL LENGTH DIMENSIONS ARE DIVIDED BY STRAND DIAMETER(=1) TO MAKE THEM DIMENSIONLESS.
 ABBREVIATIONS USED ARE EXPLAINED IN THE LIST OF SYMBOLS IN CHAPTER 2.



legs "A" and "B" for extensive jamming and out leg "C" (and "A") for compressive jamming. Each step entails the comparison of strand inter-axial distance with the distance required by the inclined and rotated strand cross-sections. If there is no jamming when the extremities of the trellis legs are reached, the diameter of the braid is decreased by a set increment and the cycle starts again. It repeats as many times as necessary to induce jamming. When there is jamming, point (D_i, Q_{li}) is recorded and the helix angle is decreased, relieving the jam. The test then returns back to stepping the legs and decreasing the diameter. The whole process is repeated until the desired range of helix angles has been covered.

Jamming In Regular Braids

The jamming phenomenon in regular braids is considerably more complex since "regular" structure is more varied than diamond. If a distance of strand between interlacing points is considered as a unit segment of strand, a regular braid consists of half alternating and half non-alternating strand segments. Diamond braids are entirely alternating. Compared to a diamond braid fabric of similar dimensions a regular braid has half the number of interlacings making it a less densely packed structure. It requires slightly less strand arc-length to form one pitch (see equation II.16). Its somewhat "looser" structure should be expected to manifest more extreme jamming

geometries.

A closer look at the "regular" structure is the key to understanding its jamming mechanism. Although elemental diamond units can be found in the regular lattice structure they are not a convenient unit for analysis, nor are they truly representative. In weave terminology, the official full pattern repeat for the analogue of regular braid, 2/2 twill, is a 4 x 4 cell. It is shown in Figure 11 though it is too unwieldy and redundant to be used as a unit of analysis. For dimensional analysis of the regular braid cell dimensions W_c , H_c , and l_o , as shown in Figure 11 will be used.

For jamming analysis attention is to be focussed on an interlacing of four half-unit segments. The alternating or non-alternating nature of these half-segments determines the distinctive geometry of regular jamming. (A non-alternating segment maintains a constant In Figure 11 the array of numbers placed around each intersection count the number of alternating half-segments in each strand pair. Observe the longitudinal orientation of the "1"-pairs compared to the transverse distribution of the "0"s and "2"s. All regular braids that have been observed during this study have been of this variety. Although woven twill jargon has right- and left-hand designations, they are absent from braid parlance. Since right and left directions lose their meaning when discussing braids which are tilted

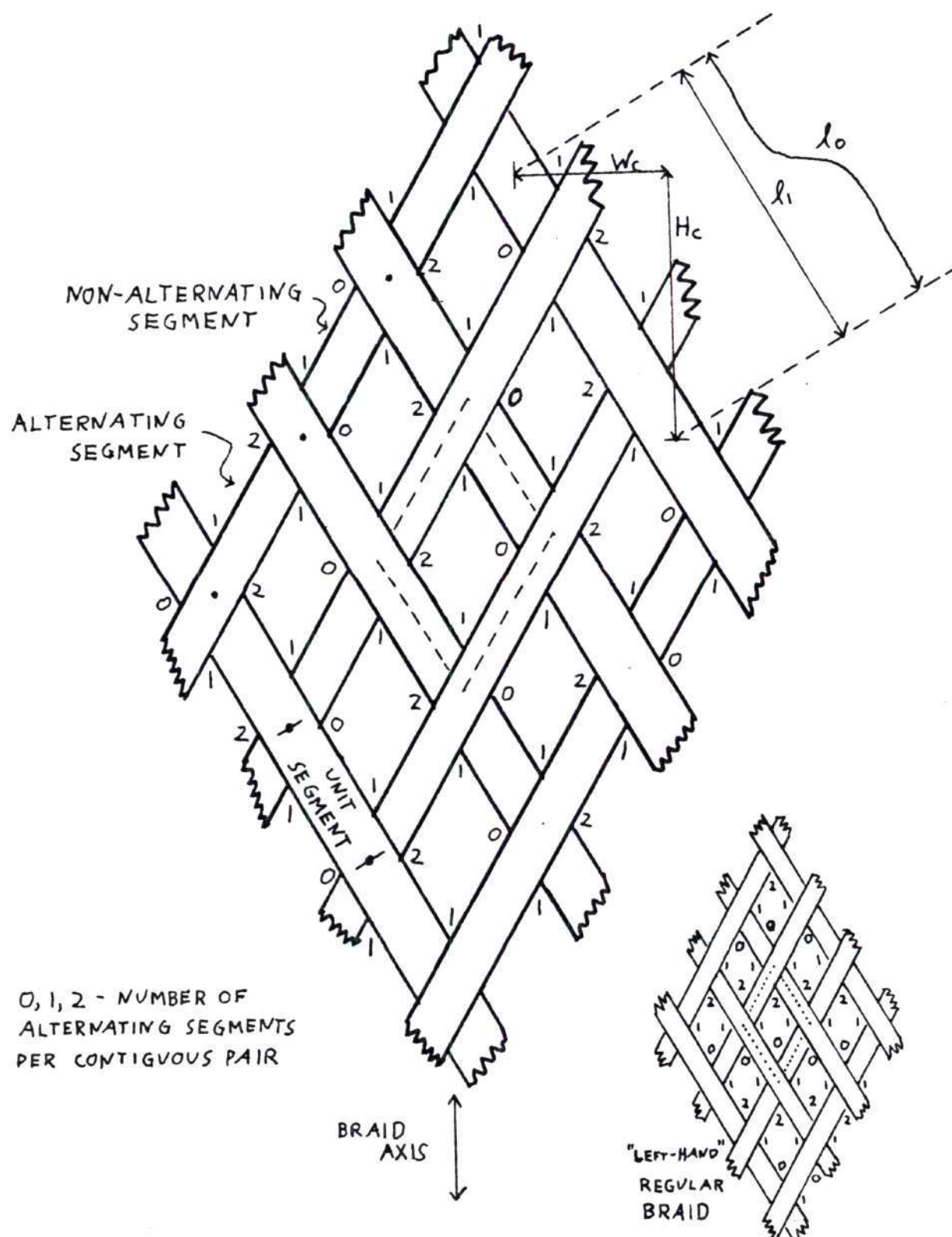


FIGURE 11.

R.H. REGULAR BRAID LATTICE STRUCTURE OF ONE FULL PATTERN REPEAT.

half-way in the middle, we will adopt the convention that the predominant pattern is the right-handed one, i.e. the structure which as one moves up either parallel set of strands, the phase of the crimp wave advances one interlacing per strand (see Figure 11).

The greater the number of alternating half-segments in a particular pair, the sooner their pivoting together is impaired. In the compressive jamming of the right-hand, regular braids although one of the transverse pairs has no alternating half-segments and therefore no reason to jam, jamming is initiated according to the geometry of the opposite "2"-pair. Transverse, compressive jamming in this case still occurs earlier than in the longitudinal, tensile direction with the "1"-pairs. Quantitative evidence for this effect can be seen in the comparison between Table 6a and Table 7b where jamming helix angles for a longitudinal "1"-pair and transverse "2"-pair are shown. Qualitatively, the asymmetry created by the right- and left-handed effects can be seen in the jamming envelopes of Figure 14, and concomitant Tables 2a and 2b.

Left-handed regular jamming is considered using an alternating "2"-pair in the longitudinal direction and a "1"-pair in the transverse. Vector analyses of incipient, left-hand, extensive jamming, compressive jamming, and jamming at a middle value, $Q_1=45$ degrees, can be seen in Tables 3a-b, 4a-b, and 5a-b. Comparison tables for

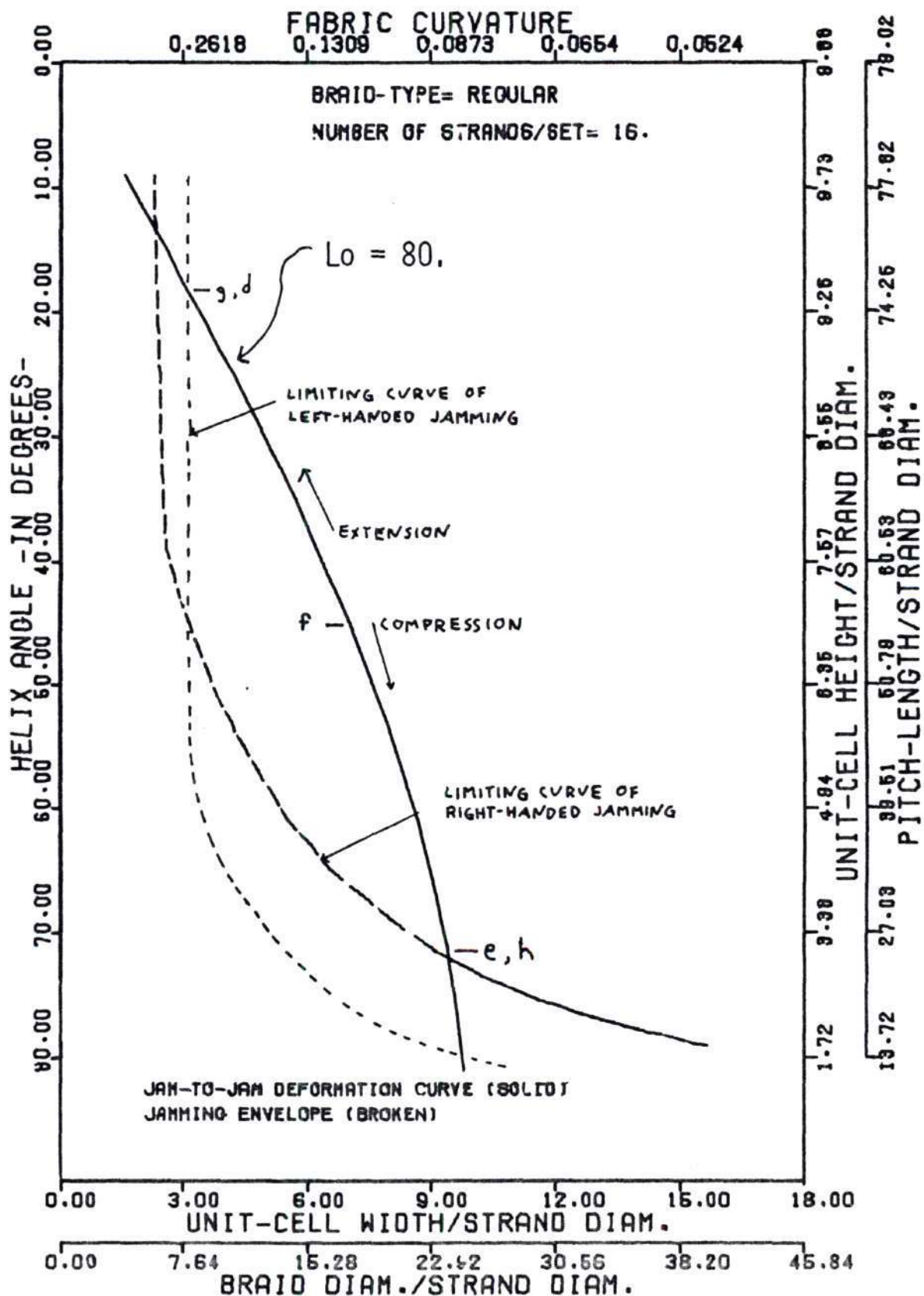


FIGURE 14. RIGHT- AND LEFT-HANDED JAMMING ENVELOPES.

Table 2a. Between-Jam Deformation of Right-Hand Regular Braid.

JAM-TO-JAM BRAID DEFORMATION CURVE										JAM ENVELOPE		CRIMP-EFFECT	
CONDITION	Q1	H	D	FK	(r_0)	HC	HC	ARC-LENGTH/PITCH=	80.000	MODE=	1		
TYPE=	2.	NUMBER OF STRANDS/SET=				16.	ARC-LENGTH/PITCH=				80.000	MODE=	1
JAMMED	3.0	78.0310	3.0340	.5084	10.0000	9.7539	1.5449	5.7612	2.2703	1-11/10			
JAMMED	11.0	77.5523	4.7994	.4108	10.0000	9.6540	1.3847	5.7312	2.2703	.012454			
JAMMED	13.0	70.9752	5.5570	.3535	10.0000	9.6224	2.2215	5.8349	2.2913	.012452			
	15.0	70.3123	6.5687	.3073	10.0000	9.5390	2.5560	5.8394	2.3128	.012449			
	17.0	75.5525	7.3525	.2720	10.0000	9.4441	2.8473	5.8394	2.3128	.012446			
	19.0	74.7656	8.1874	.2443	10.0000	9.3376	3.2452	5.9451	2.3366	.012443			
	21.0	73.7577	9.0123	.2219	10.0000	9.2197	3.5391	6.0719	2.3569	.012439			
	23.0	72.7250	9.8262	.2035	10.0000	9.0909	3.8587	6.3396	2.3796	.012434			
	25.0	71.6038	10.5242	.1892	10.0000	8.9535	4.1737	6.6185	2.4027	.012430			
	27.0	70.5292	11.172	.1752	10.0000	8.7934	4.4935	6.8185	2.423	.012425			
	29.0	69.4510	12.1923	.1640	10.0000	8.6376	4.7979	6.8186	2.4263	.012420			
	31.0	67.7225	12.3526	.1544	10.0000	8.4653	5.1265	6.3399	2.4504	.012414			
	33.0	66.2615	13.6971	.1460	10.0000	8.2927	5.3789	6.3024	2.4750	.012408			
	35.0	64.7198	14.4249	.1386	10.0000	8.1300	5.6647	6.3562	2.5000	.012403			
	37.0	63.0932	15.1352	.1321	10.0000	7.9874	5.9436	6.4113	2.5256	.012396			
	39.0	61.4018	15.8271	.1264	10.0000	7.8672	6.2153	6.477	2.5516	.012390			
	41.0	59.6295	16.4936	.1212	10.0000	7.7537	6.4794	6.9270	2.5772	.012384			
	43.0	57.7645	17.1321	.1166	10.0000	7.6231	6.7356	7.4169	2.5926	.012377			
	45.0	55.8631	17.7637	.1125	10.0000	7.4936	6.9836	7.815	3.0951	.012370			
	47.0	53.8637	18.3936	.1087	10.0000	7.357	7.2232	8.5221	3.3466	.012364			
	49.0	51.8245	18.9612	.1054	10.0000	7.2231	7.4539	9.1412	3.5897	.012357			
	51.0	49.7242	19.5456	.1023	10.0000	7.0933	7.6755	9.7353	3.8113	.012350			
	53.0	47.5512	20.0462	.0996	10.0000	6.9439	7.8878	10.5164	4.1294	.012344			
	55.0	45.3223	20.5623	.0971	10.0000	6.7930	8.0705	11.2700	4.4237	.012337			
	57.0	43.0341	21.0933	.0948	10.0000	6.6433	8.2833	12.1399	4.7673	.012331			
	59.0	40.6935	21.5597	.0928	10.0000	6.4969	8.4601	13.1552	5.1661	.012325			
	61.0	39.3072	21.9578	.0909	10.0000	6.3484	8.6185	14.3500	5.6376	.012319			
	63.0	35.8722	22.4100	.0892	10.0000	6.1940	8.8004	15.4410	6.0519	.012313			
	65.0	33.3935	22.7950	.0877	10.0000	6.0422	8.9516	17.0850	6.7093	.012308			
	67.0	30.8741	23.1522	.0864	10.0000	5.8933	9.0919	18.6004	7.3043	.012303			
	69.0	28.3170	23.4812	.0852	10.0000	5.7536	9.2210	20.4137	8.0153	.012297			
	71.0	25.7254	23.7816	.0841	10.0000	5.6215	9.3390	22.6114	8.8795	.012293			
JAMMED	73.0	23.1024	24.0529	.0831	10.0000	5.4968	9.4456	25.3441	9.9526	.012289			
JAMMED	75.0	20.4512	24.2950	.0823	10.0000	5.3564	9.5406	28.8281	11.3208	.012285			
JAMMED	77.0	17.7751	24.5075	.0816	10.0000	5.2219	9.6241	33.4225	13.1250	.012281			
JAMMED	79.0	15.0773	24.6901	.0810	10.0000	5.0847	9.6958	39.7592	15.6134	.012278			
JAMMED	81.0	12.3612	24.8426	.0805	10.0000	4.9551	9.7557	49.0606	19.2661	.012275			

ALL LENGTH DIMENSIONS ARE DIVIDED BY STRAND DIAMETER(=1) TO MAKE THEM DIMENSIONLESS.
 ABBREVIATIONS USED ARE EXPLAINED IN THE LIST OF SYMBOLS IN CHAPTER 2.

Table 2b. Between-Jam Deformation of Left-Hand Regular Braid.

JAM-TO-JAM BRAID DEFORMATION CURVE										JAM ENVELOPE		CRIMP-EFFECT
CONDITION	Q1	H	D	FK	(d _h)	NUMBER OF STRANDS/SET= 16.		ARC-LENGTH/PITCH= 80.000	MODE= 1			
						TYPE= 3.	TYPE= 3.			O	HC	
JAMMED	3.0	76.0310	3.9340	.5084	10.0000			9.7539	1.8949	7.9815	3.1343	1-L1/L0
JAMMED	11.0	77.5523	4.7984	.4168	10.0000			9.5940	1.8949	7.9815	3.1343	.012454
JAMMED	13.0	76.9792	5.6570	.3535	10.0000			9.5224	2.2215	7.9815	3.1343	.012452
JAMMED	15.0	76.3123	6.5087	.3073	10.0000			9.5390	2.5560	7.9815	3.1343	.012449
JAMMED	17.0	75.5525	7.3525	.2720	10.0000			9.4441	2.8873	7.9815	3.1343	.012445
JAMMED	19.0	74.7006	8.1874	.2443	10.0000			9.3776	3.2152	7.9815	3.1343	.012443
	21.0	73.7577	9.0123	.2219	10.0000			9.2197	3.5391	7.9815	3.1343	.012434
	23.0	72.7250	9.8262	.2035	10.0000			9.0906	3.8527	7.9815	3.1343	.012430
	25.0	71.6038	10.6282	.1892	10.0000			8.9505	4.1737	7.9815	3.1343	.012425
	27.0	70.3952	11.4172	.1752	10.0000			8.7994	4.4935	7.9815	3.1343	.012420
	29.0	69.1110	12.1923	.1640	10.0000			8.6376	4.7879	7.9815	3.1343	.012414
	31.0	67.7225	12.9526	.1544	10.0000			8.4653	5.0865	7.9815	3.1343	.012408
	33.0	66.2615	13.6971	.1460	10.0000			8.2827	5.3788	7.9815	3.1343	.012403
	35.0	64.7198	14.4249	.1386	10.0000			8.0960	5.6647	8.0841	3.1746	.012395
	37.0	63.0992	15.1352	.1321	10.0000			7.9074	5.9436	8.0841	3.1746	.012390
	39.0	61.4018	15.8271	.1264	10.0000			7.7152	6.2153	8.0841	3.1746	.012384
	41.0	59.6295	16.4996	.1212	10.0000			7.5197	6.4794	8.0841	3.1746	.012377
	43.0	57.7845	17.1521	.1166	10.0000			7.3231	6.7356	8.0841	3.1746	.012370
	45.0	55.9694	17.7837	.1125	10.0000			7.1256	6.9836	8.0841	3.1746	.012364
	47.0	53.4857	18.3936	.1087	10.0000			6.9267	7.2232	8.0841	3.1746	.012357
	49.0	51.8265	18.9812	.1054	10.0000			6.7266	7.4539	8.0841	3.1746	.012350
	51.0	49.7242	19.5456	.1023	10.0000			6.5255	7.6755	8.0841	3.1746	.012344
	53.0	47.5512	20.0662	.0996	10.0000			6.3239	7.8878	8.0841	3.1746	.012337
	55.0	45.3203	20.6023	.0971	10.0000			6.1215	8.0941	8.0841	3.1746	.012331
	57.0	43.0341	21.0933	.0948	10.0000			5.9179	8.2833	8.0841	3.1746	.012325
	59.0	40.6955	21.5597	.0928	10.0000			5.7133	8.4661	8.1893	3.2159	.012319
	61.0	38.3072	21.9978	.0909	10.0000			5.5069	8.6385	8.7594	3.4798	.012313
	63.0	35.8722	22.4100	.0892	10.0000			5.2994	8.8004	9.4148	3.6972	.012308
	65.0	33.3935	22.7950	.0877	10.0000			5.0916	8.9516	10.1762	3.9962	.012303
	67.0	30.8741	23.1522	.0864	10.0000			4.8840	9.0919	11.0716	4.3478	.012297
	69.0	28.3110	23.4812	.0852	10.0000			4.6766	9.2210	12.1399	4.7673	.012293
	71.0	25.7254	23.7816	.0841	10.0000			4.4694	9.3390	13.4362	5.2764	.012289
	73.0	23.1024	24.0529	.0831	10.0000			4.2626	9.4456	15.0425	5.9072	.012285
	75.0	20.4512	24.2950	.0823	10.0000			4.0564	9.5466	17.0850	6.7093	.012281
	77.0	17.7751	24.5075	.0816	10.0000			3.8509	9.6241	19.1670	7.5269	.012278
	79.0	15.0773	24.6901	.0810	10.0000			3.6467	9.6958	22.6114	8.4795	.012275
JAMMED	81.0	12.3612	24.8426	.0805	10.0000			3.4431	9.7557	31.7365	12.4629	.012273

ALL LENGTH DIMENSIONS ARE DIVIDED BY STRAND DIAMETER(=1) TO MAKE THEM DIMENSIONLESS.
 ABBREVIATIONS USED ARE EXPLAINED IN THE LIST OF SYMBOLS IN CHAPTER 2.

right-hand jamming geometries are given in Tables 6a-b, 7a-b, and 8a-b.

The details of the calculation of regular jamming are identical to those of diamond braids, the non-alternating segments give a slightly different series of coordinates and direction cosines which are simpler to calculate since the arc of constant radius is part of an ordinary helix.

There is one exception to this observation of similarity. When considering a "typical" regular ("l"-pair) interlacing, there is a geometric and therefore a jamming difference which depends on whether the constant radius arc occupies the maximum or minimum radial position. There are then two distinct "l"-pair geometries which manifest themselves in slightly different jamming distances (JD). These can be compared in Tables 8a (minimum radius) and 8c (maximum radius). It is therefore necessary to introduce an additional iteration in the "regular" jamming test procedure to check for inter-penetration of the second type of "l"-pair.

Before leaving the subject of regular jam phenomena, we must critically evaluate a key initial assumption of the regular model, that of equidistance of adjacent concurrent strands. As previously mentioned, the two ends of a unit strand segment of regular braid appear as they would be subject to centering forces trying to move them toward the center of their respective over- and under-lapping

sinusoidal troughs. Because the centering tendencies at the two ends are in opposite directions counteracting each other, and because due to the general slackness of the between-jam deformation zone the forces are weak, they probably do not have an important bearing on the geometric model in question. For larger forces that might start to mount at the jamming point, the strand segments would most likely be bent sideways. The net result would be a crimping of the strand within the fabric plane. The helical model that has been presented deals with crimp normal to the fabric surface. Crimp within the fabric plane that is possibly exhibited around jamming in regular braids falls outside the scope of this thesis. For discussion and analysis of this in-plane crimp in a closely related fabric structure, i.e. 2/2 woven twill, refer to [7].

CHAPTER III

THEORETICAL RESULTS AND DISCUSSION

The work in Chapter II can be separated into two main categories: 1) the arc-length calculation for the axis of a crimped strand and 2) jamming predictions based on the vector description of the strand-helix with sinusoidally varying radius. To better illustrate certain trends the basic relationships from these categories have been manipulated into several different forms. Two additional relationships included for comparison purposes are arc-length as a function of the non-crimped helix-triangle, and arc-length and jamming predictions from Brunnschweiller's flat-cell model. The majority of plotted curves combine arc-length and jamming information. The "x" terminating a curve represents the limiting jam value which prevents it from proceeding into a region of impossible braid formation.

The changing dimensions of a deforming braid can be viewed either on the macroscopic level of pitch and braid diameter or the microscopic level of unit cell dimensions. The latter is the lowest common denominator possible for the analysis. It facilitates the comparison of braids of different strand number, n , though if one restricts himself

to this level there is a danger of losing sight of the original object of study. As a remedy most of the plots have been provided with dual axes. The values given by the multiple axes are different scalings of the original two axes. The purpose is to provide the greatest amount of readily accessible information. The theoretical results are presented in four groups:

Group 1- plots of absolute strand length versus unit-cell width for various helix angles,

Group 2- plots of strand length of the crimped helix relative to strand length given by a simple helix (a measure of crimp) vs. unit-cell width for various helix angles,

Group 3- joint plots of individual braid deformation curves and jamming envelope (Q_1 vs. D),

Group 4- vector analysis of a unit strand segment in tabular form.

Group 1- Absolute Strand Arc-Length

The values for this group of plots are direct calculations from the arc-length formula (Equation II.14). As one would expect for a given helix angle a larger lateral braid dimension requires a greater length. Figures 15, 16, and 17 present the strand-length curves for diamond braids of $n = 4$, 24, and 60. When these three plots which have been normalized for unit cell dimensions are superimposed, they

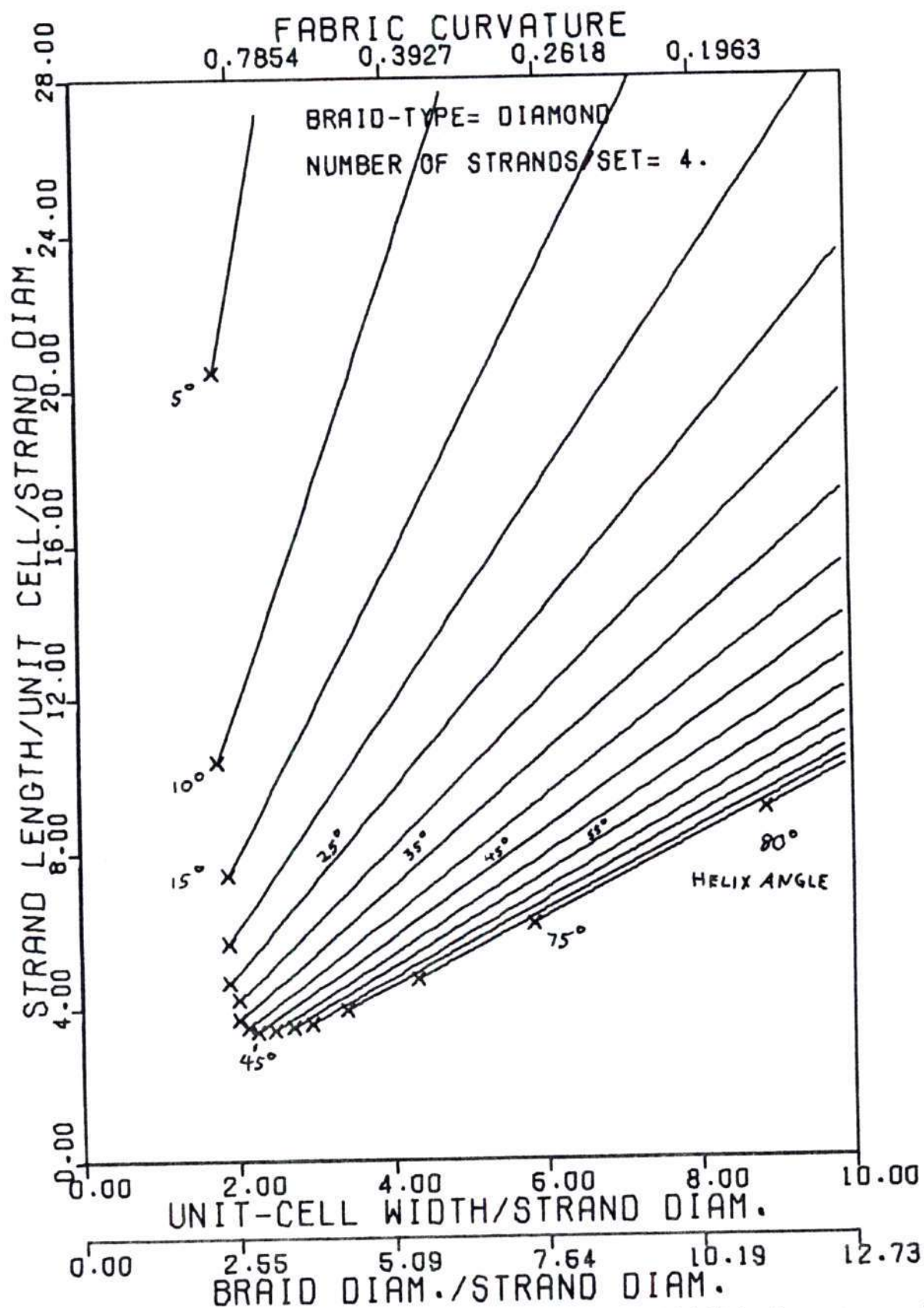


Figure 15. Unit Cell Strand Length vs. Unit Cell Width
(TYPE=1, n=4).

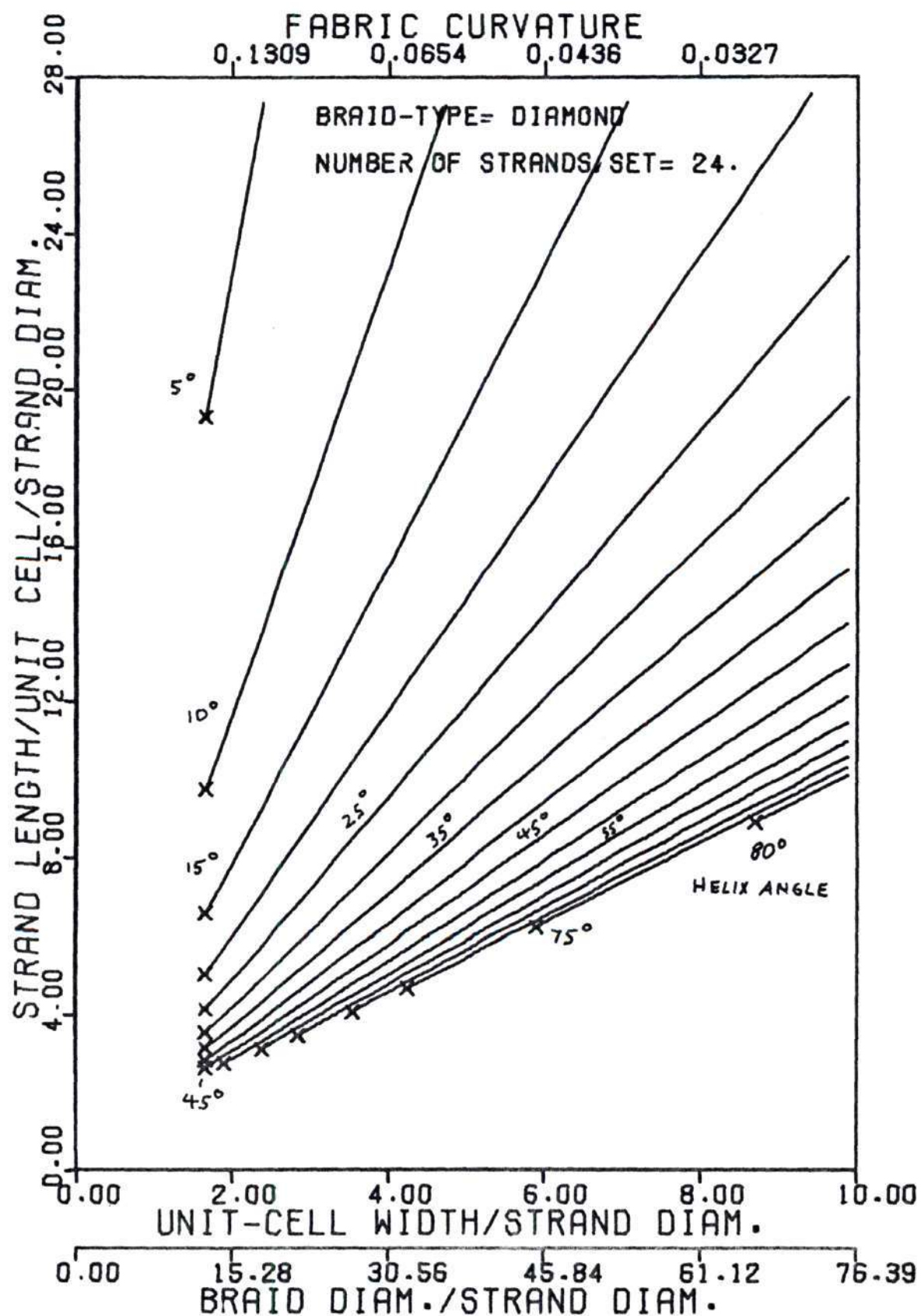


Figure 16. Unit Cell Strand Length vs. Unit Cell Width
(TYPE=1, n=24).

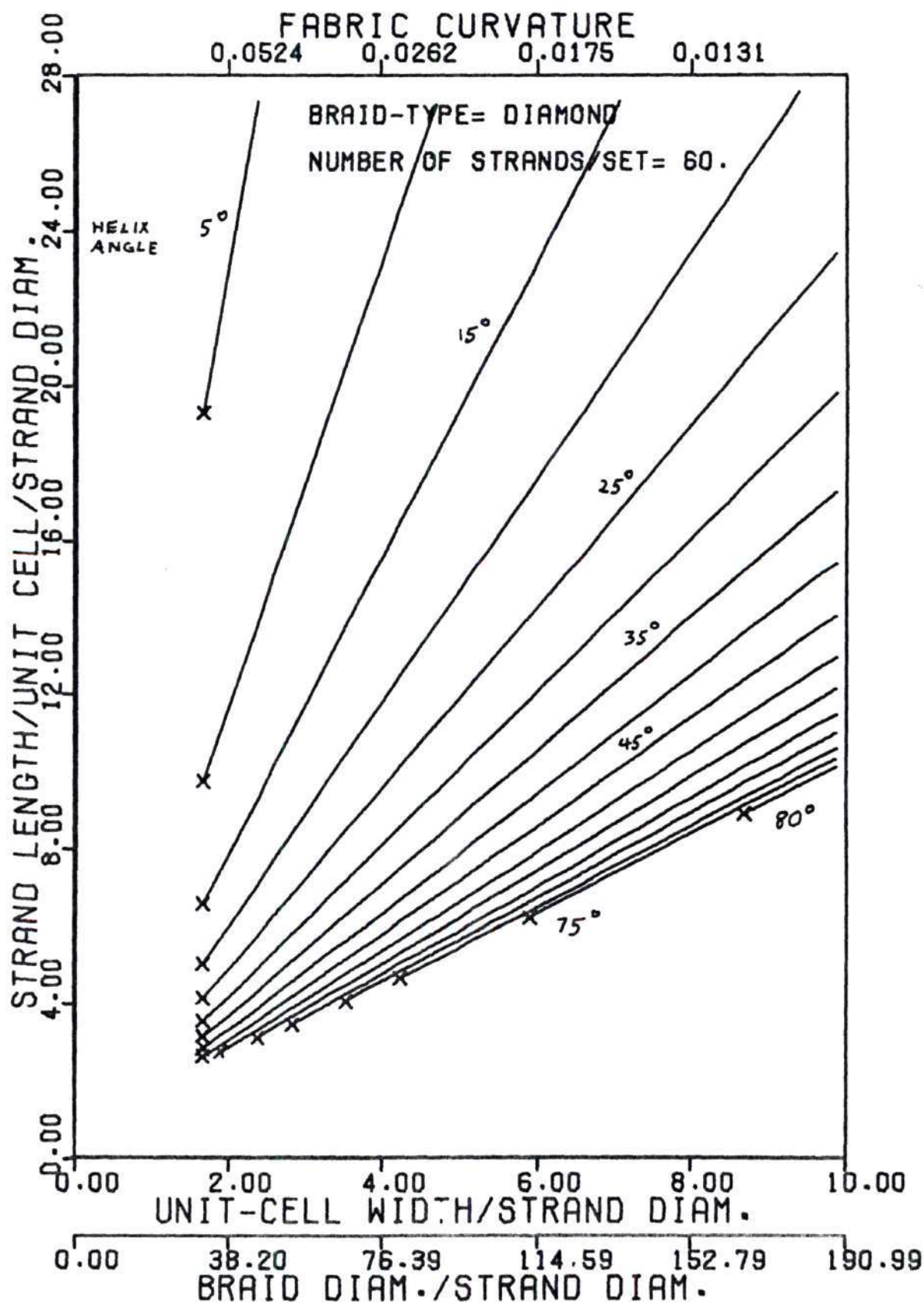


Figure 17. Unit Cell Strand Length vs- Unit Cell Width
(TYPE=1, n=60).

are almost indistinguishable with the exception of the jamming limits. As we anticipated, imposing curvature on the unit cell had no overall effect on the arc-length since the shorter path of the strand inner-segments compensate for the longer path of the outer ones. To confirm this hypothesis Brunnschweiler's arc-length formula was included in the computer program and an analogous plot made for the flat-cell model (Figure 18). If we ignore jamming, it too is nearly identical to the others. Taking another step back, if we make a similar plot of strand length given by the uncrimped helix-triangle (Figure 19), the difference found is no more than the width of the pen stroke. Where the similar arc-length curves for the crimped, flat, and uncrimped models do begin to diverge is for small unit-cell widths (W_c). However just as the divergence begins the curves are cut off due to jamming. This effect will be more visible in the second group of plots.

With respect to jamming, a considerable difference between models can be observed. The braids with smaller n , with greater curvature of the fabric wall, jam (extensively) at larger cell-widths (i.e. they jam earlier). The flat-cell model with no curvature jams later than the crimped helix model and the simple helix has no interlacings with which to jam at all.

The discussion of the effect of overall unit-cell curvature on jamming is one of very subtle differences.

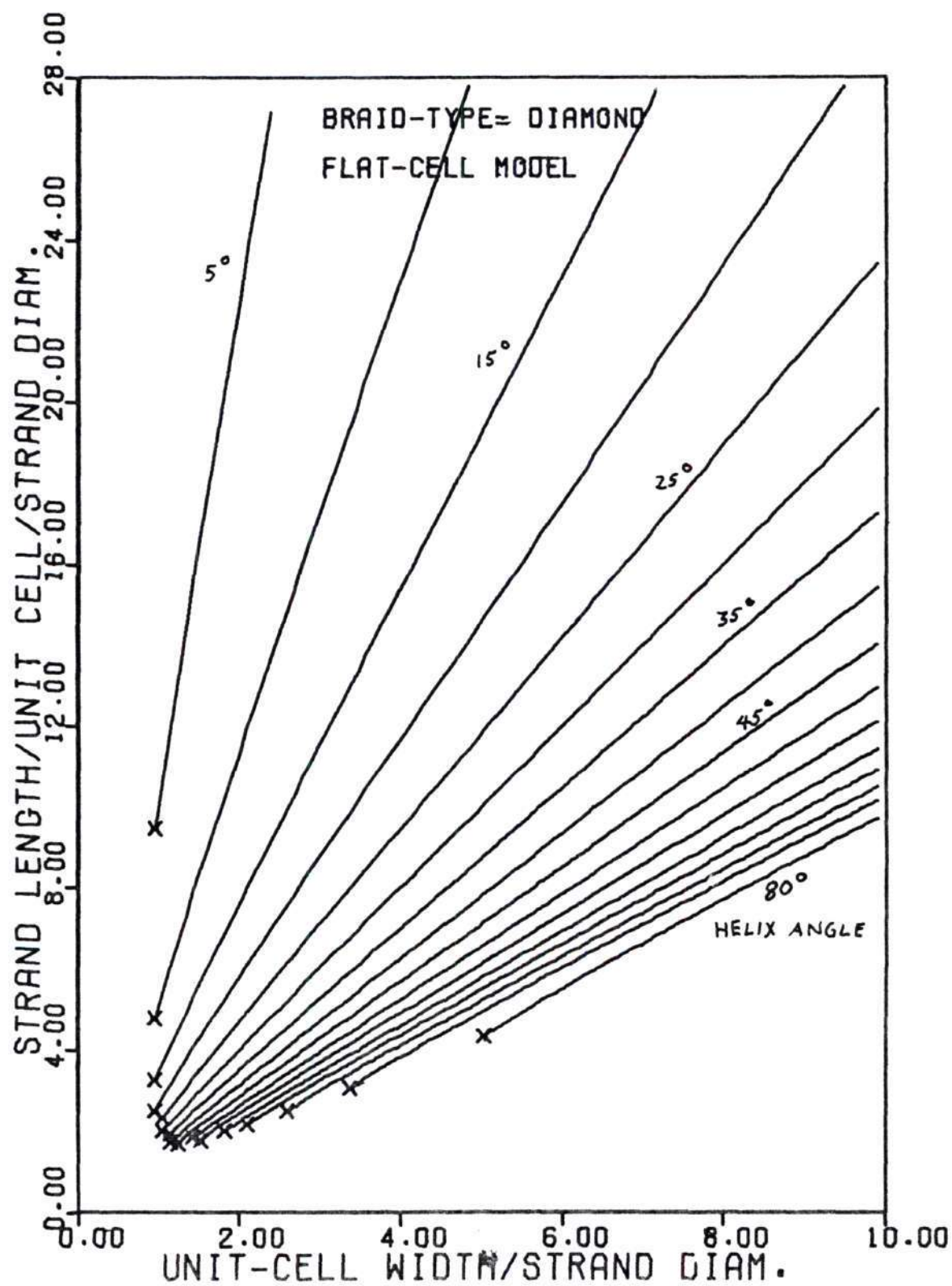


Figure 18. Unit Cell Strand Length vs. Unit Cell Width (Flat Cell Model)

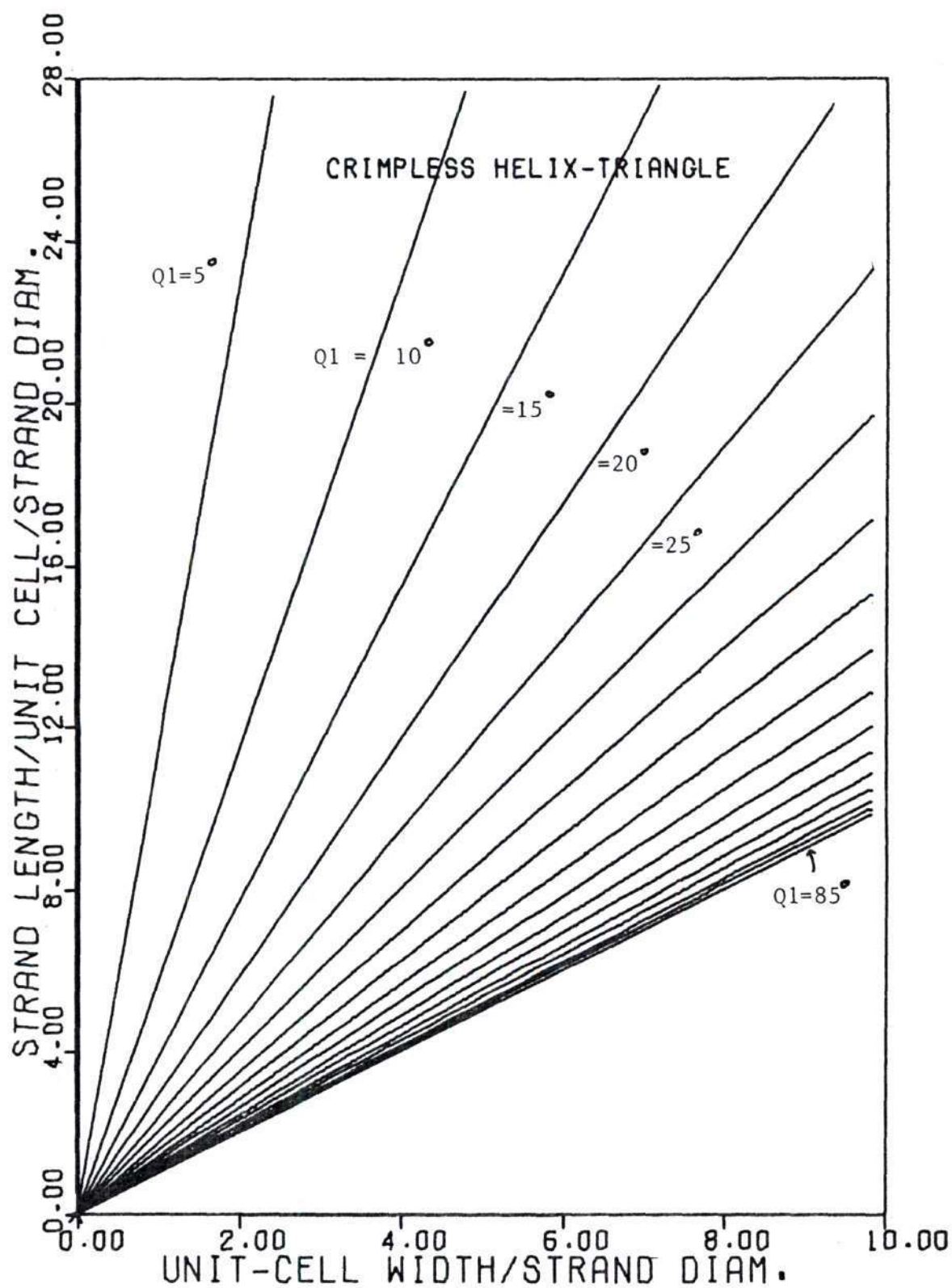


Figure 19. Unit Cell Strand Length vs. Cell Width (Helix-Triangle)

However the same jamming information on a macroscopic level can be quite helpful to, say, a practical-minded braid manufacturer. Taking the curves for helix-angle equals, say, 45 degrees from the braid plots of different n , and replotting them against a different scale with a different normalization yields Figure 20. From it a braid-maker, for braids of different n , can anticipate the smallest diameter braid that can be made with helix angle of 45 degrees. Figure 20 is a good illustration of the information generated by the type of analysis currently being undertaken compared to values gotten from the helix-triangle approach (broken line).

Group 2- Relative Strand Length, The Crimp-Effect

The degree to which the axis of a crimped helical strand departs from the nominal non-crimped helix is reflected in their length difference. The ratio of the different lengths or

$$\text{Crimp-Effect} = 1 - L_1/L_0 \quad (\text{III.1})$$

easily distinguishes between the various models. Figures 21, 22, and 23 illustrate that for small C_w , L_1 can differ from L_0 by as much as six percent ($n=4$) or ten percent ($n=24$). The amount of crimp for a given Q_1 is greater for

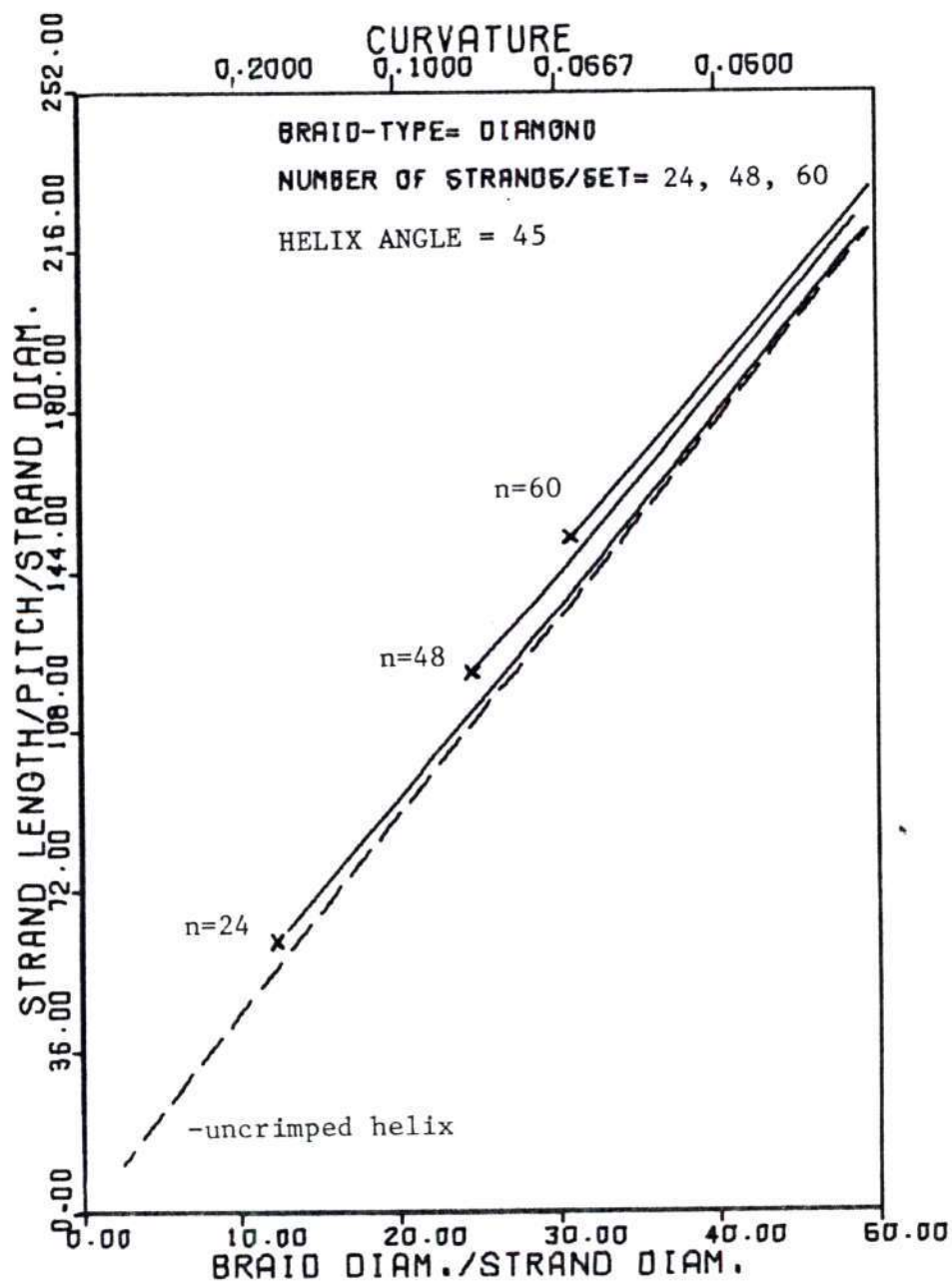


Figure 20. Strand Length at $Q_1=45$ for Different Strand Number, n .

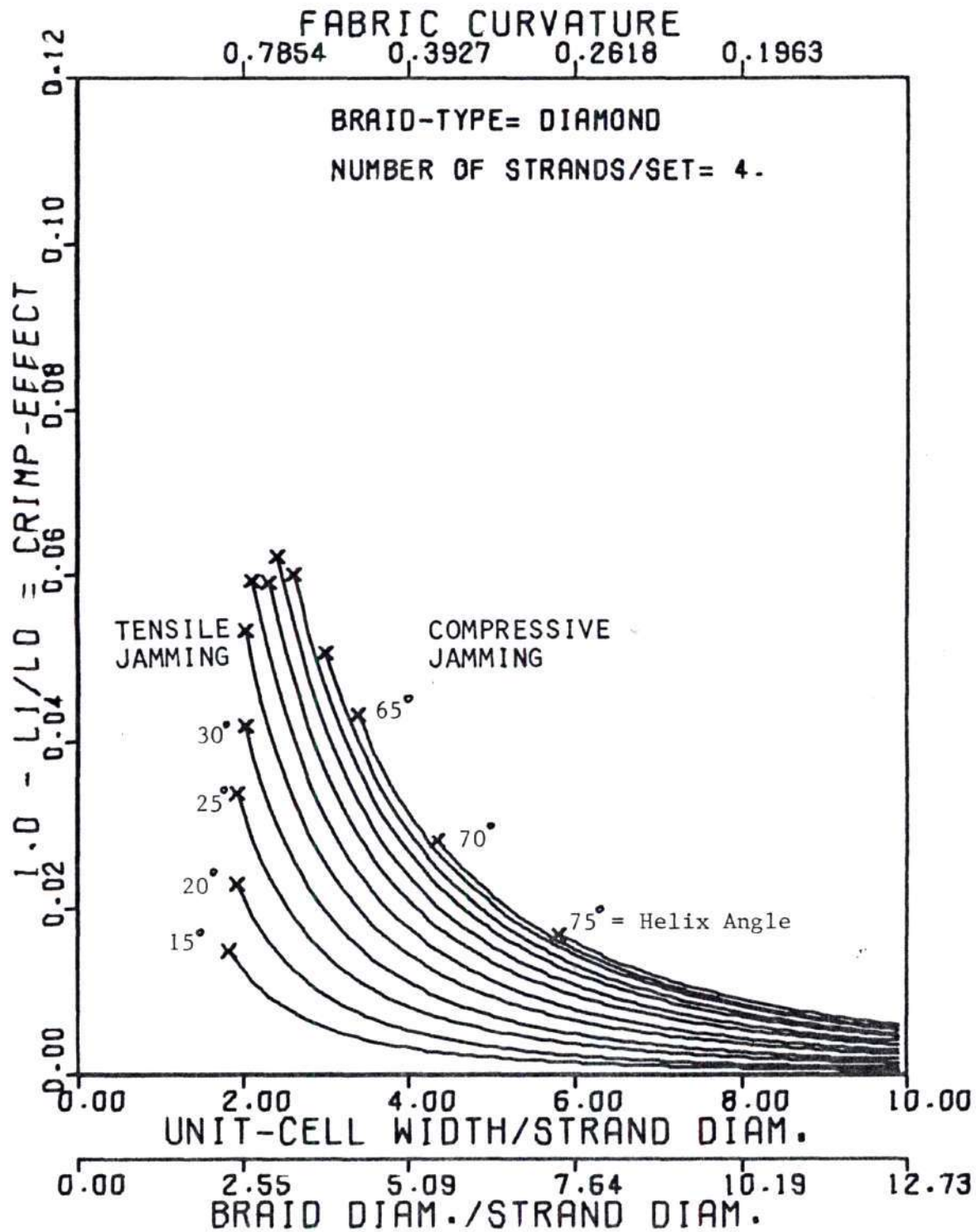


Figure 21. Crimp-Effect vs. Cell Width (TYPE=1, n=4).

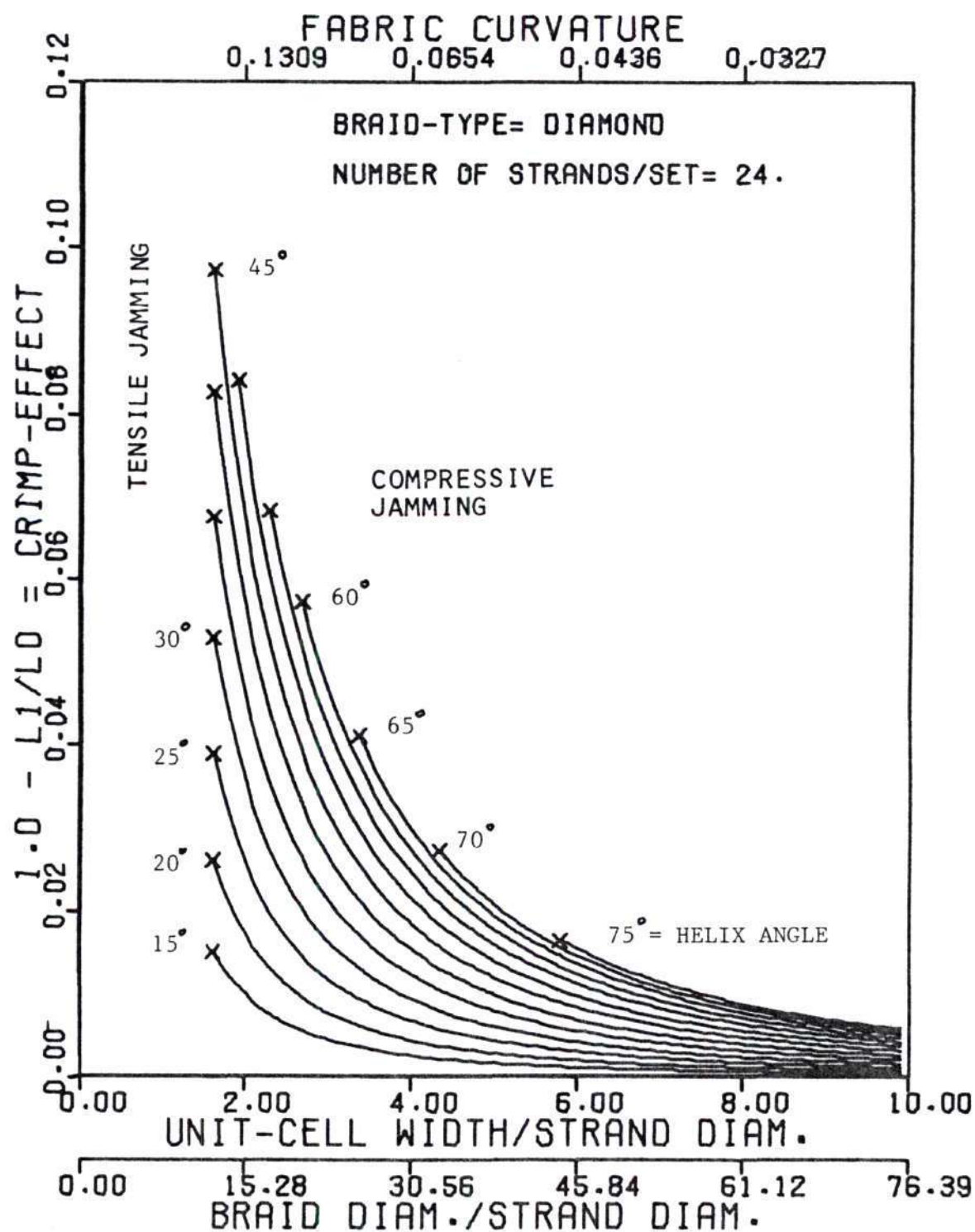


Figure 22. Crimp-Effect vs. Cell Width (TYPE=1, n=24)

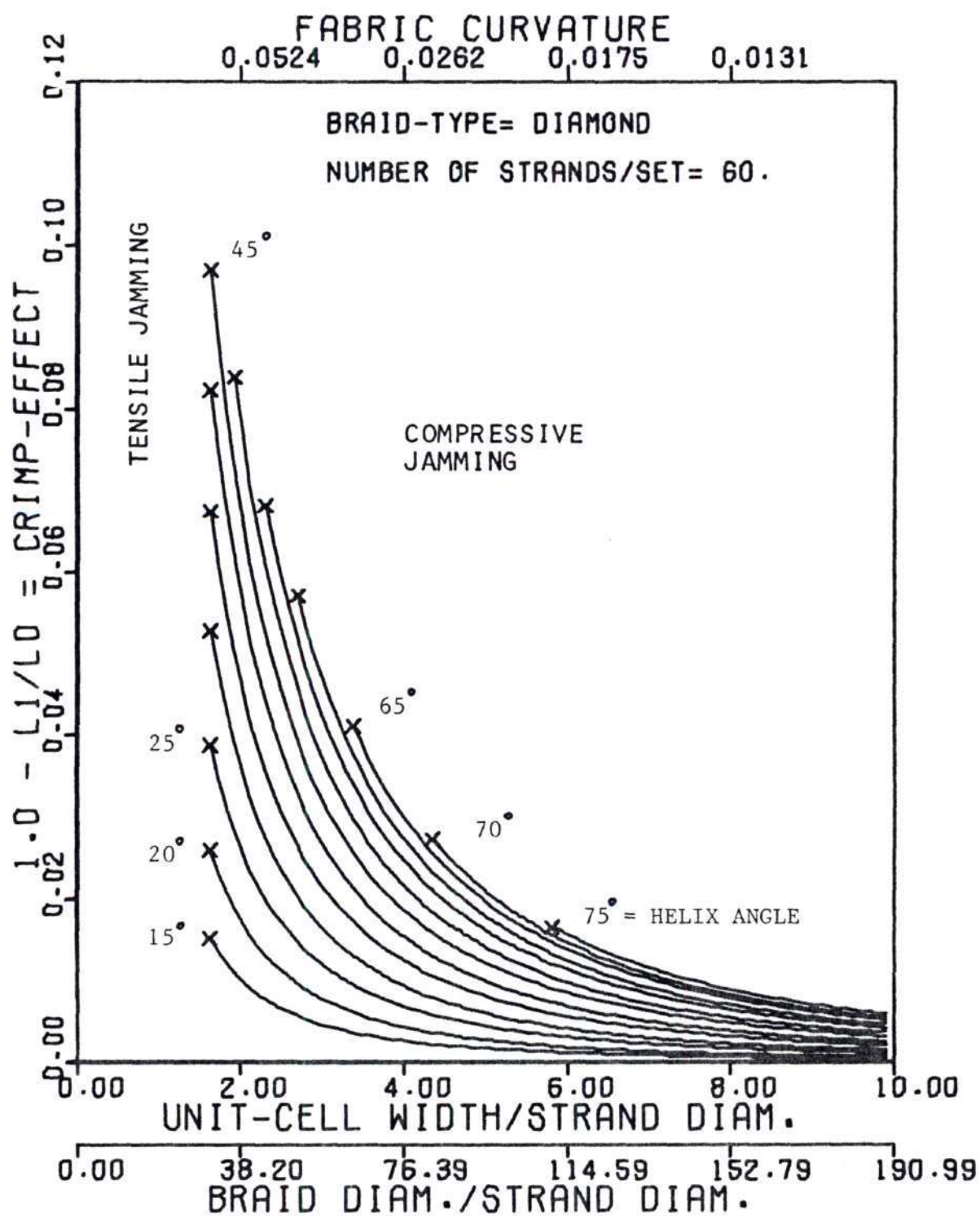


Figure 23. Crimp-Effect vs. Cell Width (TYPE=1, n=60).

braids of smaller n and greater curvature, though for all braids the effect is quite small at larger C_w . The earlier jamming of braids with small n can be seen to limit the magnitude of the crimp-effect comparing Figures 21 and 22.

Group 3- Deformation Curves And Jam Envelopes

The plots in this group have already been introduced (Figures 13 and 14). They give the potential deformation behavior of one or a whole family of braids with different L_0 and the same n . Included is the jam envelope which divides the zone of impossible braid construction from the possible. Observe that the diamond braid represented in Figure 24 exhibits a limiting C_w (about $1.6d$) for extensive jam which is independent of Q_1 and L_0 . This jamming C_w is slightly greater for unit cells of braids with smaller n , but the overall shape of the jamming envelope is generalizable for all diamond braids. The compressive jamming portion of the diamond jam envelope does not have the same steep slope or a single limiting C_w dimension. It is contingent upon the L_0 .

Jam envelopes and braid deformation curves for regular braid are pictured in Figure 25. Depending on the handedness of the braid either the extensive or compressive portion of the envelope is shifted. Comparing diamond and regular braids of $n=24$, shows that because of the longitudinal "1"-pair, a R.H. regular braid can accommodate

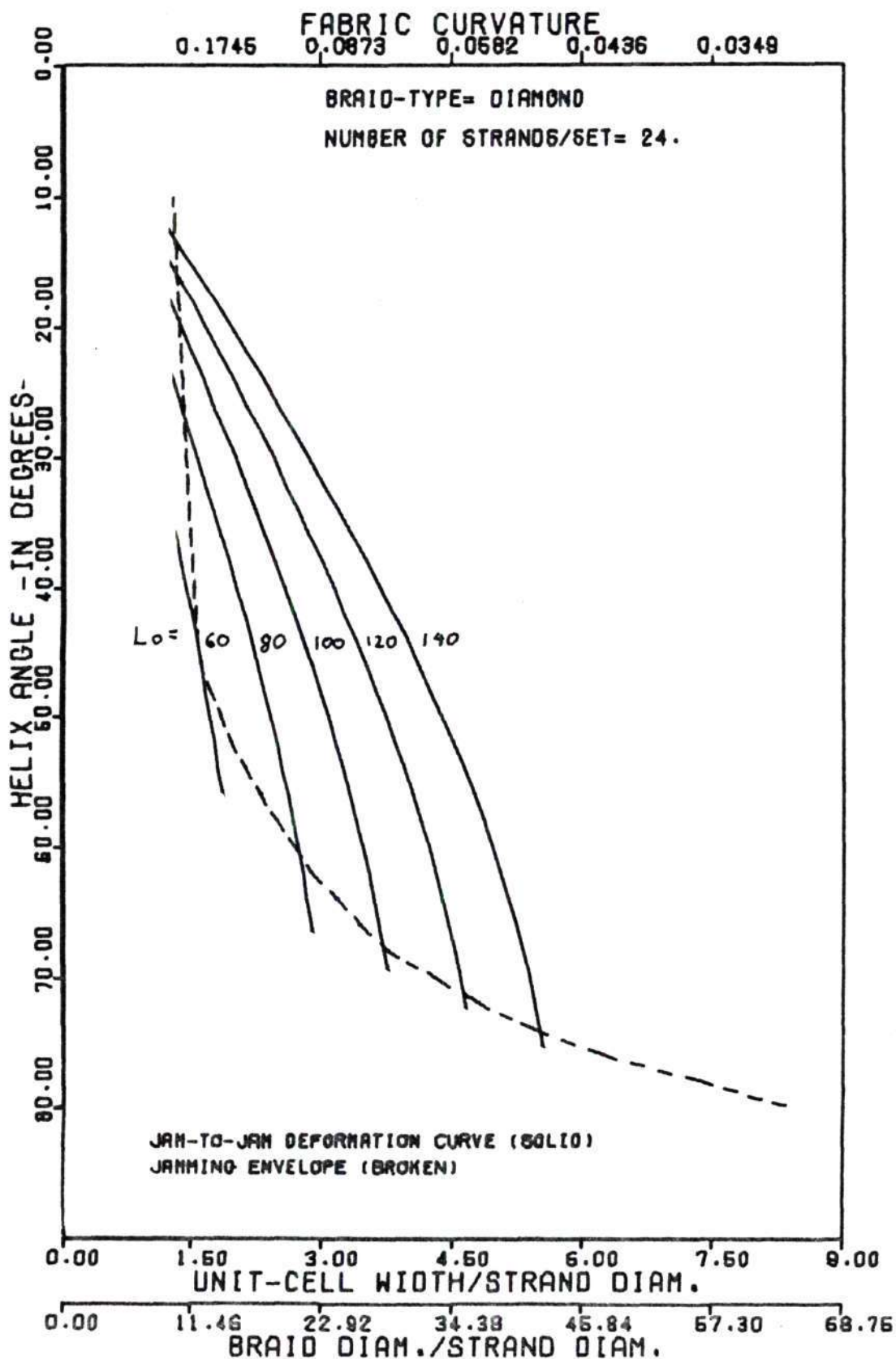


Figure 24. Braid Deformation Curves and Jamming Envelope for (TYPE=1, n=24).

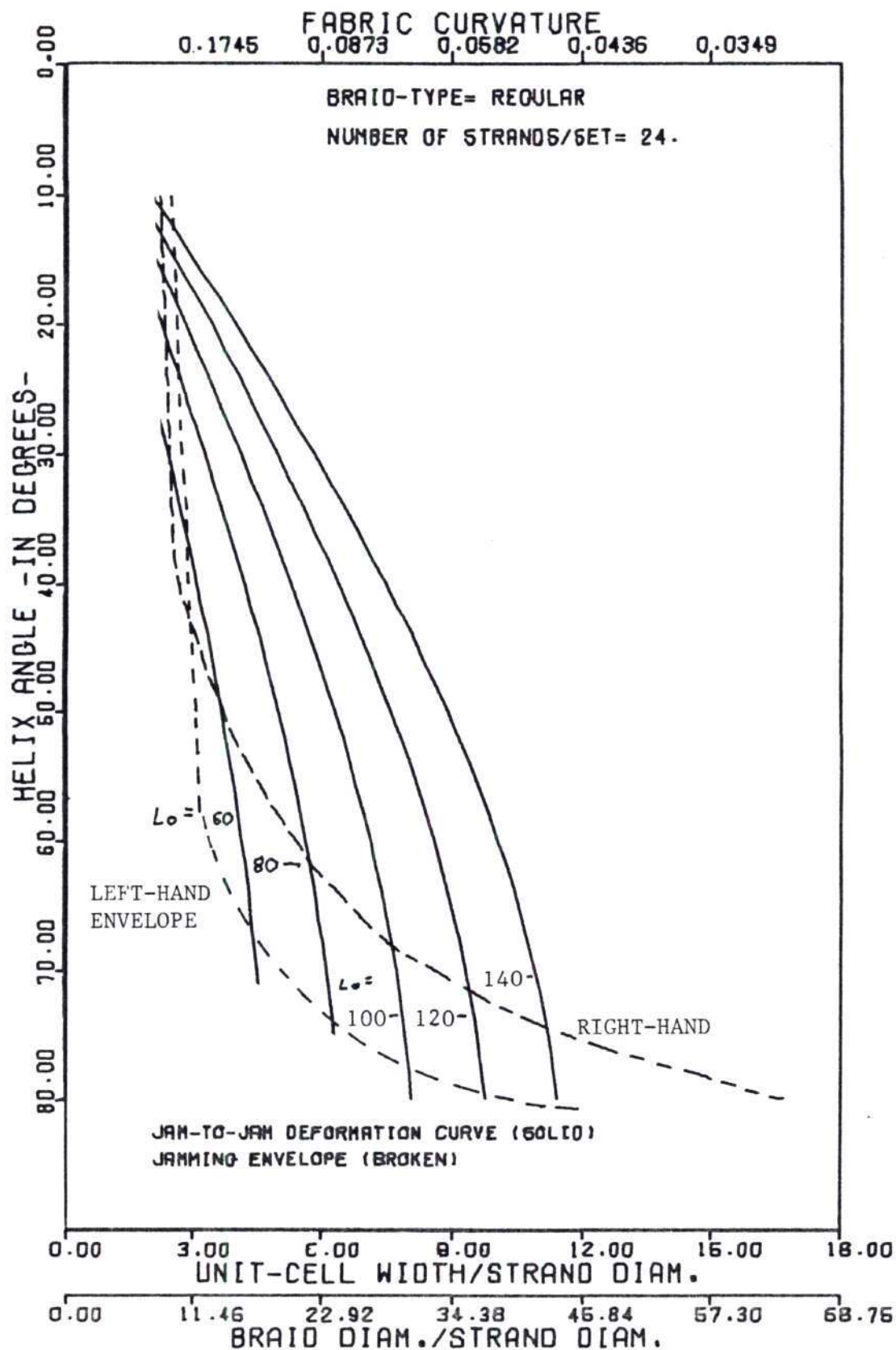


Figure 25. Braid Deformation Curves and Jamming Envelopes for (TYPE=2,3, n=24).

a shorter L_0 and that a completely jammed R.H. braid will have a smaller helix angle than its diamond counterpart. A L.H. regular braid can also have a shorter L_0 and will manifest a larger helix angle when jammed from both directions.

Group 4- Vector Analysis Tables

The previous group of results give an overall view of a deforming braid. For a detailed look at any point of interest along the deformation curve a table of vector analysis can be generated. Tables 3-8 and 9-11 are close scrutinizations of points "a" through "h" located on the deformation curves in Figures 13 and 14. The following key explains the matching of points and tables

Table	Fig.	Type	Hand	Tensile Jam Pt.	Compress. Jam Point	Mid Point
6	14	Reg.	RH	d		
7	14	Reg.	RH		e	
8	14	Reg.	RH			f
3	14	Reg.	LH	g		
4	14	Reg.	LH		h	
5	14	Reg.	LH			f
9	13	Dmd.	--	a		
10	13	Dmd.	--		b	
11	13	Dmd.	--			c

As well as signaling the onset of jam geometry the vector tables provide a wealth of other information. For instance the columns of cumulative arc-length, s , in Tables 9-11 enables the quick calculation of the percent difference between the length of an inner strand segment ($1/4$ of sine

Table 3a. Tensile Jamming Analysis of L.H. Regular Unit Cell (Extensive).

0 = 7.771E+00	Q1 = 1.800E+01	N = 1.600E+01	SD = 1.000E+03	L1/N = 4.338E+00	MODE = 1.000E+00
CLOCKWISE (ALTERNATING LEFT LEG)					
COUNTER-CLOCKWISE (ALTERNATING RIGHT LEG)					
(θ)	S	X	Y	Z	AX
1.	0.	1.000E+00	0.	0.	0.
2.	2.502E-04	9.430E-01	8.598E-02	2.340E-01	-5.591E-02
3.	1.427E-02	9.722E-01	1.712E-01	4.695E-01	-1.100E-01
4.	5.091E-02	9.380E-01	2.350E-01	7.042E-01	-1.603E-01
5.	7.454E-02	8.910E-01	3.166E-01	9.332E-01	-2.075E-01
6.	9.417E-02	8.430E-01	4.135E-01	1.172E+00	-2.445E-01
7.	1.277E-01	7.640E-01	4.922E-01	1.400E+00	-2.874E-01
8.	1.571E-01	6.832E-01	5.615E-01	1.644E+00	-3.315E-01
9.	1.871E-01	6.040E-01	6.200E-01	1.875E+00	-3.732E-01
10.	2.171E-01	5.162E-01	6.598E-01	2.112E+00	-4.173E-01
11.	2.462E-01	4.253E-01	7.590E-01	2.358E+00	-4.548E-01
12.	2.742E-01	3.333E-01	8.490E-01	2.587E+00	-4.858E-01
13.	3.022E-01	2.424E-01	9.210E-01	2.812E+00	-5.132E-01
14.	3.292E-01	1.545E-01	9.638E-01	3.052E+00	-5.362E-01
15.	3.572E-01	7.222E-02	9.742E-01	3.287E+00	-5.542E-01
16.	3.842E-01	-4.442E-02	1.025E+00	3.522E+00	-5.682E-01
17.	4.112E-01	-7.493E-02	1.076E+00	3.757E+00	-5.782E-01
18.	4.382E-01	-1.354E-01	1.127E+00	3.992E+00	-5.842E-01
19.	4.652E-01	-2.271E-01	1.176E+00	4.227E+00	-5.862E-01
20.	4.922E-01	-3.192E-01	1.226E+00	4.461E+00	-5.842E-01
21.	5.192E-01	-4.112E-01	1.276E+00	4.696E+00	-5.782E-01
22.	5.462E-01	-5.032E-01	1.326E+00	4.931E+00	-5.682E-01
23.	5.732E-01	-5.952E-01	1.376E+00	5.166E+00	-5.542E-01
24.	6.002E-01	-6.872E-01	1.426E+00	5.401E+00	-5.362E-01
25.	6.272E-01	-7.792E-01	1.476E+00	5.636E+00	-5.132E-01
26.	6.542E-01	-8.712E-01	1.526E+00	5.871E+00	-4.852E-01
27.	6.812E-01	-9.632E-01	1.576E+00	6.106E+00	-4.542E-01
28.	7.082E-01	-1.055E-01	1.626E+00	6.341E+00	-4.172E-01
29.	7.352E-01	-1.147E-01	1.676E+00	6.576E+00	-3.732E-01
30.	7.622E-01	-1.239E-01	1.726E+00	6.811E+00	-3.292E-01
31.	7.892E-01	-1.331E-01	1.776E+00	7.046E+00	-2.872E-01
32.	8.162E-01	-1.423E-01	1.826E+00	7.281E+00	-2.442E-01
33.	8.432E-01	-1.515E-01	1.876E+00	7.516E+00	-2.012E-01
34.	8.702E-01	-1.607E-01	1.926E+00	7.751E+00	-1.582E-01
35.	8.972E-01	-1.699E-01	1.976E+00	7.986E+00	-1.152E-01
36.	9.242E-01	-1.791E-01	2.026E+00	8.221E+00	-7.222E-02
37.	9.512E-01	-1.883E-01	2.076E+00	8.456E+00	-2.792E-02
38.	9.782E-01	-1.975E-01	2.126E+00	8.691E+00	-1.362E-02
39.	1.005E-01	-2.067E-01	2.176E+00	8.926E+00	-9.122E-03
40.	1.032E-01	-2.159E-01	2.226E+00	9.161E+00	-5.792E-03
41.	1.059E-01	-2.251E-01	2.276E+00	9.396E+00	-4.362E-03
42.	1.086E-01	-2.343E-01	2.326E+00	9.631E+00	-2.932E-03
43.	1.113E-01	-2.435E-01	2.376E+00	9.866E+00	-1.502E-03
44.	1.140E-01	-2.527E-01	2.426E+00	1.010E+01	-1.072E-03
45.	1.167E-01	-2.619E-01	2.476E+00	1.034E+01	-6.492E-04
46.	1.194E-01	-2.711E-01	2.526E+00	1.058E+01	-5.062E-04
47.	1.221E-01	-2.803E-01	2.576E+00	1.082E+01	-3.632E-04
48.	1.248E-01	-2.895E-01	2.626E+00	1.106E+01	-2.202E-04
49.	1.275E-01	-2.987E-01	2.676E+00	1.130E+01	-7.792E-05
50.	1.302E-01	-3.079E-01	2.726E+00	1.154E+01	-6.362E-05
51.	1.329E-01	-3.171E-01	2.776E+00	1.178E+01	-4.932E-05
52.	1.356E-01	-3.263E-01	2.826E+00	1.202E+01	-3.502E-05
53.	1.383E-01	-3.355E-01	2.876E+00	1.226E+01	-2.072E-05
54.	1.410E-01	-3.447E-01	2.926E+00	1.250E+01	-1.642E-05
55.	1.437E-01	-3.539E-01	2.976E+00	1.274E+01	-1.212E-05
56.	1.464E-01	-3.631E-01	3.026E+00	1.298E+01	-7.792E-06
57.	1.491E-01	-3.723E-01	3.076E+00	1.322E+01	-6.362E-06
58.	1.518E-01	-3.815E-01	3.126E+00	1.346E+01	-4.932E-06
59.	1.545E-01	-3.907E-01	3.176E+00	1.370E+01	-3.502E-06
60.	1.572E-01	-3.999E-01	3.226E+00	1.394E+01	-2.072E-06
61.	1.599E-01	-4.091E-01	3.276E+00	1.418E+01	-1.642E-06
62.	1.626E-01	-4.183E-01	3.326E+00	1.442E+01	-1.212E-06
63.	1.653E-01	-4.275E-01	3.376E+00	1.466E+01	-7.792E-07
64.	1.680E-01	-4.367E-01	3.426E+00	1.490E+01	-6.362E-07
65.	1.707E-01	-4.459E-01	3.476E+00	1.514E+01	-4.932E-07
66.	1.734E-01	-4.551E-01	3.526E+00	1.538E+01	-3.502E-07
67.	1.761E-01	-4.643E-01	3.576E+00	1.562E+01	-2.072E-07
68.	1.788E-01	-4.735E-01	3.626E+00	1.586E+01	-1.642E-07
69.	1.815E-01	-4.827E-01	3.676E+00	1.610E+01	-1.212E-07
70.	1.842E-01	-4.919E-01	3.726E+00	1.634E+01	-7.792E-08
71.	1.869E-01	-5.011E-01	3.776E+00	1.658E+01	-6.362E-08
72.	1.896E-01	-5.103E-01	3.826E+00	1.682E+01	-4.932E-08
73.	1.923E-01	-5.195E-01	3.876E+00	1.706E+01	-3.502E-08
74.	1.950E-01	-5.287E-01	3.926E+00	1.730E+01	-2.072E-08
75.	1.977E-01	-5.379E-01	3.976E+00	1.754E+01	-1.642E-08
76.	2.004E-01	-5.471E-01	4.026E+00	1.778E+01	-1.212E-08
77.	2.031E-01	-5.563E-01	4.076E+00	1.802E+01	-7.792E-09
78.	2.058E-01	-5.655E-01	4.126E+00	1.826E+01	-6.362E-09
79.	2.085E-01	-5.747E-01	4.176E+00	1.850E+01	-4.932E-09
80.	2.112E-01	-5.839E-01	4.226E+00	1.874E+01	-3.502E-09
81.	2.139E-01	-5.931E-01	4.276E+00	1.898E+01	-2.072E-09
82.	2.166E-01	-6.023E-01	4.326E+00	1.922E+01	-1.642E-09
83.	2.193E-01	-6.115E-01	4.376E+00	1.946E+01	-1.212E-09
84.	2.220E-01	-6.207E-01	4.426E+00	1.970E+01	-7.792E-10
85.	2.247E-01	-6.299E-01	4.476E+00	1.994E+01	-6.362E-10
86.	2.274E-01	-6.391E-01	4.526E+00	2.018E+01	-4.932E-10
87.	2.301E-01	-6.483E-01	4.576E+00	2.042E+01	-3.502E-10
88.	2.328E-01	-6.575E-01	4.626E+00	2.066E+01	-2.072E-10
89.	2.355E-01	-6.667E-01	4.676E+00	2.090E+01	-1.642E-10
90.	2.382E-01	-6.759E-01	4.726E+00	2.114E+01	-1.212E-10
91.	2.409E-01	-6.851E-01	4.776E+00	2.138E+01	-7.792E-11
92.	2.436E-01	-6.943E-01	4.826E+00	2.162E+01	-6.362E-11
93.	2.463E-01	-7.035E-01	4.876E+00	2.186E+01	-4.932E-11
94.	2.490E-01	-7.127E-01	4.926E+00	2.210E+01	-3.502E-11
95.	2.517E-01	-7.219E-01	4.976E+00	2.234E+01	-2.072E-11
96.	2.544E-01	-7.311E-01	5.026E+00	2.258E+01	-1.642E-11
97.	2.571E-01	-7.403E-01	5.076E+00	2.282E+01	-1.212E-11
98.	2.598E-01	-7.495E-01	5.126E+00	2.306E+01	-7.792E-12
99.	2.625E-01	-7.587E-01	5.176E+00	2.330E+01	-6.362E-12
100.	2.652E-01	-7.679E-01	5.226E+00	2.354E+01	-4.932E-12

Table 3b. Tensile Jamming Analysis of L.H. Regular Unit Cell (Compressive).

D = 7.77E+00		Q1 = 1.00E+01		N = 1.60E+01		SD = 1.00E+00		L1/N = 4.93E+00		MOCE = 1.00E+00	
COJINTER-CLOCKWISE (ALTERNATING TOP LEG)											
(°)	S	X	Y	Z	WX	WY	Q0	J0	GC	GT	
1.	0.	1.00E+00	0.	0.	0.	3.44E-01	2.014E+01	0.	2.24E-01	2.04E-01	
2.	2.50E-01	9.53E-01	8.59E-02	4.64E-01	-5.59E-02	3.42E-01	2.030E+01	4.18E-03	2.21E-01	2.04E-01	
3.	3.42E-01	9.72E-01	1.72E-01	4.64E-01	-1.10E-01	3.37E-01	2.076E+01	2.90E-03	2.12E-01	2.04E-01	
4.	5.93E-01	9.19E-01	2.55E-01	7.04E-01	-1.63E-01	3.24E-01	2.144E+01	2.24E-02	1.99E-01	2.55E-01	
5.	7.93E-01	8.91E-01	3.36E-01	9.39E-01	-2.05E-01	3.16E-01	2.225E+01	9.30E-02	1.91E-01	3.06E-01	
6.	9.34E-01	8.23E-01	4.25E-01	1.17E+00	-2.49E-01	3.03E-01	2.304E+01	2.52E-01	1.60E-01	3.86E-01	
7.	1.17E+00	7.64E-01	4.92E-01	1.40E+00	-2.83E-01	2.89E-01	2.395E+01	4.86E-01	1.38E-01	5.19E-01	
8.	1.37E+00	6.89E-01	5.65E-01	1.64E+00	-3.14E-01	2.72E-01	2.447E+01	7.93E-01	1.14E-01	7.45E-01	
9.	1.57E+00	6.04E-01	6.32E-01	1.87E+00	-3.32E-01	2.57E-01	2.489E+01	1.15E+00	9.08E-02	1.17E+00	
10.	1.75E+00	5.16E-01	6.96E-01	2.11E+00	-3.47E-01	2.42E-01	2.504E+01	1.56E+00	6.45E-02	2.04E+00	
11.	1.96E+00	4.25E-01	7.58E-01	2.34E+00	-3.58E-01	2.29E-01	2.500E+01	1.97E+00	5.06E-02	3.71E+00	
12.	2.19E+00	3.33E-01	8.16E-01	2.58E+00	-3.59E-01	2.19E-01	2.465E+01	2.39E+00	4.35E-02	4.94E+00	
13.	2.43E+00	2.42E-01	8.70E-01	2.81E+00	-3.36E-01	2.09E-01	2.432E+01	2.91E+00	3.40E-02	5.84E+00	
14.	2.65E+00	1.54E-01	9.29E-01	3.05E+00	-3.02E-01	2.03E-01	2.313E+01	3.23E+00	7.09E-02	6.84E+00	
15.	2.84E+00	7.12E-02	9.74E-01	3.28E+00	-2.60E-01	1.99E-01	2.201E+01	3.63E+00	9.34E-02	7.84E+00	
16.	3.02E+00	-5.64E-03	1.00E+00	3.52E+00	-2.09E-01	2.00E-01	2.072E+01	4.03E+00	1.16E-01	8.67E-01	
17.	3.17E+00	-7.49E-02	1.07E+00	3.75E+00	-1.61E-01	2.03E-01	1.935E+01	4.36E+00	1.38E-01	9.42E-01	
18.	3.30E+00	-1.35E-01	1.12E+00	3.99E+00	-1.20E-01	2.11E-01	1.802E+01	4.68E+00	1.57E-01	1.05E-01	
19.	3.39E+00	-1.66E-01	1.16E+00	4.22E+00	-8.72E-02	2.21E-01	1.687E+01	4.98E+00	1.72E-01	2.91E-01	
20.	3.43E+00	-1.87E-01	1.19E+00	4.46E+00	-1.46E-01	2.35E-01	1.609E+01	5.31E+00	1.82E-01	2.60E-01	
21.	3.42E+00	-2.57E-01	1.24E+00	4.69E+00	-1.04E-01	2.51E-01	1.581E+01	5.72E+00	1.95E-01	2.56E-01	
22.	3.37E+00	-3.77E-01	1.29E+00	4.92E+00	-5.84E-02	2.70E-01	1.581E+01	6.15E+00	2.12E-01	2.74E-01	
23.	3.28E+00	-5.00E-01	1.34E+00	5.15E+00	-3.72E-02	2.69E-01	1.581E+01	6.58E+00	2.19E-01	2.74E-01	
24.	3.17E+00	-6.25E-01	1.39E+00	5.38E+00	-2.61E-02	2.68E-01	1.581E+01	7.01E+00	2.19E-01	2.74E-01	
25.	3.05E+00	-7.49E-02	1.44E+00	5.61E+00	-1.46E-02	2.67E-01	1.581E+01	7.44E+00	2.19E-01	2.74E-01	
26.	2.92E+00	-8.72E-02	1.49E+00	5.84E+00	-8.48E-03	2.66E-01	1.581E+01	7.87E+00	2.19E-01	2.74E-01	
27.	2.79E+00	-1.00E-01	1.54E+00	6.07E+00	-7.39E-03	2.65E-01	1.581E+01	8.30E+00	2.19E-01	2.74E-01	
28.	2.66E+00	-1.17E-01	1.59E+00	6.30E+00	-6.28E-03	2.63E-01	1.581E+01	8.73E+00	2.19E-01	2.74E-01	
29.	2.53E+00	-1.35E-01	1.64E+00	6.53E+00	-5.17E-03	2.62E-01	1.581E+01	9.16E+00	2.19E-01	2.74E-01	
30.	2.40E+00	-1.54E-01	1.69E+00	6.76E+00	-4.06E-03	2.60E-01	1.581E+01	9.59E+00	2.19E-01	2.74E-01	
31.	2.27E+00	-1.72E-01	1.74E+00	6.99E+00	-2.95E-03	2.59E-01	1.581E+01	1.00E+00	2.19E-01	2.74E-01	
32.	2.14E+00	-1.91E-01	1.79E+00	7.22E+00	-1.84E-03	2.57E-01	1.581E+01	1.04E+00	2.19E-01	2.74E-01	
33.	2.01E+00	-2.10E-01	1.84E+00	7.45E+00	-7.34E-04	2.55E-01	1.581E+01	1.08E+00	2.19E-01	2.74E-01	
34.	1.88E+00	-2.29E-01	1.89E+00	7.68E+00	-6.23E-04	2.53E-01	1.581E+01	1.12E+00	2.19E-01	2.74E-01	
35.	1.75E+00	-2.48E-01	1.94E+00	7.91E+00	-5.12E-04	2.51E-01	1.581E+01	1.16E+00	2.19E-01	2.74E-01	
36.	1.62E+00	-2.67E-01	1.99E+00	8.14E+00	-4.01E-04	2.49E-01	1.581E+01	1.20E+00	2.19E-01	2.74E-01	
37.	1.49E+00	-2.86E-01	2.04E+00	8.37E+00	-2.90E-04	2.47E-01	1.581E+01	1.24E+00	2.19E-01	2.74E-01	
38.	1.36E+00	-3.05E-01	2.09E+00	8.60E+00	-1.79E-04	2.45E-01	1.581E+01	1.28E+00	2.19E-01	2.74E-01	
39.	1.23E+00	-3.24E-01	2.14E+00	8.83E+00	-7.84E-05	2.43E-01	1.581E+01	1.32E+00	2.19E-01	2.74E-01	
40.	1.10E+00	-3.43E-01	2.19E+00	9.06E+00	3.17E-05	2.41E-01	1.581E+01	1.36E+00	2.19E-01	2.74E-01	
41.	9.74E-01	-3.62E-01	2.24E+00	9.29E+00	1.06E-04	2.39E-01	1.581E+01	1.40E+00	2.19E-01	2.74E-01	
42.	8.57E-01	-3.81E-01	2.29E+00	9.52E+00	-1.05E-04	2.37E-01	1.581E+01	1.44E+00	2.19E-01	2.74E-01	
43.	7.40E-01	-4.00E-01	2.34E+00	9.75E+00	-2.04E-04	2.35E-01	1.581E+01	1.48E+00	2.19E-01	2.74E-01	
44.	6.23E-01	-4.19E-01	2.39E+00	9.98E+00	-3.03E-04	2.33E-01	1.581E+01	1.52E+00	2.19E-01	2.74E-01	
45.	5.06E-01	-4.38E-01	2.44E+00	1.02E+00	-4.02E-04	2.31E-01	1.581E+01	1.56E+00	2.19E-01	2.74E-01	
46.	3.89E-01	-4.57E-01	2.49E+00	1.04E+00	-5.01E-04	2.29E-01	1.581E+01	1.60E+00	2.19E-01	2.74E-01	
47.	2.72E-01	-4.76E-01	2.54E+00	1.06E+00	-6.00E-04	2.27E-01	1.581E+01	1.64E+00	2.19E-01	2.74E-01	
48.	1.55E-01	-4.95E-01	2.59E+00	1.08E+00	-7.00E-04	2.25E-01	1.581E+01	1.68E+00	2.19E-01	2.74E-01	
49.	3.97E-02	-5.14E-01	2.64E+00	1.10E+00	-8.00E-04	2.23E-01	1.581E+01	1.72E+00	2.19E-01	2.74E-01	
50.	0.	-5.33E-01	2.69E+00	1.12E+00	-9.00E-04	2.21E-01	1.581E+01	1.76E+00	2.19E-01	2.74E-01	
51.	0.	-5.52E-01	2.74E+00	1.14E+00	-1.00E-03	2.19E-01	1.581E+01	1.80E+00	2.19E-01	2.74E-01	
52.	0.	-5.71E-01	2.79E+00	1.16E+00	-1.10E-03	2.17E-01	1.581E+01	1.84E+00	2.19E-01	2.74E-01	
53.	0.	-5.90E-01	2.84E+00	1.18E+00	-1.20E-03	2.15E-01	1.581E+01	1.88E+00	2.19E-01	2.74E-01	
54.	0.	-6.09E-01	2.89E+00	1.20E+00	-1.30E-03	2.13E-01	1.581E+01	1.92E+00	2.19E-01	2.74E-01	
55.	0.	-6.28E-01	2.94E+00	1.22E+00	-1.40E-03	2.11E-01	1.581E+01	1.96E+00	2.19E-01	2.74E-01	
56.	0.	-6.47E-01	2.99E+00	1.24E+00	-1.50E-03	2.09E-01	1.581E+01	2.00E+00	2.19E-01	2.74E-01	
57.	0.	-6.66E-01	3.04E+00	1.26E+00	-1.60E-03	2.07E-01	1.581E+01	2.04E+00	2.19E-01	2.74E-01	
58.	0.	-6.85E-01	3.09E+00	1.28E+00	-1.70E-03	2.05E-01	1.581E+01	2.08E+00	2.19E-01	2.74E-01	
59.	0.	-7.04E-01	3.14E+00	1.30E+00	-1.80E-03	2.03E-01	1.581E+01	2.12E+00	2.19E-01	2.74E-01	
60.	0.	-7.23E-01	3.19E+00	1.32E+00	-1.90E-03	2.01E-01	1.581E+01	2.16E+00	2.19E-01	2.74E-01	
61.	0.	-7.42E-01	3.24E+00	1.34E+00	-2.00E-03	2.00E-01	1.581E+01	2.20E+00	2.19E-01	2.74E-01	
62.	0.	-7.61E-01	3.29E+00	1.36E+00	-2.10E-03	1.98E-01	1.581E+01	2.24E+00	2.19E-01	2.74E-01	
63.	0.	-7.80E-01	3.34E+00	1.38E+00	-2.20E-03	1.96E-01	1.581E+01	2.28E+00	2.19E-01	2.74E-01	
64.	0.	-7.99E-01	3.39E+00	1.40E+00	-2.30E-03	1.94E-01	1.581E+01	2.32E+00	2.19E-01	2.74E-01	
65.	0.	-8.18E-01	3.44E+00	1.42E+00	-2.40E-03	1.92E-01	1.581E+01	2.36E+00	2.19E-01	2.74E-01	
66.	0.	-8.37E-01	3.49E+00	1.44E+00	-2.50E-03	1.90E-01	1.581E+01	2.40E+00	2.19E-01	2.74E-01	
67.	0.	-8.56E-01	3.54E+00	1.46E+00	-2.60E-03	1.88E-01	1.581E+01	2.44E+00	2.19E-01	2.74E-01	
68.	0.	-8.75E-01	3.59E+00	1.48E+00	-2.70E-03	1.86E-01	1.581E+01	2.48E+00	2.19E-01	2.74E-01	
69.	0.	-8.94E-01	3.64E+00	1.50E+00	-2.80E-03	1.84E-01	1.581E+01	2.52E+00	2.19E-01	2.74E-01	
70.	0.	-9.13E-01	3.69E+00	1.52E+00	-2.90E-03	1.82E-01	1.581E+01	2.56E+00	2.19E-01	2.74E-01	
71.	0.	-9.32E-01	3.74E+00	1.54E+00	-3.00E-03	1.80E-01	1.581E+01	2.60E+00	2.19E-01	2.74E-01	
72.	0.	-9.51E-01	3.79E+00	1.56E+00	-3.10E-03	1.78E-01	1.581E+01	2.64E+00	2.19E-01	2.74E-01	
73.	0.	-9.70E-01	3.84E+00	1.58E+00	-3.20E-03	1.76E-01	1.581E+01	2.68E+00	2.19E-01	2.74E-01	
74.	0.	-9.89E-01	3.89E+00	1.60E+00	-3.30E-03	1.74E-01	1.581E+01	2.72E+00	2.19E-01	2.74E-01	
75.	0.	-1.00E-01	3.94E+00	1.62E+00	-3.40E-03	1.72E-01	1.581E+01	2.76E+00	2.19E-01	2.74E-01	
76.	0.	-1.00E-01	3.99E+00	1.64E+00	-3.50E-03	1.70E-01	1.581E+01	2.80E+00	2.19E-01	2.74E-01	
77.	0.	-1.00E-01	4.04E+00	1.66E+00	-3.60E-03	1.68E-01	1.581E+01	2.84E+00	2.19E-01	2.74E-01	
78.	0.	-1.00E-01	4.09E+00	1.68E+00	-3.70E-03	1.66E-01	1.581E+01	2.88E+00	2.19E-01	2.74E-01	
79.	0.	-1.00E-01	4.14E+00	1.70E+00	-3.80E-03	1.64E-01	1.581E+01	2.92E+00	2.19E-01	2.74E-01	
80.	0.	-1.00E-01	4.19E+00	1.72E+00	-3.90E-03	1.62E-01	1.581E+01	2.96E+00	2.19E-01	2.74E-01	
81.	0.	-1.00E-01	4.24E+00	1.74E+00	-4.00E-03	1.60E-01	1.581E+01	3.00E+00	2.19E-01	2.74E-01	
82.	0.	-1.00E-01	4.29E+00	1.76E+00	-4.10E-03	1.58E-01	1.581E+01	3.04E+00	2.19E-01	2.74E-01	
83.	0.	-1.00E-01	4.34E+00	1.78E+00	-4.20E-03	1.56E-01					

Table 4b. Compressive Jamming Analysis of L.H. Regular Unit Cell (Compressive).

0=	2.332E+01	Q1=	7.200E+01	N=	1.60E+01	SD=	1.000E+00	L1/N=	4.939E+0J	MODE=	1.000E+00
COUNTER-CLOCKWISE (ALTERNATING TOP LEG)											
(e)	S	X	Y	Z	WX	WY	00	J0	GC	GT	
1.	0.	1.00E+00	0.	0.	0.	9.54E-01	7.26E+01	0.	2.45E-01	5.56E-02	
2.	2.56E-01	9.95E-01	2.49E-01	7.53E-02	-6.66E-02	9.52E-01	7.26E+01	1.557E-03	2.55E-01	5.65E-02	
3.	3.327E-02	9.95E-01	2.49E-01	1.52E-01	-1.37E-01	9.45E-01	7.27E+01	1.074E-02	2.58E-01	5.67E-02	
4.	5.33E-02	9.95E-01	2.49E-01	2.28E-01	-1.937E-01	9.35E-01	7.27E+01	1.074E-02	2.58E-01	5.67E-02	
5.	7.83E-02	9.95E-01	2.49E-01	3.03E-01	-2.51E-01	9.21E-01	7.27E+01	9.040E-02	2.61E-01	5.69E-02	
6.	9.94E-02	9.95E-01	2.49E-01	3.81E-01	-3.02E-01	9.06E-01	7.29E+01	1.155E-01	2.62E-01	5.70E-02	
7.	1.17E-01	9.95E-01	2.49E-01	4.62E-01	-3.51E-01	8.93E-01	7.29E+01	1.793E-01	1.85E-01	1.07E-01	
8.	1.37E-01	9.95E-01	2.49E-01	5.46E-01	-3.94E-01	8.72E-01	7.29E+01	2.575E-01	1.56E-01	1.07E-01	
9.	1.57E-01	9.95E-01	2.49E-01	6.34E-01	-4.25E-01	8.56E-01	7.29E+01	3.495E-01	1.33E-01	1.91E-02	
10.	1.77E-01	9.95E-01	2.49E-01	7.26E-01	-4.52E-01	8.41E-01	7.29E+01	4.538E-01	1.08E-01	2.93E-01	
11.	1.97E-01	9.95E-01	2.49E-01	8.21E-01	-4.74E-01	8.29E-01	7.29E+01	5.684E-01	7.94E-02	5.56E-01	
12.	2.16E-01	9.95E-01	2.49E-01	9.19E-01	-4.90E-01	8.20E-01	7.27E+01	6.949E-01	5.36E-02	1.00E+00	
13.	2.35E-01	9.95E-01	2.49E-01	1.02E-01	-4.99E-01	8.12E-01	7.26E+01	8.247E-01	2.78E-02	4.06E+03	
14.	2.53E-01	9.95E-01	2.49E-01	1.14E-01	-5.03E-01	8.14E-01	7.24E+01	9.624E-01	1.44E-02	1.41E+01	
15.	2.71E-01	9.95E-01	2.49E-01	1.26E-01	-5.03E-01	8.14E-01	7.22E+01	1.105E-00	7.50E-02	2.34E+00	
16.	2.89E-01	9.95E-01	2.49E-01	1.37E-01	-5.03E-01	8.14E-01	7.19E+01	1.255E+00	6.55E-02	7.11E+00	
17.	3.07E-01	9.95E-01	2.49E-01	1.48E-01	-5.03E-01	8.14E-01	7.17E+01	1.397E+00	8.06E-02	3.40E+01	
18.	3.25E-01	9.95E-01	2.49E-01	1.59E-01	-5.03E-01	8.14E-01	7.15E+01	1.545E+00	1.26E-01	2.04E+01	
19.	3.43E-01	9.95E-01	2.49E-01	1.70E-01	-5.03E-01	8.14E-01	7.14E+01	1.694E+00	2.24E-01	4.45E+01	
20.	3.61E-01	9.95E-01	2.49E-01	1.81E-01	-5.03E-01	8.14E-01	7.13E+01	1.845E+00	1.35E-01	1.17E+01	
21.	3.79E-01	9.95E-01	2.49E-01	1.92E-01	-5.03E-01	8.14E-01	7.12E+01	1.996E+00	1.493E-01	1.09E+01	
CLOCKWISE (NON-ALTERNATING BOTTOM LEG)											
(e)	S	X	Y	Z	WX	WY	00	J0	GC	GT	
1.	0.	1.00E+00	0.	0.	0.	9.47E-01	7.127E+01	0.	7.85E-02	2.65E-02	
2.	2.56E-01	9.95E-01	2.49E-01	-7.63E-02	-1.89E-02	9.46E-01	7.127E+01	4.5557E-03	7.85E-02	2.65E-02	
3.	3.327E-02	9.95E-01	2.49E-01	-1.52E-01	-3.71E-02	9.46E-01	7.127E+01	1.679E-02	7.85E-02	2.65E-02	
4.	5.33E-02	9.95E-01	2.49E-01	-2.28E-01	-5.53E-02	9.46E-01	7.127E+01	3.646E-02	7.85E-02	2.65E-02	
5.	7.83E-02	9.95E-01	2.49E-01	-3.03E-01	-7.43E-02	9.46E-01	7.127E+01	6.508E-02	7.85E-02	2.65E-02	
6.	9.94E-02	9.95E-01	2.49E-01	-3.81E-01	-9.29E-02	9.46E-01	7.127E+01	1.155E-01	7.85E-02	2.65E-02	
7.	1.17E-01	9.95E-01	2.49E-01	-4.62E-01	-1.13E-01	9.46E-01	7.127E+01	1.795E-01	7.85E-02	2.65E-02	
8.	1.37E-01	9.95E-01	2.49E-01	-5.46E-01	-1.34E-01	9.46E-01	7.127E+01	2.575E-01	7.85E-02	2.65E-02	
9.	1.57E-01	9.95E-01	2.49E-01	-6.34E-01	-1.49E-01	9.46E-01	7.127E+01	3.495E-01	7.85E-02	2.65E-02	
10.	1.77E-01	9.95E-01	2.49E-01	-7.26E-01	-1.66E-01	9.46E-01	7.127E+01	4.538E-01	7.85E-02	2.65E-02	
11.	1.97E-01	9.95E-01	2.49E-01	-8.21E-01	-1.84E-01	9.46E-01	7.127E+01	5.684E-01	7.85E-02	2.65E-02	
12.	2.16E-01	9.95E-01	2.49E-01	-9.19E-01	-2.03E-01	9.46E-01	7.127E+01	6.949E-01	7.85E-02	2.65E-02	
13.	2.35E-01	9.95E-01	2.49E-01	-1.02E-01	-2.21E-01	9.46E-01	7.127E+01	8.247E-01	7.85E-02	2.65E-02	
14.	2.53E-01	9.95E-01	2.49E-01	-1.14E-01	-2.31E-01	9.46E-01	7.127E+01	9.624E-01	7.85E-02	2.65E-02	
15.	2.71E-01	9.95E-01	2.49E-01	-1.26E-01	-2.41E-01	9.46E-01	7.127E+01	1.105E+00	7.85E-02	2.65E-02	
16.	2.89E-01	9.95E-01	2.49E-01	-1.37E-01	-2.49E-01	9.46E-01	7.127E+01	1.250E+00	7.85E-02	2.65E-02	
17.	3.07E-01	9.95E-01	2.49E-01	-1.48E-01	-2.56E-01	9.46E-01	7.127E+01	1.397E+00	7.85E-02	2.65E-02	
18.	3.25E-01	9.95E-01	2.49E-01	-1.59E-01	-2.62E-01	9.46E-01	7.127E+01	1.545E+00	7.85E-02	2.65E-02	
19.	3.43E-01	9.95E-01	2.49E-01	-1.70E-01	-2.67E-01	9.46E-01	7.127E+01	1.694E+00	7.85E-02	2.65E-02	
20.	3.61E-01	9.95E-01	2.49E-01	-1.81E-01	-2.72E-01	9.46E-01	7.127E+01	1.845E+00	7.85E-02	2.65E-02	
21.	3.79E-01	9.95E-01	2.49E-01	-1.92E-01	-2.76E-01	9.46E-01	7.127E+01	1.996E+00	7.85E-02	2.65E-02	

Table 5b. Mid-Point Jamming Analysis of L.H. Regular Unit Cell (Compressive).

D= 1.778E+01												Q1= 4.500E+01												N= 1.600E+01												SO= 1.000E+00												L1/N= 4.938E+00												MOCE= 1.000E+00																																																																																																																																																																																																																																																																																																																																																																																																																																																																																																																																																																																																																																																																																																																																																																																																																																																																																																																																																																																																																																																																																																																																																																																																																																																																																																																																																																																																																																																																																																																																																																																																																																																																																																																																																																																																																																																																																																																																																																																																																																																																																																																																																																																																																																																																																																																																																																																																																																																																																																																																																																																																																																																																																																																																																																																																																																																																																																																																																																																																																																																																																																																																																																																																																																																																																																																																																																																																																																																																																																																																																																																																																																																																																																																																																																																																																																																																																																																																																																																																																																																																																																																																																																																																																																																																																																																																																																																																																																																																																																																																																																																																																																																																																																																																																																																																																																																																																																																																																																																																																																																																																																																																																																																																																																																																																																																																																																																																																																																																																																																																																																																																																																																																																																																																																																																																																																																																																																																																																																																																																																																																																																																																																																																																																																																																																																																																																																																																																																																																																																																																																																																																																																																																																																																																																																																																																																																																																																																																																																																																																																																																																																																																																																																																																																																																																																																																																																																																																																																																																																																																																																																																																																																																																																																																																																																																																																																																																																																																																																																																																																																																																																																																																																																																																																																																																																											
(8)												COUNTER-CLOCKWISE												(ALTERNATING TOP LEG)												CLOCKWISE (NON-ALTERNATING BOTTOM LEG)												(9)																																																																																																																																																																																																																																																																																																																																																																																																																																																																																																																																																																																																																																																																																																																																																																																																																																																																																																																																																																																																																																																																																																																																																																																																																																																																																																																																																																																																																																																																																																																																																																																																																																																																																																																																																																																																																																																																																																																																																																																																																																																																																																																																																																																																																																																																																																																																																																																																																																																																																																																																																																																																																																																																																																																																																																																																																																																																																																																																																																																																																																																																																																																																																																																																																																																																																																																																																																																																																																																																																																																																																																																																																																																																																																																																																																																																																																																																																																																																																																																																																																																																																																																																																																																																																																																																																																																																																																																																																																																																																																																																																																																																																																																																																																																																																																																																																																																																																																																																																																																																																																																																																																																																																																																																																																																																																																																																																																																																																																																																																																																																																																																																																																																																																																																																																																																																																																																																																																																																																																																																																																																																																																																																																																																																																																																																																																																																																																																																																																																																																																																																																																																																																																																																																																																																																																																																																																																																																																																																																																																																																																																																																																																																																																																																																																																																																																																																																																																																																																																																																																																																																																																																																																																																																																																																																																																																																																																																																																																																																																																																																																																																																																																																																																																																																																																																																																																							
Y												Z												W												X												Y												Z												W												X																																																																																																																																																																																																																																																																																																																																																																																																																																																																																																																																																																																																																																																																																																																																																																																																																																																																																																																																																																																																																																																																																																																																																																																																																																																																																																																																																																																																																																																																																																																																																																																																																																																																																																																																																																																																																																																																																																																																																																																																																																																																																																																																																																																																																																																																																																																																																																																																																																																																																																																																																																																																																																																																																																																																																																																																																																																																																																																																																																																																																																																																																																																																																																																																																																																																																																																																																																																																																																																																																																																																																																																																																																																																																																																																																																																																																																																																																																																																																																																																																																																																																																																																																																																																																																																																																																																																																																																																																																																																																																																																																																																																																																																																																																																																																																																																																																																																																																																																																																																																																																																																																																																																																																																																																																																																																																																																																																																																																																																																																																																																																																																																																																																																																																																																																																																																																																																																																																																																																																																																																																																																																																																																																																																																																																																																																																																																																																																																																																																																																																																																																																																																																																																																																																																																																																																																																																																																																																																																																																																																																																																																																																																																																																																																																																																																																																																																																																																																																																																																																																																																																																																																																																																																																																																																																																																																																																																																																																																																																																																																																																																																																																																																																																																																																																																																																			
0.												0.												0.												0.												0.												0.												0.												0.												0.												0.												0.												0.												0.												0.												0.												0.												0.												0.												0.												0.												0.												0.												0.												0.												0.												0.												0.												0.												0.												0.												0.												0.												0.												0.												0.												0.												0.												0.												0.												0.												0.												0.												0.												0.												0.												0.												0.												0.												0.												0.												0.												0.												0.												0.												0.												0.												0.												0.												0.												0.												0.												0.												0.												0.												0.												0.												0.												0.												0.												0.												0.												0.												0.												0.												0.												0.												0.												0.												0.												0.												0.												0.												0.												0.												0.												0.												0.												0.												0.												0.												0.												0.												0.												0.												0.												0.												0.												0.												0.												0.												0.												0.												0.												0.												0.												0.												0.												0.												0.												0.												0.												0.												0.												0.												0.												0.												0.												0.												0.												0.												0.												0.												0.												0.												0.												0.												0.												0.												0.												0.												0.												0.												0.												0.												0.												0.												0.												0.												0.												0.												0.												0.												0.												0.												0.												0.												0.												0.												0.												0.												0.												0.												0.												0.												0.												0.												0.												0.												0.												0.												0.												0.												0.												0.												0.												0.												0.												0.												0.												0.												0.												0.												0.												0.												0.												0.												0.												0.												0.												0.												0.												0.												0.												0.												0.												0.												0.												0.												0.												0.												0.												0.												0.												0.												0.												0.												0.												0.												0.												0.												0.												0.												0.												0.												0.												0.												0.												0.												0.												0.												0.												0.												0.												0.												0.												0.												0.												0.												0.												0.												0.												0.												0.												0.												0.												0.												0.												0.												0.												0.												0.												0.												0.												0.												0.												0.												0.												0.												0.												0.												0.												0.												0.												0.												0.												0.												0.												0.												0.												0.												0.												0.												0.												0.												0.												0.												0.												0.												0.												0.												0.												0.												0.												0.												0.												0.												0.												0.												0.												0.												0.												0.												0.												0.												0.												0.												0.												0.												0.												0.												0.												0.												0.												0.												0.												0.												0.												0.												0.												0.												0.												0.												0.												0.												0.												0.												0.												0.												0.												0.												0.												0.												0.												0.												0.												0.												0.												0.												0.												0.												0.												0.												0.												0.												0.												0.												0.												0.												0.												0.												0.												0.												0.												0.												0.												0.												0.												0.												0.												0.												0.												0.												0.												0.												0.												0.												0.												0.												0.												0.												0.												0.												0.												0.												0.												0.												0.												0.												0.												0.												0.												0.												0.												0.												0.												0.												0.												0.												0.												0.												0.												0.												0.												0.												0.												0.												0.												0.												0.												0.												0.												0.												0.												0.												0.												0.												0.												0.												0.												0.												0.												0.												0.												0.												0.												0.												0.												0.												0.												0.												0.												0.												0.												0.												0.												0.												0.												0.												0.												0.												0.												0.												0.												0.												0.												0.												0.												0.												0.												0.												0.												0.												0.												0.												0.												0.												0.												0.												0.												0.												0.												0.												0.												0.												0.												0.												0.												0.												0.												0.												0.												0.												0.												0.												0.												0.												0.												0.												0.												0.												0.												0.												0.												0.												0.												0.												0.												0.												0.												0.												0.												0.												0.												0.												0.												0.												0.												0.												0.												0.												0.												0.												0.												0.												0.												0.												0.												0.												0.												0.												0.												0.												0.												0.												0.												0.												0.												0.												0.												0.												0.												0.												0.												0.												0.												0.												0.												0.												0.												0.												0.												0.												0.												0.												0.												0.												0.												0.												0.												0.												0.												0.												0.												0.												0.												0.												0.												0.												0.												0.												0.												0.												0.												0.												0.												0.												0.												0.												0.												0.												0.												0.												0.												0.												0.												0.												0.												0.												0.												0.												0.												0.												0.												0.												0.												0.												0.												0.												0.												0.												0.												0.												0.												0.												0.												0.												0.												0.												0.												0.												0.												0.												0.												0.												0.												0.												0.												0.												0.												0.												0.												0.												0.												0.												0.												0.												0.												0.												0.												0.												0.												0.												0.												0.												0.												0.												0.												0.												0.												0.												0.												0.												0.												0.												0.												0.												0.												0.												0.												0.												0.												0.												0.												0.												0.												0.												0.												0.												0.												0.												0.												0.												0.												0.												0.												0.												0.												0.												0.												0.												0.												0.												0.												0.												0.												0.												0.												0.												0.												0.												0.												0.												0.												0.												0.												0.												0.												0.												0.												0.												0.												0.												0.												0.												0.												0.												0.												0.												0.												0.												0.												0.												0.												0.												0.												0.												0.												0.												0.												0.												0.												0.												0.												0.												0.												0.												0.												0.												0.												0.												0.												0.												0.												0.												0.												0.												0.												0.												0.												0.</											

Table 6b. Tensile Jamming Analysis of R.H. Regular Unit Cell (Compressive).

D= 7.771E+00												C1= 1.000E+01												N= 1.600E+01												SD= 1.000E+00												L1/N= 4.938E+00												MORE= 1.000E+00																																																																																																																																																																																																																																																																																																																																																																																																																																																																																																																																																																																																																																																																																																																																																																																																																																																																																																																																																																																																																																																																																																																																																																																																																																																																																																																																																																																																																																																																																																																																																																																																																																																																																																																																																																																																																																																																																																																																																																																																																																																																																																																																																																																																																																																																																																																																																																																																																																																																																																																																																																																																																																																																																																																																																																																																																																																																																																																																																																																																																																																																																																																																																																																																																																																																																																																																																																																																																																																																																																																																																																																																																																																																																																																																																																																																																																																																																																																																																																																																																																																																																																																																																																																																																																																																																																																																																																																																																																																																																																																																																																																																																																																																																																																																																																																																																																																																																																																																																																																																																																																																																			
COUNTER-CLOCKWISE												COUNTER-CLOCKWISE												COUNTER-CLOCKWISE												COUNTER-CLOCKWISE												COUNTER-CLOCKWISE												COUNTER-CLOCKWISE												COUNTER-CLOCKWISE												COUNTER-CLOCKWISE												COUNTER-CLOCKWISE												COUNTER-CLOCKWISE												COUNTER-CLOCKWISE												COUNTER-CLOCKWISE												COUNTER-CLOCKWISE												COUNTER-CLOCKWISE												COUNTER-CLOCKWISE												COUNTER-CLOCKWISE												COUNTER-CLOCKWISE												COUNTER-CLOCKWISE												COUNTER-CLOCKWISE												COUNTER-CLOCKWISE												COUNTER-CLOCKWISE												COUNTER-CLOCKWISE												COUNTER-CLOCKWISE												COUNTER-CLOCKWISE												COUNTER-CLOCKWISE												COUNTER-CLOCKWISE												COUNTER-CLOCKWISE												COUNTER-CLOCKWISE												COUNTER-CLOCKWISE												COUNTER-CLOCKWISE												COUNTER-CLOCKWISE												COUNTER-CLOCKWISE												COUNTER-CLOCKWISE												COUNTER-CLOCKWISE												COUNTER-CLOCKWISE												COUNTER-CLOCKWISE												COUNTER-CLOCKWISE												COUNTER-CLOCKWISE												COUNTER-CLOCKWISE												COUNTER-CLOCKWISE												COUNTER-CLOCKWISE												COUNTER-CLOCKWISE												COUNTER-CLOCKWISE												COUNTER-CLOCKWISE												COUNTER-CLOCKWISE												COUNTER-CLOCKWISE												COUNTER-CLOCKWISE												COUNTER-CLOCKWISE												COUNTER-CLOCKWISE												COUNTER-CLOCKWISE												COUNTER-CLOCKWISE												COUNTER-CLOCKWISE												COUNTER-CLOCKWISE												COUNTER-CLOCKWISE												COUNTER-CLOCKWISE												COUNTER-CLOCKWISE												COUNTER-CLOCKWISE												COUNTER-CLOCKWISE												COUNTER-CLOCKWISE												COUNTER-CLOCKWISE												COUNTER-CLOCKWISE												COUNTER-CLOCKWISE												COUNTER-CLOCKWISE												COUNTER-CLOCKWISE												COUNTER-CLOCKWISE												COUNTER-CLOCKWISE												COUNTER-CLOCKWISE												COUNTER-CLOCKWISE												COUNTER-CLOCKWISE												COUNTER-CLOCKWISE												COUNTER-CLOCKWISE												COUNTER-CLOCKWISE												COUNTER-CLOCKWISE												COUNTER-CLOCKWISE												COUNTER-CLOCKWISE												COUNTER-CLOCKWISE												COUNTER-CLOCKWISE												COUNTER-CLOCKWISE												COUNTER-CLOCKWISE												COUNTER-CLOCKWISE												COUNTER-CLOCKWISE												COUNTER-CLOCKWISE												COUNTER-CLOCKWISE												COUNTER-CLOCKWISE												COUNTER-CLOCKWISE												COUNTER-CLOCKWISE												COUNTER-CLOCKWISE												COUNTER-CLOCKWISE												COUNTER-CLOCKWISE												COUNTER-CLOCKWISE												COUNTER-CLOCKWISE												COUNTER-CLOCKWISE												COUNTER-CLOCKWISE												COUNTER-CLOCKWISE												COUNTER-CLOCKWISE												COUNTER-CLOCKWISE												COUNTER-CLOCKWISE												COUNTER-CLOCKWISE												COUNTER-CLOCKWISE												COUNTER-CLOCKWISE												COUNTER-CLOCKWISE												COUNTER-CLOCKWISE												COUNTER-CLOCKWISE												COUNTER-CLOCKWISE												COUNTER-CLOCKWISE												COUNTER-CLOCKWISE												COUNTER-CLOCKWISE												COUNTER-CLOCKWISE												COUNTER-CLOCKWISE												COUNTER-CLOCKWISE												COUNTER-CLOCKWISE												COUNTER-CLOCKWISE												COUNTER-CLOCKWISE												COUNTER-CLOCKWISE												COUNTER-CLOCKWISE												COUNTER-CLOCKWISE												COUNTER-CLOCKWISE												COUNTER-CLOCKWISE												COUNTER-CLOCKWISE												COUNTER-CLOCKWISE												COUNTER-CLOCKWISE												COUNTER-CLOCKWISE												COUNTER-CLOCKWISE												COUNTER-CLOCKWISE												COUNTER-CLOCKWISE												COUNTER-CLOCKWISE												COUNTER-CLOCKWISE												COUNTER-CLOCKWISE												COUNTER-CLOCKWISE												COUNTER-CLOCKWISE												COUNTER-CLOCKWISE												COUNTER-CLOCKWISE												COUNTER-CLOCKWISE												COUNTER-CLOCKWISE												COUNTER-CLOCKWISE												COUNTER-CLOCKWISE												COUNTER-CLOCKWISE												COUNTER-CLOCKWISE												COUNTER-CLOCKWISE												COUNTER-CLOCKWISE												COUNTER-CLOCKWISE												COUNTER-CLOCKWISE												COUNTER-CLOCKWISE												COUNTER-CLOCKWISE												COUNTER-CLOCKWISE												COUNTER-CLOCKWISE												COUNTER-CLOCKWISE												COUNTER-CLOCKWISE												COUNTER-CLOCKWISE												COUNTER-CLOCKWISE												COUNTER-CLOCKWISE												COUNTER-CLOCKWISE												COUNTER-CLOCKWISE												COUNTER-CLOCKWISE												COUNTER-CLOCKWISE												COUNTER-CLOCKWISE												COUNTER-CLOCKWISE												COUNTER-CLOCKWISE												COUNTER-CLOCKWISE												COUNTER-CLOCKWISE												COUNTER-CLOCKWISE												COUNTER-CLOCKWISE												COUNTER-CLOCKWISE												COUNTER-CLOCKWISE												COUNTER-CLOCKWISE												COUNTER-CLOCKWISE												COUNTER-CLOCKWISE												COUNTER-CLOCKWISE												COUNTER-CLOCKWISE												COUNTER-CLOCKWISE												COUNTER-CLOCKWISE												COUNTER-CLOCKWISE												COUNTER-CLOCKWISE												COUNTER-CLOCKWISE												COUNTER-CLOCKWISE												COUNTER-CLOCKWISE												COUNTER-CLOCKWISE												COUNTER-CLOCKWISE												COUNTER-CLOCKWISE												COUNTER-CLOCKWISE												COUNTER-CLOCKWISE												COUNTER-CLOCKWISE												COUNTER-CLOCKWISE												COUNTER-CLOCKWISE												COUNTER-CLOCKWISE												COUNTER-CLOCKWISE												COUNTER-CLOCKWISE												COUNTER-CLOCKWISE												COUNTER-CLOCKWISE												COUNTER-CLOCKWISE												COUNTER-CLOCKWISE												COUNTER-CLOCKWISE												COUNTER-CLOCKWISE												COUNTER-CLOCKWISE												COUNTER-CLOCKWISE												COUNTER-CLOCKWISE												COUNTER-CLOCKWISE												COUNTER-CLOCKWISE												COUNTER-CLOCKWISE												COUNTER-CLOCKWISE												COUNTER-CLOCKWISE												COUNTER-CLOCKWISE												COUNTER-CLOCKWISE												COUNTER-CLOCKWISE												COUNTER-CLOCKWISE												COUNTER-CLOCKWISE												COUNTER-CLOCKWISE												COUNTER-CLOCKWISE												COUNTER-CLOCKWISE												COUNTER-CLOCKWISE												COUNTER-CLOCKWISE												COUNTER-CLOCKWISE												COUNTER-CLOCKWISE												COUNTER-CLOCKWISE												COUNTER-CLOCKWISE												COUNTER-CLOCKWISE												COUNTER-CLOCKWISE												COUNTER-CLOCKWISE												COUNTER-CLOCKWISE												COUNTER-CLOCKWISE												COUNTER-CLOCKWISE												COUNTER-CLOCKWISE												COUNTER-CLOCKWISE												COUNTER-CLOCKWISE												COUNTER-CLOCKWISE												COUNTER-CLOCKWISE												COUNTER-CLOCKWISE												COUNTER-CLOCKWISE												COUNTER-CLOCKWISE												COUNTER-CLOCKWISE												COUNTER-CLOCKWISE												COUNTER-CLOCKWISE												COUNTER-CLOCKWISE												COUNTER-CLOCKWISE												COUNTER-CLOCKWISE												COUNTER-CLOCKWISE												COUNTER-CLOCKWISE												COUNTER-CLOCKWISE												COUNTER-CLOCKWISE												COUNTER-CLOCKWISE												COUNTER-CLOCKWISE												COUNTER-CLOCKWISE												COUNTER-CLOCKWISE												COUNTER-CLOCKWISE												COUNTER-CLOCKWISE												COUNTER-CLOCKWISE												COUNTER-CLOCKWISE												COUNTER-CLOCKWISE												COUNTER-CLOCKWISE												COUNTER-CLOCKWISE												COUNTER-CLOCKWISE												COUNTER-CLOCKWISE												COUNTER-CLOCKWISE												COUNTER-CLOCKWISE												COUNTER-CLOCKWISE												COUNTER-CLOCKWISE												COUNTER-CLOCKWISE												COUNTER-CLOCKWISE												COUNTER-CLOCKWISE												COUNTER-CLOCKWISE												COUNTER-CLOCKWISE												COUNTER-CLOCKWISE												COUNTER-CLOCKWISE												COUNTER-CLOCKWISE												COUNTER-CLOCKWISE												COUNTER-CLOCKWISE												COUNTER-CLOCKWISE												COUNTER-CLOCKWISE												COUNTER-CLOCKWISE												COUNTER-CLOCKWISE												COUNTER-CLOCKWISE												COUNTER-CLOCKWISE												COUNTER-CLOCKWISE												COUNTER-CLOCKWISE												COUNTER-CLOCKWISE												COUNTER-CLOCKWISE												COUNTER-CLOCKWISE												COUNTER-CLOCKWISE												COUNTER-CLOCKWISE												COUNTER-CLOCKWISE												COUNTER-CLOCKWISE												COUNTER-CLOCKWISE												COUNTER-CLOCKWISE												COUNTER-CLOCKWISE												COUNTER-CLOCKWISE												COUNTER-CLOCKWISE												COUNTER-CLOCKWISE												COUNTER-CLOCKWISE												COUNTER-CLOCKWISE												COUNTER-CLOCKWISE												COUNTER-CLOCKWISE												COUNTER-CLOCKWISE												COUNTER-CLOCKWISE												COUNTER-CLOCKWISE												COUNTER-CLOCKWISE												COUNTER-CLOCKWISE												COUNTER-CLOCKWISE												COUNTER-CLOCKWISE												COUNTER-CLOCKWISE												COUNTER-CLOCKWISE												COUNTER-CLOCKWISE												COUNTER-CLOCKWISE												COUNTER-CLOCKWISE												COUNTER-CLOCKWISE												COUNTER-CLOCKWISE												COUNTER-CLOCKWISE												COUNTER-CLOCKWISE												COUNTER-CLOCKWISE												COUNTER-CLOCKWISE												COUNTER-CLOCKWISE												COUNTER-CLOCKWISE												COUNTER-CLOCKWISE												COUNTER-CLOCKWISE												COUNTER-CLOCKWISE												COUNTER-CLOCKWISE												COUNTER-CLOCKWISE												COUNTER-CLOCKWISE												COUNTER-CLOCKWISE												COUNTER-CLOCKWISE												COUNTER-CLOCKWISE												COUNTER-CLOCKWISE												COUNTER-CLOCKWISE												COUNTER-CLOCKWISE												COUNTER-CLOCKWISE												COUNTER-CLOCKWISE												COUNTER-CLOCKWISE												COUNTER-CLOCKWISE												COUNTER-CLOCKWISE												COUNTER-CLOCKWISE												COUNTER-CLOCKWISE												COUNTER-CLOCKWISE												COUNTER-CLOCKWISE												COUNTER-CLOCKWISE												COUNTER-CLOCKWISE												COUNTER-CLOCKWISE												COUNTER-CLOCKWISE												COUNTER-CLOCKWISE												COUNTER-CLOCKWISE												COUNTER-CLOCKWISE												COUNTER-CLOCKWISE												COUNTER-CLOCKWISE												COUNTER-CLOCKWISE												COUNTER-CLOCKWISE												COUNTER-CLOCKWISE												COUNTER-CLOCKWISE												COUNTER-CLOCKWISE												COUNTER-CLOCKWISE												COUNTER-CLOCKWISE												COUNTER-CLOCKWISE												COUNTER-CLOCKWISE												COUNTER-CLOCKWISE												COUNTER-CLOCKWISE												COUNTER-CLOCKWISE												COUNTER-CLOCKWISE												COUNTER-CLOCKWISE												COUNTER-CLOCKWISE												COUNTER-CLOCKWISE												COUNTER-CLOCKWISE												COUNTER-CLOCKWISE												COUNTER-CLOCKWISE												COUNTER-CLOCKWISE												COUNTER-CLOCKWISE												COUNTER-CLOCKWISE												COUNTER-CLOCKWISE												COUNTER-CLOCKWISE												COUNTER-CLOCKWISE												COUNTER-CLOCKWISE												COUNTER-CLOCKWISE												COUNTER-CLOCKWISE												COUNTER-CLOCKWISE												COUNTER-CLOCKWISE												COUNTER-CLOCKWISE												COUNTER-CLOCKWISE												COUNTER-CLOCKWISE												COUNTER-CLOCKWISE												COUNTER-CLOCKWISE												COUNTER-CLOCKWISE												COUNTER-CLOCKWISE												COUNTER-CLOCKWISE												COUNTER-CLOCKWISE												COUNTER-CLOCKWISE												COUNTER-CLOCKWISE												COUNTER-CLOCKWISE												COUNTER-CLOCKWISE												COUNTER-CLOCKWISE												COUNTER-CLOCKWISE												COUNTER-CLOCKWISE												COUNTER-CLOCKWISE												COUNTER-CLOCKWISE												COUNTER-CLOCKWISE												COUNTER-CLOCKWISE												COUNTER-CLOCKWISE												COUNTER-CLOCKWISE												COUNTER-CLOCKWISE												COUNTER-CLOCKWISE												COUNTER-CLOCKWISE												COUNTER-CLOCKWISE												COUNTER-CLOCKWISE												COUNTER-CLOCKWISE												COUNTER-CLOCKWISE												COUNTER-CLOCKWISE												COUNTER-CLOCKWISE												COUNTER-CLOCKWISE												COUNTER-CLOCKWISE												COUNTER-CLOCKWISE												COUNTER-CLOCKWISE												COUNTER-CLOCKWISE												COUNTER-CLOCKWISE												COUNTER-CLOCKWISE												COUNTER-CLOCKWISE												COUNTER-CLOCKWISE												COUNTER-CLOCK											

Table 7b. Compressive Jamming Analysis of R.H. Regular Unit Cell (Compressive).

D= 2.392E+01	Q1= 7.200E+01	N= 1.000E+01	SD= 1.000E+00	LI/A= 4.939E+00	MODE= 1.000E+00					
COUNTER-CLOCKWISE (ALTERNATING TOP LEG)										
(°)	S	X	Y	Z	WX	WY	Q0	JO	GC	GT
1.	0.	1.000E+00	0.	0.	0.	9.500E-01	7.260E-01	0.	2.610E-01	5.956E-02
2.	1.360E-01	9.914E-01	2.440E-01	7.031E-02	-0.602E-02	9.520E-01	7.269E-01	-0.335E-04	2.500E-01	5.944E-02
3.	3.427E-01	9.653E-01	4.942E-01	1.520E-01	-2.317E-01	9.440E-01	7.270E-01	-2.212E-03	2.500E-01	5.974E-02
4.	5.930E-01	9.200E-01	7.303E-01	2.200E-01	-3.970E-01	9.330E-01	7.274E-01	-2.316E-03	2.340E-01	5.950E-02
5.	7.994E-01	8.604E-01	9.712E-01	3.050E-01	-5.010E-01	9.230E-01	7.284E-01	-2.340E-03	2.210E-01	5.900E-02
6.	9.570E-01	7.990E-01	1.207E+00	3.810E-01	-6.010E-01	9.000E-01	7.290E-01	-2.340E-03	2.000E-01	5.704E-02
7.	1.070E-01	7.000E-01	1.440E+00	4.570E-01	-3.510E-01	8.430E-01	7.295E-01	7.365E-02	1.800E-01	1.774E-01
8.	1.370E-01	6.000E-01	1.670E+00	5.340E-01	-3.910E-01	8.730E-01	7.294E-01	1.325E-01	1.560E-01	1.390E-01
9.	1.570E-01	5.000E-01	1.890E+00	6.100E-01	-4.570E-01	8.930E-01	7.294E-01	2.302E-01	1.320E-01	1.017E-01
10.	1.700E-01	4.000E-01	2.110E+00	6.860E-01	-4.530E-01	8.740E-01	7.294E-01	3.620E-01	1.060E-01	2.849E-01
11.	1.800E-01	3.000E-01	2.330E+00	7.630E-01	-4.710E-01	8.280E-01	7.287E-01	5.440E-01	7.900E-02	4.680E-01
12.	2.000E-01	2.000E-01	2.560E+00	8.390E-01	-4.860E-01	8.280E-01	7.270E-01	6.520E-01	5.720E-02	1.097E+00
13.	2.100E-01	1.000E-01	2.780E+00	9.150E-01	-4.960E-01	9.130E-01	7.260E-01	8.360E-01	2.720E-02	4.067E+00
14.	2.200E-01	0.	2.990E+00	9.920E-01	-4.90E-01	8.130E-01	7.242E-01	1.130E+00	1.440E-02	1.413E-01
15.	2.300E-01	-0.500E-01	3.190E+00	1.060E+00	-4.90E-01	8.130E-01	7.220E-01	1.420E+00	5.330E-02	2.244E+00
16.	2.400E-01	-1.000E-01	3.390E+00	1.140E+00	-4.810E-01	8.130E-01	7.194E-01	1.760E+00	8.140E-02	7.112E-01
17.	2.440E-01	-1.400E-01	3.570E+00	1.220E+00	-4.670E-01	8.260E-01	7.176E-01	1.540E+00	8.630E-02	3.407E-01
18.	2.450E-01	-1.600E-01	3.730E+00	1.290E+00	-4.460E-01	8.370E-01	7.156E-01	1.706E+00	1.080E-01	2.305E-01
19.	2.450E-01	-1.600E-01	3.950E+00	1.370E+00	-4.210E-01	8.430E-01	7.141E-01	1.864E+00	1.250E-01	1.442E-01
20.	2.450E-01	-1.600E-01	4.170E+00	1.450E+00	-3.920E-01	8.620E-01	7.130E-01	2.015E+00	1.360E-01	1.171E-01
21.	2.450E-01	-1.600E-01	4.380E+00	1.520E+00	-3.620E-01	8.740E-01	7.127E-01	2.161E+00	1.400E-01	1.092E-01
CLOCKWISE (ALTERNATING BOTTOM LEG)										
(°)	S	X	Y	Z	WX	WY	Q0	JO	GC	GT
1.	0.	0.	0.	0.	0.	9.470E-01	7.127E-01	0.	1.400E-01	1.092E-01
2.	2.370E-01	3.940E-03	2.231E-01	-7.631E-02	3.233E-02	9.470E-01	7.170E-01	-6.335E-04	1.360E-01	1.171E-01
3.	4.760E-01	1.560E-01	4.500E-01	-1.520E-01	9.330E-02	9.456E-01	7.141E-01	-2.212E-03	1.250E-01	1.440E-01
4.	7.160E-01	3.450E-02	6.770E-01	-2.280E-01	9.230E-02	9.420E-01	7.156E-01	-2.316E-03	1.080E-01	2.045E-01
5.	9.590E-01	5.990E-02	9.007E-01	-3.050E-01	1.158E-01	9.420E-01	7.176E-01	-2.340E-03	8.630E-02	3.407E-01
6.	1.200E+00	7.990E-01	1.130E+00	-3.810E-01	1.330E-01	9.410E-01	7.194E-01	2.308E-02	5.140E-02	7.112E-01
7.	1.450E+00	1.070E-01	1.371E+00	-4.570E-01	1.440E-01	9.410E-01	7.220E-01	7.365E-02	3.530E-02	2.244E+00
8.	1.700E+00	1.370E-01	1.600E+00	-5.340E-01	1.430E-01	9.410E-01	7.242E-01	1.325E-01	1.440E-02	1.413E-01
9.	1.950E+00	1.570E-01	1.890E+00	-6.100E-01	1.470E-01	9.400E-01	7.260E-01	2.302E-01	2.720E-02	4.067E+00
10.	2.200E+00	1.700E-01	2.110E+00	-6.860E-01	1.470E-01	9.400E-01	7.270E-01	3.620E-01	5.320E-02	1.097E+00
11.	2.400E+00	1.800E-01	2.330E+00	-7.630E-01	1.200E-01	9.400E-01	7.287E-01	5.440E-01	7.900E-02	4.680E-01
12.	2.500E+00	1.900E-01	2.560E+00	-8.390E-01	9.650E-02	9.512E-01	7.294E-01	6.520E-01	1.060E-01	2.849E-01
13.	2.590E+00	2.000E-01	2.780E+00	-9.150E-01	6.550E-02	9.500E-01	7.294E-01	8.360E-01	1.320E-01	1.017E-01
14.	2.650E+00	2.100E-01	2.990E+00	-9.920E-01	2.790E-02	9.500E-01	7.294E-01	1.017E+00	1.560E-01	1.390E-01
15.	2.700E+00	2.200E-01	3.190E+00	-1.060E+00	1.370E-02	9.500E-01	7.294E-01	1.325E-01	1.800E-01	1.017E-01
16.	2.740E+00	2.300E-01	3.390E+00	-1.140E+00	-6.560E-02	9.460E-01	7.290E-01	1.760E+00	2.020E-02	8.729E-02
17.	2.770E+00	2.400E-01	3.570E+00	-1.220E+00	-1.000E-01	9.470E-01	7.294E-01	2.161E+00	2.210E-01	7.405E-02
18.	2.790E+00	2.500E-01	3.730E+00	-1.290E+00	-1.780E-01	9.380E-01	7.270E-01	1.864E+00	2.390E-01	6.530E-02
19.	2.800E+00	2.600E-01	3.950E+00	-1.370E+00	-2.030E-01	9.340E-01	7.270E-01	2.015E+00	2.500E-01	5.664E-02
20.	2.800E+00	2.600E-01	4.170E+00	-1.450E+00	-3.020E-01	9.040E-01	7.260E-01	2.161E+00	2.500E-01	5.664E-02
21.	2.800E+00	2.600E-01	4.380E+00	-1.520E+00	-3.620E-01	8.800E-01	7.260E-01	2.161E+00	2.610E-01	5.565E-02

Table 8c. Mid-Point Jamming Analysis of R.H. Regular Unit Cell (Extensive),
(Non-Alternating Leg Occupies Maximum Radial Position).

0=	2.776E+01	Q1=	4.500E+01	N=	1.600E+01	SO=	1.000E+00	L1/N=	4.938E+00	MODE=	1.000E+00
COUNTER-CLOCKWISE (NON-ALTERNATING LEFT LEG)											
(°)	S	X	Y	Z	WX	WY	WZ	Q0	JD	GC	GT
0.	0.	0.	0.	0.	0.	0.	0.	0.	0.	0.	0.
1.	1.33E-02	4.537E-03	1.279E-01	1.742E-01	7.762E-02	6.462E-01	4.334E-01	4.334E-01	3.031E-02	1.579E-01	2.27E-01
2.	1.33E-02	1.742E-01	3.304E-01	3.304E-01	7.357E-02	6.474E-01	4.373E-01	4.373E-01	1.221E-01	1.547E-01	2.27E-01
3.	5.33E-02	3.935E-02	4.972E-01	5.288E-01	1.031E-01	6.837E-01	4.172E-01	4.172E-01	2.733E-01	1.447E-01	3.08E-01
4.	7.33E-02	1.020E+00	6.032E-02	6.032E-02	1.341E-01	6.937E-01	4.473E-01	4.473E-01	4.741E-01	1.279E-01	5.31E-01
5.	9.31E-02	1.277E+00	1.253E-01	1.253E-01	1.504E-01	6.937E-01	4.533E-01	4.533E-01	7.132E-01	1.074E-01	8.95E-01
6.	1.17E-01	1.536E+00	1.463E-01	1.463E-01	1.723E-01	6.976E-01	4.593E-01	4.593E-01	9.403E-01	8.472E-02	8.95E-01
7.	1.37E-01	1.795E+00	1.913E-01	1.913E-01	1.844E-01	7.023E-01	4.650E-01	4.650E-01	1.269E+00	6.037E-02	1.793E+00
8.	1.57E-01	2.055E+00	2.379E-01	2.379E-01	1.834E-01	7.139E-01	4.694E-01	4.694E-01	1.571E+00	3.386E-02	4.286E+00
9.	1.77E-01	2.315E+00	2.845E-01	2.845E-01	1.792E-01	7.074E-01	4.737E-01	4.737E-01	1.935E+00	3.206E-02	6.734E+00
10.	1.97E-01	2.574E+00	3.291E-01	3.291E-01	1.638E-01	7.000E-01	4.764E-01	4.764E-01	2.222E+00	6.602E-02	1.66E+00
11.	2.15E-01	2.832E+00	3.699E-01	3.699E-01	1.422E-01	6.932E-01	4.782E-01	4.782E-01	2.506E+00	9.142E-02	8.77E-01
12.	2.33E-01	3.090E+00	4.040E-01	4.040E-01	1.199E-01	7.313E-01	4.782E-01	4.782E-01	2.786E+00	1.164E-01	5.51E-01
13.	2.50E-01	3.348E+00	4.319E-01	4.319E-01	8.666E-02	7.352E-01	4.775E-01	4.775E-01	3.069E+00	1.409E-01	3.85E-01
14.	2.74E-01	3.597E+00	4.495E-01	4.495E-01	4.702E-02	7.375E-01	4.760E-01	4.760E-01	3.353E+00	1.647E-01	2.86E-01
15.	2.94E-01	3.847E+00	4.554E-01	4.554E-01	2.019E-02	7.360E-01	4.740E-01	4.740E-01	3.984E+00	1.969E-01	2.08E-01
16.	3.14E-01	4.094E+00	4.495E-01	4.495E-01	-4.869E-02	7.316E-01	4.716E-01	4.716E-01	4.355E+00	2.068E-01	1.973E-01
17.	3.34E-01	4.338E+00	4.301E-01	4.301E-01	1.032E-01	7.232E-01	4.693E-01	4.693E-01	4.728E+00	2.237E-01	1.64E-01
18.	3.54E-01	4.582E+00	3.905E-01	3.905E-01	1.605E-01	7.103E-01	4.674E-01	4.674E-01	5.101E+00	2.366E-01	1.48E-01
19.	3.74E-01	4.822E+00	3.421E-01	3.421E-01	2.193E-01	6.928E-01	4.661E-01	4.661E-01	5.472E+00	2.447E-01	1.31E-01
20.	3.97E-01	5.062E+00	2.851E-01	2.851E-01	2.773E-01	6.709E-01	4.657E-01	4.657E-01	6.186E+00	2.475E-01	1.35E-01
21.	3.37E-01	5.062E+00	2.851E-01	2.851E-01	-2.773E-01	6.709E-01	4.657E-01	4.657E-01	6.186E+00	2.475E-01	1.35E-01

CLOCKWISE (NON-ALTERNATING LEFT LEG)

Table 8d. Mid-Point Jamming Analysis of R.H. Regular Unit Cell (Compressive),
(Non-Alternating Leg Occupies Maximum Radial Position).

D= 1.775E+00	Q1= 4.500E+01	N= 1.600E+01	SD= 1.000E+00	L1/N= 4.938E+00	MODE= 1.000E+00					
COUNTER-CLOCKWISE (ALTERNATING TOP LEG)										
(θ)	S	X	Y	Z	WX	WY	Q0	J0	GC	GT
1.	0.	0.	0.	0.	0.	0.	4.234E+01	0.	1.579E-01	2.20E-01
2.	2.50E+00	4.537E+03	1.609E+01	1.744E+01	3.72E-02	0.856E-01	4.34E+01	2.160E+02	1.54E-01	2.33E-01
3.	3.92E+02	5.30E+00	1.798E+02	3.32E+01	3.492E+01	6.84E-01	4.37E+01	7.58E-01	1.49E-01	2.74E-01
4.	5.91E+02	7.63E+00	3.995E+02	4.97E+01	5.238E+01	1.00E-01	4.41E+01	1.94E-01	1.39E-01	4.47E-01
5.	7.55E+02	1.03E+00	6.93E+00	6.59E+01	6.94E+01	6.98E-01	4.43E+01	3.45E+01	1.47E-01	5.31E-01
6.	9.81E+02	1.27E+00	1.05E+01	8.39E+01	8.73E+01	1.55E-01	4.47E+01	6.33E+01	1.47E-01	9.93E-02
7.	1.17E+03	1.53E+00	1.40E+01	1.01E+02	1.04E+02	1.73E-01	4.50E+01	9.18E+01	6.57E-01	7.79E+00
8.	1.37E+03	1.79E+00	1.79E+01	1.14E+02	1.17E+02	7.07E-01	4.65E+01	1.22E+00	7.96E-02	4.23E+00
9.	1.57E+03	2.05E+00	2.07E+01	1.36E+02	1.39E+02	7.07E-01	4.69E+01	1.54E+00	3.20E-02	6.73E+00
10.	1.75E+03	2.31E+00	2.34E+01	1.59E+02	1.57E+02	1.73E-01	4.73E+01	1.86E+00	4.41E-02	1.51E+00
11.	1.96E+03	2.57E+00	2.62E+01	1.81E+02	1.74E+02	7.20E-01	4.78E+01	2.18E+00	6.69E-02	1.63E+00
12.	2.16E+03	2.83E+00	2.89E+01	2.03E+02	1.92E+02	7.25E-01	4.77E+01	2.57E+00	9.14E-02	4.76E-01
13.	2.35E+03	3.09E+00	3.16E+01	2.25E+02	2.09E+02	7.37E-01	4.78E+01	3.14E+00	1.16E-01	5.51E-01
14.	2.55E+03	3.35E+00	3.43E+01	2.47E+02	2.27E+02	7.32E-01	4.77E+01	3.28E+00	1.44E-01	3.82E-01
15.	2.74E+03	3.61E+00	3.70E+01	2.69E+02	2.45E+02	7.30E-01	4.76E+01	3.63E+00	1.67E-01	2.95E-02
16.	2.94E+03	3.87E+00	3.97E+01	2.91E+02	2.61E+02	7.35E-01	4.74E+01	3.72E+00	1.86E-01	2.25E-02
17.	3.14E+03	4.13E+00	4.24E+01	3.13E+02	2.79E+02	7.31E-01	4.71E+01	4.30E+00	2.56E-01	1.75E-01
18.	3.33E+03	4.39E+00	4.51E+01	3.35E+02	2.96E+02	7.23E-01	4.69E+01	4.64E+00	2.37E-01	1.62E-01
19.	3.53E+03	4.65E+00	4.78E+01	3.57E+02	3.14E+02	7.13E-01	4.67E+01	4.71E+00	2.36E-01	1.46E-01
20.	3.73E+03	4.91E+00	5.05E+01	3.79E+02	3.31E+02	6.98E-01	4.66E+01	5.30E+00	2.47E-01	1.38E-01
21.	3.92E+03	5.06E+00	5.32E+01	4.01E+02	3.49E+02	6.70E-01	4.65E+01	5.63E+00	2.475E-01	1.35E-01
CLOCKWISE (ALTERNATING BOTTOM LEG)										
(θ)	S	X	Y	Z	WX	WY	Q0	J0	GC	GT
1.	0.	0.	0.	0.	0.	0.	4.657E+01	0.	2.475E-01	1.35E-01
2.	2.40E+00	1.920E+03	1.83E+01	1.746E+01	6.23E-02	7.24E-01	4.66E+01	2.16E-02	2.447E-01	1.34E-01
3.	4.81E+01	9.49E+01	3.67E+01	3.492E+01	1.23E-01	7.17E-01	4.67E+01	7.62E-02	2.36E-01	1.46E-01
4.	7.23E+01	2.23E+02	5.47E+01	5.238E+01	1.81E-01	7.07E-01	4.69E+01	1.94E-01	2.37E-01	1.62E-01
5.	9.64E+01	4.75E+01	7.63E+01	6.94E+01	2.33E-01	6.94E-01	4.71E+01	3.45E-01	2.36E-01	1.67E-01
6.	1.20E+02	6.69E+01	9.80E+01	8.73E+01	2.83E-01	6.79E-01	4.74E+01	6.33E+01	1.66E-01	2.25E-01
7.	1.45E+02	9.40E+01	1.20E+02	1.04E+02	3.26E-01	6.62E-01	4.76E+01	9.18E+01	1.647E-01	2.56E-01
8.	1.70E+02	1.40E+02	1.20E+02	1.22E+02	3.61E-01	6.61E-01	4.77E+01	1.22E+00	1.64E-01	3.52E-01
9.	1.95E+02	1.85E+02	1.45E+02	1.39E+02	3.96E-01	6.29E-01	4.78E+01	1.54E+00	5.52E-01	5.52E-01
10.	2.20E+02	2.30E+02	1.70E+02	1.57E+02	4.13E-01	6.14E-01	4.77E+01	1.86E+00	9.14E-02	9.76E-01
11.	2.45E+02	2.75E+02	1.95E+02	1.74E+02	4.29E-01	6.01E-01	4.76E+01	2.18E+00	6.92E-02	1.60E+00
12.	2.70E+02	3.20E+02	2.20E+02	1.92E+02	4.37E-01	5.91E-01	4.76E+01	2.50E+00	4.91E-02	3.51E+00
13.	2.95E+02	3.65E+02	2.45E+02	2.09E+02	4.43E-01	5.83E-01	4.69E+01	2.82E+00	3.26E-02	6.73E+00
14.	3.20E+02	4.10E+02	2.70E+02	2.27E+02	4.34E-01	5.79E-01	4.65E+01	3.14E+00	3.96E-02	4.75E+00
15.	3.45E+02	4.55E+02	2.95E+02	2.44E+02	4.21E-01	5.78E-01	4.59E+01	3.46E+00	6.97E-02	1.79E+00
16.	3.70E+02	5.00E+02	3.20E+02	2.61E+02	4.00E-01	5.81E-01	4.53E+01	3.78E+00	8.32E-02	8.95E-01
17.	3.95E+02	5.45E+02	3.45E+02	2.79E+02	3.82E-01	5.86E-01	4.47E+01	4.10E+00	1.07E-01	3.51E-01
18.	4.20E+02	5.90E+02	3.70E+02	2.96E+02	3.63E-01	5.95E-01	4.41E+01	4.42E+00	1.27E-01	3.50E-01
19.	4.45E+02	6.35E+02	3.95E+02	3.14E+02	3.33E-01	6.06E-01	4.37E+01	4.74E+00	1.44E-01	2.74E-01
20.	4.70E+02	6.80E+02	4.20E+02	3.31E+02	2.95E-01	6.19E-01	4.34E+01	5.06E+00	1.54E-01	2.34E-01
21.	4.95E+02	7.25E+02	4.45E+02	3.49E+02	2.67E-01	6.34E-01	4.33E+01	5.38E+00	1.54E-01	2.20E-01

Table 10a. Compressive Jamming Analysis of Diamond Unit Cell (Extensive).

D= 2.352E+01	Q1= 7.200E+01	N= 1.600E+01	SD= 1.000E+00	L1/N= 4.975E+00	MODE= 1.000E+00					
(θ)										
COUNTER-CLOCKWISE (ALTERNATING RIGHT LEG)										
	S	X	Y	Z	WX	WY	CO	JO	GC	GT
1.	0.	1.000E+00	0.	0.	0.	9.547E-01	7.269E+01	0.	2.669E-01	5.747E-02
2.	6.51E-01	9.455E-01	2.415E-01	7.533E-02	-6.721E-02	9.524E-01	7.270E+01	1.184E-02	2.639E-01	5.744E-02
3.	3.37E-02	9.601E-01	4.822E-01	1.507E-01	-1.324E-01	9.457E-01	7.274E+01	8.459E-02	2.558E-01	6.050E-02
4.	5.34E-02	9.243E-01	7.224E-01	2.260E-01	-1.954E-01	9.350E-01	7.279E+01	4.178E-01	2.433E-01	6.622E-02
5.	7.43E-02	8.639E-01	9.533E-01	3.013E-01	-2.537E-01	9.213E-01	7.286E+01	4.003E-01	2.322E-01	7.624E-02
6.	9.43E-02	7.957E-01	1.442E+00	3.767E-01	-3.058E-01	9.053E-01	7.292E+01	6.427E-01	2.061E-01	8.371E-02
7.	1.17E-01	7.102E-01	1.822E+00	4.526E-01	-3.519E-01	8.893E-01	7.297E+01	9.130E-01	1.837E-01	1.092E-01
8.	1.37E-01	6.135E-01	1.864E+00	5.277E-01	-3.861E-01	8.741E-01	7.303E+01	1.203E+00	1.569E-01	1.416E-01
9.	1.57E-01	5.172E-01	1.871E+00	6.027E-01	-4.203E-01	8.584E-01	7.308E+01	1.509E+00	1.321E-01	1.952E-01
10.	1.77E-01	4.232E-01	2.040E+00	6.780E-01	-4.545E-01	8.402E-01	7.312E+01	1.823E+00	1.085E-01	2.495E-01
11.	1.95E-01	3.311E-01	2.304E+00	7.533E-01	-4.774E-01	8.240E-01	7.316E+01	2.160E+00	8.109E-02	3.133E-01
12.	2.11E-01	2.494E-01	2.514E+00	8.267E-01	-4.945E-01	8.104E-01	7.319E+01	2.606E+00	5.383E-02	4.133E-01
13.	2.25E-01	1.891E-01	2.722E+00	9.043E-01	-5.095E-01	8.000E-01	7.322E+01	3.135E+00	2.735E-02	4.702E-01
14.	2.37E-01	1.422E-01	2.924E+00	9.793E-01	-5.014E-01	8.109E-01	7.323E+01	3.577E+00	1.503E-02	5.184E-01
15.	2.47E-01	1.068E-01	3.125E+00	1.055E+00	-4.934E-01	8.123E-01	7.324E+01	4.027E+00	7.703E-02	5.575E-01
16.	2.55E-01	8.468E-02	3.325E+00	1.137E+00	-4.853E-01	8.173E-01	7.325E+01	4.469E+00	6.387E-02	5.894E-01
17.	2.62E-01	6.620E-02	3.525E+00	1.205E+00	-4.634E-01	8.254E-01	7.326E+01	5.156E+00	5.942E-02	6.135E-01
18.	2.67E-01	5.728E-02	3.723E+00	1.281E+00	-4.444E-01	8.360E-01	7.326E+01	5.784E+00	1.120E-01	2.050E-01
19.	2.70E-01	4.761E-02	3.923E+00	1.356E+00	-4.223E-01	8.494E-01	7.326E+01	6.262E+00	1.298E-01	1.450E-01
20.	2.71E-01	3.721E-02	4.124E+00	1.431E+00	-3.974E-01	8.616E-01	7.326E+01	6.785E+00	1.412E-01	1.140E-01
21.	2.72E-01	2.604E-02	4.327E+00	1.507E+00	-3.624E-01	8.749E-01	7.326E+01	7.257E+00	1.451E-01	1.101E-01

(θ)										
CLOCKWISE (ALTERNATING LEFT LEG)										
	S	X	Y	Z	WX	WY	CO	JO	GC	GT
1.	0.	1.000E+00	0.	0.	0.	-9.547E-01	7.269E+01	0.	1.459E-01	-1.101E-01
2.	2.36E-01	2.975E-01	-2.221E-01	7.533E-02	3.373E-02	-9.566E-01	7.269E+01	1.984E-02	1.412E-01	-1.193E-01
3.	4.71E-01	1.571E-01	-4.479E-01	1.507E-01	6.870E-02	-9.455E-01	7.274E+01	8.855E-02	1.298E-01	-1.458E-01
4.	7.07E-01	3.479E-01	-6.639E-01	2.260E-01	9.431E-02	-9.440E-01	7.279E+01	2.173E-01	1.120E-01	-2.052E-01
5.	9.46E-01	6.032E-01	-8.947E-01	3.013E-01	1.182E-01	-9.424E-01	7.286E+01	4.033E-01	8.946E-02	-2.401E-01
6.	1.18E-01	9.129E-01	-1.123E+00	3.767E-01	1.364E-01	-9.412E-01	7.292E+01	6.427E-01	6.381E-02	-2.045E-01
7.	1.39E-01	8.263E-01	-1.323E+00	4.526E-01	1.481E-01	-9.406E-01	7.297E+01	9.130E-01	3.700E-02	-2.192E-01
8.	1.54E-01	7.393E-01	-1.547E+00	5.277E-01	1.529E-01	-9.410E-01	7.303E+01	1.203E+00	2.735E-02	-2.343E-01
9.	1.74E-01	6.420E-01	-1.742E+00	6.027E-01	1.569E-01	-9.424E-01	7.308E+01	1.509E+00	2.061E-02	-2.495E-01
10.	1.93E-01	5.494E-01	-1.932E+00	6.780E-01	1.612E-01	-9.447E-01	7.312E+01	1.823E+00	1.321E-02	-2.647E-01
11.	2.10E-01	4.568E-01	-2.104E+00	7.533E-01	1.652E-01	-9.477E-01	7.316E+01	2.160E+00	8.109E-02	-2.800E-01
12.	2.25E-01	3.642E-01	-2.257E+00	8.267E-01	1.691E-01	-9.509E-01	7.319E+01	2.606E+00	5.383E-02	-2.952E-01
13.	2.37E-01	2.716E-01	-2.373E+00	9.043E-01	1.728E-01	-9.538E-01	7.322E+01	3.135E+00	2.735E-02	-3.104E-01
14.	2.47E-01	1.790E-01	-2.474E+00	9.793E-01	1.765E-01	-9.558E-01	7.323E+01	3.577E+00	1.503E-02	-3.256E-01
15.	2.55E-01	1.362E-01	-2.552E+00	1.055E+00	1.800E-01	-9.581E-01	7.324E+01	4.027E+00	7.703E-02	-3.408E-01
16.	2.62E-01	9.492E-02	-2.624E+00	1.137E+00	1.836E-01	-9.588E-01	7.324E+01	4.469E+00	6.387E-02	-3.560E-01
17.	2.67E-01	8.468E-02	-2.674E+00	1.205E+00	1.872E-01	-9.588E-01	7.325E+01	4.911E+00	5.942E-02	-3.712E-01
18.	2.70E-01	7.432E-02	-2.704E+00	1.281E+00	1.908E-01	-9.588E-01	7.325E+01	5.353E+00	2.433E-02	-3.864E-01
19.	2.71E-01	6.392E-02	-2.714E+00	1.356E+00	1.944E-01	-9.588E-01	7.326E+01	5.784E+00	2.558E-02	-4.016E-01
20.	2.72E-01	5.252E-02	-2.724E+00	1.431E+00	1.979E-01	-9.588E-01	7.326E+01	6.262E+00	2.638E-02	-4.168E-01
21.	2.72E-01	4.112E-02	-2.724E+00	1.507E+00	1.979E-01	-9.588E-01	7.326E+01	6.785E+00	2.665E-02	-4.320E-01

Table 10b. Compressive Jamming Analysis of Diamond Unit Cell (Compressive).

D= 2.362E+01		Q1= 7.200E+01		N= 1.600E+01		SD= 1.000E+00		LI/N= 4.876E+00		MODE= 1.000E+02	
COUNTER-CLOCKWISE (ALTERNATING TOP LEG)											
(°)	S	A	Y	Z	WX	WY	CO	JO	GC	GT	
1.	0.	1.000E+00	0.	0.	0.	9.547E-01	7.240E+01	9.163E-01	2.666E-01	5.644E-02	
2.	1.935E-02	2.572E-01	0.	0.	0.	9.547E-01	7.240E+01	9.163E-01	2.666E-01	5.644E-02	
3.	3.327E-04	9.619E-01	4.422E-01	1.507E-01	0.724E-02	9.547E-01	7.240E+01	9.163E-01	2.666E-01	5.644E-02	
4.	5.335E-02	7.540E-01	9.244E-01	7.244E-01	1.334E-01	9.547E-01	7.240E+01	9.163E-01	2.666E-01	5.644E-02	
5.	7.935E-02	1.016E+00	9.666E-01	3.017E-01	1.994E-01	9.547E-01	7.240E+01	9.163E-01	2.666E-01	5.644E-02	
6.	9.412E-02	1.272E+00	7.590E-01	3.767E-01	3.038E-01	9.547E-01	7.240E+01	9.163E-01	2.666E-01	5.644E-02	
7.	1.171E-01	1.527E+00	7.150E-01	4.521E-01	4.533E-01	9.547E-01	7.240E+01	9.163E-01	2.666E-01	5.644E-02	
8.	1.371E-01	1.766E+00	6.135E-01	5.273E-01	5.273E-01	9.547E-01	7.240E+01	9.163E-01	2.666E-01	5.644E-02	
9.	1.571E-01	2.004E+00	5.072E-01	6.027E-01	6.027E-01	9.547E-01	7.240E+01	9.163E-01	2.666E-01	5.644E-02	
10.	1.768E-01	2.242E+00	3.931E-01	6.780E-01	6.780E-01	9.547E-01	7.240E+01	9.163E-01	2.666E-01	5.644E-02	
11.	1.968E-01	2.480E+00	2.731E-01	7.533E-01	7.533E-01	9.547E-01	7.240E+01	9.163E-01	2.666E-01	5.644E-02	
12.	2.168E-01	2.718E+00	1.493E-01	8.285E-01	8.285E-01	9.547E-01	7.240E+01	9.163E-01	2.666E-01	5.644E-02	
13.	2.368E-01	2.956E+00	2.354E-02	9.037E-01	9.037E-01	9.547E-01	7.240E+01	9.163E-01	2.666E-01	5.644E-02	
14.	2.568E-01	3.194E+00	-1.622E-01	9.790E-01	9.790E-01	9.547E-01	7.240E+01	9.163E-01	2.666E-01	5.644E-02	
15.	2.768E-01	3.432E+00	-2.622E-01	1.054E+00	1.054E+00	9.547E-01	7.240E+01	9.163E-01	2.666E-01	5.644E-02	
16.	2.968E-01	3.670E+00	-3.568E-01	1.130E+00	1.130E+00	9.547E-01	7.240E+01	9.163E-01	2.666E-01	5.644E-02	
17.	3.168E-01	3.908E+00	-4.508E-01	1.206E+00	1.206E+00	9.547E-01	7.240E+01	9.163E-01	2.666E-01	5.644E-02	
18.	3.368E-01	4.146E+00	-5.448E-01	1.282E+00	1.282E+00	9.547E-01	7.240E+01	9.163E-01	2.666E-01	5.644E-02	
19.	3.568E-01	4.384E+00	-6.388E-01	1.358E+00	1.358E+00	9.547E-01	7.240E+01	9.163E-01	2.666E-01	5.644E-02	
20.	3.768E-01	4.622E+00	-7.328E-01	1.434E+00	1.434E+00	9.547E-01	7.240E+01	9.163E-01	2.666E-01	5.644E-02	
21.	3.968E-01	4.860E+00	-8.268E-01	1.510E+00	1.510E+00	9.547E-01	7.240E+01	9.163E-01	2.666E-01	5.644E-02	
22.	4.168E-01	5.098E+00	-9.208E-01	1.586E+00	1.586E+00	9.547E-01	7.240E+01	9.163E-01	2.666E-01	5.644E-02	
23.	4.368E-01	5.336E+00	-1.014E-01	1.662E+00	1.662E+00	9.547E-01	7.240E+01	9.163E-01	2.666E-01	5.644E-02	
24.	4.568E-01	5.574E+00	-1.102E-01	1.738E+00	1.738E+00	9.547E-01	7.240E+01	9.163E-01	2.666E-01	5.644E-02	
25.	4.768E-01	5.812E+00	-1.190E-01	1.814E+00	1.814E+00	9.547E-01	7.240E+01	9.163E-01	2.666E-01	5.644E-02	
26.	4.968E-01	6.050E+00	-1.278E-01	1.890E+00	1.890E+00	9.547E-01	7.240E+01	9.163E-01	2.666E-01	5.644E-02	
27.	5.168E-01	6.288E+00	-1.366E-01	1.966E+00	1.966E+00	9.547E-01	7.240E+01	9.163E-01	2.666E-01	5.644E-02	
28.	5.368E-01	6.526E+00	-1.454E-01	2.042E+00	2.042E+00	9.547E-01	7.240E+01	9.163E-01	2.666E-01	5.644E-02	
29.	5.568E-01	6.764E+00	-1.542E-01	2.118E+00	2.118E+00	9.547E-01	7.240E+01	9.163E-01	2.666E-01	5.644E-02	
30.	5.768E-01	7.002E+00	-1.630E-01	2.194E+00	2.194E+00	9.547E-01	7.240E+01	9.163E-01	2.666E-01	5.644E-02	
31.	5.968E-01	7.240E+00	-1.718E-01	2.270E+00	2.270E+00	9.547E-01	7.240E+01	9.163E-01	2.666E-01	5.644E-02	
32.	6.168E-01	7.478E+00	-1.806E-01	2.346E+00	2.346E+00	9.547E-01	7.240E+01	9.163E-01	2.666E-01	5.644E-02	
33.	6.368E-01	7.716E+00	-1.894E-01	2.422E+00	2.422E+00	9.547E-01	7.240E+01	9.163E-01	2.666E-01	5.644E-02	
34.	6.568E-01	7.954E+00	-1.982E-01	2.498E+00	2.498E+00	9.547E-01	7.240E+01	9.163E-01	2.666E-01	5.644E-02	
35.	6.768E-01	8.192E+00	-2.070E-01	2.574E+00	2.574E+00	9.547E-01	7.240E+01	9.163E-01	2.666E-01	5.644E-02	
36.	6.968E-01	8.430E+00	-2.158E-01	2.650E+00	2.650E+00	9.547E-01	7.240E+01	9.163E-01	2.666E-01	5.644E-02	
37.	7.168E-01	8.668E+00	-2.246E-01	2.726E+00	2.726E+00	9.547E-01	7.240E+01	9.163E-01	2.666E-01	5.644E-02	
38.	7.368E-01	8.906E+00	-2.334E-01	2.802E+00	2.802E+00	9.547E-01	7.240E+01	9.163E-01	2.666E-01	5.644E-02	
39.	7.568E-01	9.144E+00	-2.422E-01	2.878E+00	2.878E+00	9.547E-01	7.240E+01	9.163E-01	2.666E-01	5.644E-02	
40.	7.768E-01	9.382E+00	-2.510E-01	2.954E+00	2.954E+00	9.547E-01	7.240E+01	9.163E-01	2.666E-01	5.644E-02	
41.	7.968E-01	9.620E+00	-2.598E-01	3.030E+00	3.030E+00	9.547E-01	7.240E+01	9.163E-01	2.666E-01	5.644E-02	
42.	8.168E-01	9.858E+00	-2.686E-01	3.106E+00	3.106E+00	9.547E-01	7.240E+01	9.163E-01	2.666E-01	5.644E-02	
43.	8.368E-01	10.096E+00	-2.774E-01	3.182E+00	3.182E+00	9.547E-01	7.240E+01	9.163E-01	2.666E-01	5.644E-02	
44.	8.568E-01	10.334E+00	-2.862E-01	3.258E+00	3.258E+00	9.547E-01	7.240E+01	9.163E-01	2.666E-01	5.644E-02	
45.	8.768E-01	10.572E+00	-2.950E-01	3.334E+00	3.334E+00	9.547E-01	7.240E+01	9.163E-01	2.666E-01	5.644E-02	
46.	8.968E-01	10.810E+00	-3.038E-01	3.410E+00	3.410E+00	9.547E-01	7.240E+01	9.163E-01	2.666E-01	5.644E-02	
47.	9.168E-01	11.048E+00	-3.126E-01	3.486E+00	3.486E+00	9.547E-01	7.240E+01	9.163E-01	2.666E-01	5.644E-02	
48.	9.368E-01	11.286E+00	-3.214E-01	3.562E+00	3.562E+00	9.547E-01	7.240E+01	9.163E-01	2.666E-01	5.644E-02	
49.	9.568E-01	11.524E+00	-3.302E-01	3.638E+00	3.638E+00	9.547E-01	7.240E+01	9.163E-01	2.666E-01	5.644E-02	
50.	9.768E-01	11.762E+00	-3.390E-01	3.714E+00	3.714E+00	9.547E-01	7.240E+01	9.163E-01	2.666E-01	5.644E-02	
51.	9.968E-01	12.000E+00	-3.478E-01	3.790E+00	3.790E+00	9.547E-01	7.240E+01	9.163E-01	2.666E-01	5.644E-02	
52.	1.016E+00	12.238E+00	-3.566E-01	3.866E+00	3.866E+00	9.547E-01	7.240E+01	9.163E-01	2.666E-01	5.644E-02	
53.	1.036E+00	12.476E+00	-3.654E-01	3.942E+00	3.942E+00	9.547E-01	7.240E+01	9.163E-01	2.666E-01	5.644E-02	
54.	1.056E+00	12.714E+00	-3.742E-01	4.018E+00	4.018E+00	9.547E-01	7.240E+01	9.163E-01	2.666E-01	5.644E-02	
55.	1.076E+00	12.952E+00	-3.830E-01	4.094E+00	4.094E+00	9.547E-01	7.240E+01	9.163E-01	2.666E-01	5.644E-02	
56.	1.096E+00	13.190E+00	-3.918E-01	4.170E+00	4.170E+00	9.547E-01	7.240E+01	9.163E-01	2.666E-01	5.644E-02	
57.	1.116E+00	13.428E+00	-4.006E-01	4.246E+00	4.246E+00	9.547E-01	7.240E+01	9.163E-01	2.666E-01	5.644E-02	
58.	1.136E+00	13.666E+00	-4.094E-01	4.322E+00	4.322E+00	9.547E-01	7.240E+01	9.163E-01	2.666E-01	5.644E-02	
59.	1.156E+00	13.904E+00	-4.182E-01	4.398E+00	4.398E+00	9.547E-01	7.240E+01	9.163E-01	2.666E-01	5.644E-02	
60.	1.176E+00	14.142E+00	-4.270E-01	4.474E+00	4.474E+00	9.547E-01	7.240E+01	9.163E-01	2.666E-01	5.644E-02	
61.	1.196E+00	14.380E+00	-4.358E-01	4.550E+00	4.550E+00	9.547E-01	7.240E+01	9.163E-01	2.666E-01	5.644E-02	
62.	1.216E+00	14.618E+00	-4.446E-01	4.626E+00	4.626E+00	9.547E-01	7.240E+01	9.163E-01	2.666E-01	5.644E-02	
63.	1.236E+00	14.856E+00	-4.534E-01	4.702E+00	4.702E+00	9.547E-01	7.240E+01	9.163E-01	2.666E-01	5.644E-02	
64.	1.256E+00	15.094E+00	-4.622E-01	4.778E+00	4.778E+00	9.547E-01	7.240E+01	9.163E-01	2.666E-01	5.644E-02	
65.	1.276E+00	15.332E+00	-4.710E-01	4.854E+00	4.854E+00	9.547E-01	7.240E+01	9.163E-01	2.666E-01	5.644E-02	
66.	1.296E+00	15.570E+00	-4.798E-01	4.930E+00	4.930E+00	9.547E-01	7.240E+01	9.163E-01	2.666E-01	5.644E-02	
67.	1.316E+00	15.808E+00	-4.886E-01	5.006E+00	5.006E+00	9.547E-01	7.240E+01	9.163E-01	2.666E-01	5.644E-02	
68.	1.336E+00	16.046E+00	-4.974E-01	5.082E+00	5.082E+00	9.547E-01	7.240E+01	9.163E-01	2.666E-01	5.644E-02	
69.	1.356E+00	16.284E+00	-5.062E-01	5.158E+00	5.158E+00	9.547E-01	7.240E+01	9.163E-01	2.666E-01	5.644E-02	
70.	1.376E+00	16.522E+00	-5.150E-01	5.234E+00	5.234E+00	9.547E-01	7.240E+01	9.163E-01	2.666E-01	5.644E-02	
71.	1.396E+00	16.760E+00	-5.238E-01	5.310E+00	5.310E+00	9.547E-01	7.240E+01	9.163E-01	2.666E-01	5.644E-02	
72.	1.416E+00	17.000E+00	-5.326E-01	5.386E+00	5.386E+00	9.547E-01	7.240E+01	9.163E-01	2.666E-01	5.644E-02	
73.	1.436E+00	17.238E+00	-5.414E-01	5.462E+00	5.462E+00	9.547E-01	7.240E+01	9.163E-01	2.666E-01	5.644E-02	
74.	1.456E+00	17.476E+00	-5.502E-01	5.538E+00	5.538E+00	9.547E-01	7.240E+01	9.163E-01	2.666E-01	5.644E-02	
75.	1.476E+00	17.714E+00	-5.590E-01	5.614E+00	5.614E+00	9.547E-01	7.240E+01	9.163E-01	2.666E-01	5.644E-02	
76.	1.496E+00	17.952E+00	-5.678E-01	5.690E+00	5.690E+00	9.547E-01	7.240E+01	9.163E-01	2.666E-01	5.644E-02	
77.	1.516E+00	18.190E+00</									

Table 11a. Mid-Point Jamming Analysis of Diamond Unit Cell (Extensive).

D= 1.756E+01												Q1= .4500E+01												N= 1.600E+01												S0= 1.000E+00												L1/N= 4.475E+00												M0/E= 1.000E+00																																																																																																																																																																																																																																																																																																																																																																																																																																																																																				
COUNTER-CLOCKWISE												CLOCKWISE												COUNTER-CLOCKWISE												CLOCKWISE												COUNTER-CLOCKWISE												CLOCKWISE												COUNTER-CLOCKWISE												CLOCKWISE																																																																																																																																																																																																																																																																																																																																																																																																																																																												
(0)												(0)												(0)												(0)												(0)												(0)												(0)												(0)												(0)												(0)																																																																																																																																																																																																																																																																																																																																																																																																																																				
S	X	Y	Z	WX	MY	Q0	JD	GC	GT	S	X	Y	Z	WX	MY	Q0	JD	GC	GT	S	X	Y	Z	WX	MY	Q0	JD	GC	GT	S	X	Y	Z	WX	MY	Q0	JD	GC	GT	S	X	Y	Z	WX	MY	Q0	JD	GC	GT																																																																																																																																																																																																																																																																																																																																																																																																																																																																																															
1.	0.	1.000E+00	0.	0.	0.	7.200E-01	4.659E+01	0.	2.500E-01	1.750E-01	1.	0.	1.000E+00	0.	0.	0.	7.200E-01	4.659E+01	0.	2.500E-01	1.750E-01	1.	0.	1.000E+00	0.	0.	0.	7.200E-01	4.659E+01	0.	2.500E-01	1.750E-01	1.	0.	1.000E+00	0.	0.	0.	7.200E-01	4.659E+01	0.	2.500E-01	1.750E-01	1.	0.	1.000E+00	0.	0.	0.	7.200E-01	4.659E+01	0.	2.500E-01	1.750E-01																																																																																																																																																																																																																																																																																																																																																																																																																																																																																										
2.	1.400E-02	9.400E-01	1.720E-01	-6.310E-02	7.200E-02	4.668E+01	1.130E-01	2.410E-01	1.400E-01	2.	1.400E-02	9.400E-01	1.720E-01	-6.310E-02	7.200E-02	4.668E+01	1.130E-01	2.410E-01	1.400E-01	2.	1.400E-02	9.400E-01	1.720E-01	-6.310E-02	7.200E-02	4.668E+01	1.130E-01	2.410E-01	1.400E-01	2.	1.400E-02	9.400E-01	1.720E-01	-6.310E-02	7.200E-02	4.668E+01	1.130E-01	2.410E-01	1.400E-01	2.	1.400E-02	9.400E-01	1.720E-01	-6.310E-02	7.200E-02	4.668E+01	1.130E-01	2.410E-01	1.400E-01	2.	1.400E-02	9.400E-01	1.720E-01	-6.310E-02	7.200E-02	4.668E+01	1.130E-01	2.410E-01	1.400E-01																																																																																																																																																																																																																																																																																																																																																																																																																																																																																					
3.	1.400E-02	9.400E-01	3.630E-01	-1.240E-01	7.170E-01	4.676E+01	2.530E-01	2.410E-01	1.400E-01	3.	1.400E-02	9.400E-01	3.630E-01	-1.240E-01	7.170E-01	4.676E+01	2.530E-01	2.410E-01	1.400E-01	3.	1.400E-02	9.400E-01	3.630E-01	-1.240E-01	7.170E-01	4.676E+01	2.530E-01	2.410E-01	1.400E-01	3.	1.400E-02	9.400E-01	3.630E-01	-1.240E-01	7.170E-01	4.676E+01	2.530E-01	2.410E-01	1.400E-01	3.	1.400E-02	9.400E-01	3.630E-01	-1.240E-01	7.170E-01	4.676E+01	2.530E-01	2.410E-01	1.400E-01	3.	1.400E-02	9.400E-01	3.630E-01	-1.240E-01	7.170E-01	4.676E+01	2.530E-01	2.410E-01	1.400E-01																																																																																																																																																																																																																																																																																																																																																																																																																																																																																					
4.	5.940E-02	9.400E-01	5.940E-01	-1.430E-01	7.070E-01	4.696E+01	4.380E-01	2.410E-01	1.400E-01	4.	5.940E-02	9.400E-01	5.940E-01	-1.430E-01	7.070E-01	4.696E+01	4.380E-01	2.410E-01	1.400E-01	4.	5.940E-02	9.400E-01	5.940E-01	-1.430E-01	7.070E-01	4.696E+01	4.380E-01	2.410E-01	1.400E-01	4.	5.940E-02	9.400E-01	5.940E-01	-1.430E-01	7.070E-01	4.696E+01	4.380E-01	2.410E-01	1.400E-01	4.	5.940E-02	9.400E-01	5.940E-01	-1.430E-01	7.070E-01	4.696E+01	4.380E-01	2.410E-01	1.400E-01	4.	5.940E-02	9.400E-01	5.940E-01	-1.430E-01	7.070E-01	4.696E+01	4.380E-01	2.410E-01	1.400E-01																																																																																																																																																																																																																																																																																																																																																																																																																																																																																					
5.	7.940E-02	9.400E-01	7.940E-01	-1.430E-01	6.940E-01	4.720E+01	6.590E-01	1.670E-01	2.410E-01	5.	7.940E-02	9.400E-01	7.940E-01	-1.430E-01	6.940E-01	4.720E+01	6.590E-01	1.670E-01	2.410E-01	5.	7.940E-02	9.400E-01	7.940E-01	-1.430E-01	6.940E-01	4.720E+01	6.590E-01	1.670E-01	2.410E-01	5.	7.940E-02	9.400E-01	7.940E-01	-1.430E-01	6.940E-01	4.720E+01	6.590E-01	1.670E-01	2.410E-01	5.	7.940E-02	9.400E-01	7.940E-01	-1.430E-01	6.940E-01	4.720E+01	6.590E-01	1.670E-01	2.410E-01	5.	7.940E-02	9.400E-01	7.940E-01	-1.430E-01	6.940E-01	4.720E+01	6.590E-01	1.670E-01	2.410E-01	5.	7.940E-02	9.400E-01	7.940E-01	-1.430E-01	6.940E-01	4.720E+01	6.590E-01	1.670E-01	2.410E-01	5.	7.940E-02	9.400E-01	7.940E-01	-1.430E-01	6.940E-01	4.720E+01	6.590E-01	1.670E-01	2.410E-01	5.	7.940E-02	9.400E-01	7.940E-01	-1.430E-01	6.940E-01	4.720E+01	6.590E-01	1.670E-01	2.410E-01	5.	7.940E-02	9.400E-01	7.940E-01	-1.430E-01	6.940E-01	4.720E+01	6.590E-01	1.670E-01	2.410E-01	5.	7.940E-02	9.400E-01	7.940E-01	-1.430E-01	6.940E-01	4.720E+01	6.590E-01	1.670E-01	2.410E-01	5.	7.940E-02	9.400E-01	7.940E-01	-1.430E-01	6.940E-01	4.720E+01	6.590E-01	1.670E-01	2.410E-01	5.	7.940E-02	9.400E-01	7.940E-01	-1.430E-01	6.940E-01	4.720E+01	6.590E-01	1.670E-01	2.410E-01	5.	7.940E-02	9.400E-01	7.940E-01	-1.430E-01	6.940E-01	4.720E+01	6.590E-01	1.670E-01	2.410E-01	5.	7.940E-02	9.400E-01	7.940E-01	-1.430E-01	6.940E-01	4.720E+01	6.590E-01	1.670E-01	2.410E-01	5.	7.940E-02	9.400E-01	7.940E-01	-1.430E-01	6.940E-01	4.720E+01	6.590E-01	1.670E-01	2.410E-01	5.	7.940E-02	9.400E-01	7.940E-01	-1.430E-01	6.940E-01	4.720E+01	6.590E-01	1.670E-01	2.410E-01	5.	7.940E-02	9.400E-01	7.940E-01	-1.430E-01	6.940E-01	4.720E+01	6.590E-01	1.670E-01	2.410E-01	5.	7.940E-02	9.400E-01	7.940E-01	-1.430E-01	6.940E-01	4.720E+01	6.590E-01	1.670E-01	2.410E-01	5.	7.940E-02	9.400E-01	7.940E-01	-1.430E-01	6.940E-01	4.720E+01	6.590E-01	1.670E-01	2.410E-01	5.	7.940E-02	9.400E-01	7.940E-01	-1.430E-01	6.940E-01	4.720E+01	6.590E-01	1.670E-01	2.410E-01	5.	7.940E-02	9.400E-01	7.940E-01	-1.430E-01	6.940E-01	4.720E+01	6.590E-01	1.670E-01	2.410E-01	5.	7.940E-02	9.400E-01	7.940E-01	-1.430E-01	6.940E-01	4.720E+01	6.590E-01	1.670E-01	2.410E-01	5.	7.940E-02	9.400E-01	7.940E-01	-1.430E-01	6.940E-01	4.720E+01	6.590E-01	1.670E-01	2.410E-01	5.	7.940E-02	9.400E-01	7.940E-01	-1.430E-01	6.940E-01	4.720E+01	6.590E-01	1.670E-01	2.410E-01	5.	7.940E-02	9.400E-01	7.940E-01	-1.430E-01	6.940E-01	4.720E+01	6.590E-01	1.670E-01	2.410E-01	5.	7.940E-02	9.400E-01	7.940E-01	-1.430E-01	6.940E-01	4.720E+01	6.590E-01	1.670E-01	2.410E-01	5.	7.940E-02	9.400E-01	7.940E-01	-1.430E-01	6.940E-01	4.720E+01	6.590E-01	1.670E-01	2.410E-01	5.	7.940E-02	9.400E-01	7.940E-01	-1.430E-01	6.940E-01	4.720E+01	6.590E-01	1.670E-01	2.410E-01	5.	7.940E-02	9.400E-01	7.940E-01	-1.430E-01	6.940E-01	4.720E+01	6.590E-01	1.670E-01	2.410E-01	5.	7.940E-02	9.400E-01	7.940E-01	-1.430E-01	6.940E-01	4.720E+01	6.590E-01	1.670E-01	2.410E-01	5.	7.940E-02	9.400E-01	7.940E-01	-1.430E-01	6.940E-01	4.720E+01	6.590E-01	1.670E-01	2.410E-01	5.	7.940E-02	9.400E-01	7.940E-01	-1.430E-01	6.940E-01	4.720E+01	6.590E-01	1.670E-01	2.410E-01	5.	7.940E-02	9.400E-01	7.940E-01	-1.430E-01	6.940E-01	4.720E+01	6.590E-01	1.670E-01	2.410E-01	5.	7.940E-02	9.400E-01	7.940E-01	-1.430E-01	6.940E-01	4.720E+01	6.590E-01	1.670E-01	2.410E-01	5.	7.940E-02	9.400E-01	7.940E-01	-1.430E-01	6.940E-01	4.720E+01	6.590E-01	1.670E-01	2.410E-01	5.	7.940E-02	9.400E-01	7.940E-01	-1.430E-01	6.940E-01	4.720E+01	6.590E-01	1.670E-01	2.410E-01	5.	7.940E-02	9.400E-01	7.940E-01	-1.430E-01	6.940E-01	4.720E+01	6.590E-01	1.670E-01	2.410E-01	5.	7.940E-02	9.400E-01	7.940E-01	-1.430E-01	6.940E-01	4.720E+01	6.590E-01	1.670E-01	2.410E-01	5.	7.940E-02	9.400E-01	7.940E-01	-1.430E-01	6.940E-01	4.720E+01	6.590E-01	1.670E-01	2.410E-01	5.	7.940E-02	9.400E-01	7.940E-01	-1.430E-01	6.940E-01	4.720E+01	6.590E-01	1.670E-01	2.410E-01	5.	7.940E-02	9.400E-01	7.940E-01	-1.430E-01	6.940E-01	4.720E+01	6.590E-01	1.670E-01	2.410E-01	5.	7.940E-02	9.400E-01	7.940E-01	-1.430E-01	6.940E-01	4.720E+01	6.590E-01	1.670E-01	2.410E-01	5.	7.940E-02	9.400E-01	7.940E-01	-1.430E-01	6.940E-01	4.720E+01	6.590E-01	1.670E-01	2.410E-01	5.	7.940E-02	9.400E-01	7.940E-01	-1.430E-01	6.940E-01	4.720E+01	6.590E-01	1.670E-01	2.410E-01	5.	7.940E-02	9.400E-01	7.940E-01	-1.430E-01	6.940E-01	4.720E+01	6.590E-01	1.670E-01	2.410E-01	5.	7.940E-02	9.400E-01	7.940E-01	-1.430E-01	6.940E-01	4.720E+01	6.590E-01	1.670E-01	2.410E-01	5.	7.940E-02	9.400E-01	7.940E-01	-1.430E-01	6.940E-01	4.720E+01	6.590E-01	1.670E-01	2.410E-01	5.	7.940E-02	9.400E-01	7.940E-01	-1.430E-01	6.940E-01	4.720E+01	6.590E-01	1.670E-01	2.410E-01	5.	7.940E-02	9.400E-01	7.940E-01	-1.430E-01	6.940E-01	4.720E+01	6.590E-01	1.670E-01	2.410E-01	5.	7.940E-02	9.400E-01	7.940E-01	-1.430E-01	6.940E-01	4.720E+01	6.590E-01	1.670E-01	2.410E-01	5.	7.940E-02	9.400E-01	7.940E-01	-1.430E-01	6.940E-01	4.720E+01	6.590E-01	1.670E-01	2.410E-01	5.	7.940E-02	9.400E-01	7.940E-01	-1.430E-01	6.940E-01	4.720E+01	6.590E-01	1.670E-

Table 11b. Mid-Point Jamming Analysis of Diamond Unit Cell (Compressive).

D = 1.756E+01	Q1 = 4.510E+01	N = 1.000E+01	SD = 1.000E+00	L1/N = 4.975E+00	MODE = 1.000E+00
COUNTER-CLOCKWISE (ALTERNATING TOP LEG)					
0.	0.	0.	0.	0.	0.
1.	1.000E+00	1.724E+01	0.	7.264E+01	2.503E+01
2.	2.000E+00	1.724E+01	0.314E+02	7.262E+01	2.503E+01
3.	3.000E+00	1.724E+01	0.314E+02	7.262E+01	2.503E+01
4.	4.000E+00	1.724E+01	0.314E+02	7.262E+01	2.503E+01
5.	5.000E+00	1.724E+01	0.314E+02	7.262E+01	2.503E+01
6.	6.000E+00	1.724E+01	0.314E+02	7.262E+01	2.503E+01
7.	7.000E+00	1.724E+01	0.314E+02	7.262E+01	2.503E+01
8.	8.000E+00	1.724E+01	0.314E+02	7.262E+01	2.503E+01
9.	9.000E+00	1.724E+01	0.314E+02	7.262E+01	2.503E+01
10.	1.000E+00	1.724E+01	0.314E+02	7.262E+01	2.503E+01
11.	1.000E+00	1.724E+01	0.314E+02	7.262E+01	2.503E+01
12.	1.000E+00	1.724E+01	0.314E+02	7.262E+01	2.503E+01
13.	1.000E+00	1.724E+01	0.314E+02	7.262E+01	2.503E+01
14.	1.000E+00	1.724E+01	0.314E+02	7.262E+01	2.503E+01
15.	1.000E+00	1.724E+01	0.314E+02	7.262E+01	2.503E+01
16.	1.000E+00	1.724E+01	0.314E+02	7.262E+01	2.503E+01
17.	1.000E+00	1.724E+01	0.314E+02	7.262E+01	2.503E+01
18.	1.000E+00	1.724E+01	0.314E+02	7.262E+01	2.503E+01
19.	1.000E+00	1.724E+01	0.314E+02	7.262E+01	2.503E+01
20.	1.000E+00	1.724E+01	0.314E+02	7.262E+01	2.503E+01
21.	1.000E+00	1.724E+01	0.314E+02	7.262E+01	2.503E+01
22.	1.000E+00	1.724E+01	0.314E+02	7.262E+01	2.503E+01
23.	1.000E+00	1.724E+01	0.314E+02	7.262E+01	2.503E+01
24.	1.000E+00	1.724E+01	0.314E+02	7.262E+01	2.503E+01
25.	1.000E+00	1.724E+01	0.314E+02	7.262E+01	2.503E+01
26.	1.000E+00	1.724E+01	0.314E+02	7.262E+01	2.503E+01
27.	1.000E+00	1.724E+01	0.314E+02	7.262E+01	2.503E+01
28.	1.000E+00	1.724E+01	0.314E+02	7.262E+01	2.503E+01
29.	1.000E+00	1.724E+01	0.314E+02	7.262E+01	2.503E+01
30.	1.000E+00	1.724E+01	0.314E+02	7.262E+01	2.503E+01
31.	1.000E+00	1.724E+01	0.314E+02	7.262E+01	2.503E+01
32.	1.000E+00	1.724E+01	0.314E+02	7.262E+01	2.503E+01
33.	1.000E+00	1.724E+01	0.314E+02	7.262E+01	2.503E+01
34.	1.000E+00	1.724E+01	0.314E+02	7.262E+01	2.503E+01
35.	1.000E+00	1.724E+01	0.314E+02	7.262E+01	2.503E+01
36.	1.000E+00	1.724E+01	0.314E+02	7.262E+01	2.503E+01
37.	1.000E+00	1.724E+01	0.314E+02	7.262E+01	2.503E+01
38.	1.000E+00	1.724E+01	0.314E+02	7.262E+01	2.503E+01
39.	1.000E+00	1.724E+01	0.314E+02	7.262E+01	2.503E+01
40.	1.000E+00	1.724E+01	0.314E+02	7.262E+01	2.503E+01
41.	1.000E+00	1.724E+01	0.314E+02	7.262E+01	2.503E+01
42.	1.000E+00	1.724E+01	0.314E+02	7.262E+01	2.503E+01
43.	1.000E+00	1.724E+01	0.314E+02	7.262E+01	2.503E+01
44.	1.000E+00	1.724E+01	0.314E+02	7.262E+01	2.503E+01
45.	1.000E+00	1.724E+01	0.314E+02	7.262E+01	2.503E+01
46.	1.000E+00	1.724E+01	0.314E+02	7.262E+01	2.503E+01
47.	1.000E+00	1.724E+01	0.314E+02	7.262E+01	2.503E+01
48.	1.000E+00	1.724E+01	0.314E+02	7.262E+01	2.503E+01
49.	1.000E+00	1.724E+01	0.314E+02	7.262E+01	2.503E+01
50.	1.000E+00	1.724E+01	0.314E+02	7.262E+01	2.503E+01
51.	1.000E+00	1.724E+01	0.314E+02	7.262E+01	2.503E+01
52.	1.000E+00	1.724E+01	0.314E+02	7.262E+01	2.503E+01
53.	1.000E+00	1.724E+01	0.314E+02	7.262E+01	2.503E+01
54.	1.000E+00	1.724E+01	0.314E+02	7.262E+01	2.503E+01
55.	1.000E+00	1.724E+01	0.314E+02	7.262E+01	2.503E+01
56.	1.000E+00	1.724E+01	0.314E+02	7.262E+01	2.503E+01
57.	1.000E+00	1.724E+01	0.314E+02	7.262E+01	2.503E+01
58.	1.000E+00	1.724E+01	0.314E+02	7.262E+01	2.503E+01
59.	1.000E+00	1.724E+01	0.314E+02	7.262E+01	2.503E+01
60.	1.000E+00	1.724E+01	0.314E+02	7.262E+01	2.503E+01
61.	1.000E+00	1.724E+01	0.314E+02	7.262E+01	2.503E+01
62.	1.000E+00	1.724E+01	0.314E+02	7.262E+01	2.503E+01
63.	1.000E+00	1.724E+01	0.314E+02	7.262E+01	2.503E+01
64.	1.000E+00	1.724E+01	0.314E+02	7.262E+01	2.503E+01
65.	1.000E+00	1.724E+01	0.314E+02	7.262E+01	2.503E+01
66.	1.000E+00	1.724E+01	0.314E+02	7.262E+01	2.503E+01
67.	1.000E+00	1.724E+01	0.314E+02	7.262E+01	2.503E+01
68.	1.000E+00	1.724E+01	0.314E+02	7.262E+01	2.503E+01
69.	1.000E+00	1.724E+01	0.314E+02	7.262E+01	2.503E+01
70.	1.000E+00	1.724E+01	0.314E+02	7.262E+01	2.503E+01
71.	1.000E+00	1.724E+01	0.314E+02	7.262E+01	2.503E+01
72.	1.000E+00	1.724E+01	0.314E+02	7.262E+01	2.503E+01
73.	1.000E+00	1.724E+01	0.314E+02	7.262E+01	2.503E+01
74.	1.000E+00	1.724E+01	0.314E+02	7.262E+01	2.503E+01
75.	1.000E+00	1.724E+01	0.314E+02	7.262E+01	2.503E+01
76.	1.000E+00	1.724E+01	0.314E+02	7.262E+01	2.503E+01
77.	1.000E+00	1.724E+01	0.314E+02	7.262E+01	2.503E+01
78.	1.000E+00	1.724E+01	0.314E+02	7.262E+01	2.503E+01
79.	1.000E+00	1.724E+01	0.314E+02	7.262E+01	2.503E+01
80.	1.000E+00	1.724E+01	0.314E+02	7.262E+01	2.503E+01
81.	1.000E+00	1.724E+01	0.314E+02	7.262E+01	2.503E+01
82.	1.000E+00	1.724E+01	0.314E+02	7.262E+01	2.503E+01
83.	1.000E+00	1.724E+01	0.314E+02	7.262E+01	2.503E+01
84.	1.000E+00	1.724E+01	0.314E+02	7.262E+01	2.503E+01
85.	1.000E+00	1.724E+01	0.314E+02	7.262E+01	2.503E+01
86.	1.000E+00	1.724E+01	0.314E+02	7.262E+01	2.503E+01
87.	1.000E+00	1.724E+01	0.314E+02	7.262E+01	2.503E+01
88.	1.000E+00	1.724E+01	0.314E+02	7.262E+01	2.503E+01
89.	1.000E+00	1.724E+01	0.314E+02	7.262E+01	2.503E+01
90.	1.000E+00	1.724E+01	0.314E+02	7.262E+01	2.503E+01
91.	1.000E+00	1.724E+01	0.314E+02	7.262E+01	2.503E+01
92.	1.000E+00	1.724E+01	0.314E+02	7.262E+01	2.503E+01
93.	1.000E+00	1.724E+01	0.314E+02	7.262E+01	2.503E+01
94.	1.000E+00	1.724E+01	0.314E+02	7.262E+01	2.503E+01
95.	1.000E+00	1.724E+01	0.314E+02	7.262E+01	2.503E+01
96.	1.000E+00	1.724E+01	0.314E+02	7.262E+01	2.503E+01
97.	1.000E+00	1.724E+01	0.314E+02	7.262E+01	2.503E+01
98.	1.000E+00	1.724E+01	0.314E+02	7.262E+01	2.503E+01
99.	1.000E+00	1.724E+01	0.314E+02	7.262E+01	2.503E+01
100.	1.000E+00	1.724E+01	0.314E+02	7.262E+01	2.503E+01

CLOCKWISE (ALTERNATING BOTTOM LEG)					
0.	0.	0.	0.	0.	0.
1.	1.000E+00	1.724E+01	0.314E+02	7.262E+01	2.503E+01
2.	2.000E+00	1.724E+01	0.314E+02	7.262E+01	2.503E+01
3.	3.000E+00	1.724E+01	0.314E+02	7.262E+01	2.503E+01
4.	4.000E+00	1.724E+01	0.314E+02	7.262E+01	2.503E+01
5.	5.000E+00	1.724E+01	0.314E+02	7.262E+01	2.503E+01
6.	6.000E+00	1.724E+01	0.314E+02	7.262E+01	2.503E+01
7.	7.000E+00	1.724E+01	0.314E+02	7.262E+01	2.503E+01
8.	8.000E+00	1.724E+01	0.314E+02	7.262E+01	2.503E+01
9.	9.000E+00	1.724E+01	0.314E+02	7.262E+01	2.503E+01
10.	1.000E+00	1.724E+01	0.314E+02	7.262E+01	2.503E+01
11.	1.000E+00	1.724E+01	0.314E+02	7.262E+01	2.503E+01
12.	1.000E+00	1.724E+01	0.314E+02	7.262E+01	2.503E+01
13.	1.000E+00	1.724E+01	0.314E+02	7.262E+01	2.503E+01
14.	1.000E+00	1.724E+01	0.314E+02	7.262E+01	2.503E+01
15.	1.000E+00	1.724E+01	0.314E+02	7.262E+01	2.503E+01
16.	1.000E+00	1.724E+01	0.314E+02	7.262E+01	2.503E+01
17.	1.000E+00	1.724E+01	0.314E+02	7.262E+01	2.503E+01
18.	1.000E+00	1.724E+01	0.314E+02	7.262E+01	2.503E+01
19.	1.000E+00	1.724E+01	0.314E+02	7.262E+01	2.503E+01
20.	1.000E+00	1.724E+01	0.314E+02	7.262E+01	2.503E+01
21.	1.000E+00	1.724E+01	0.314E+02	7.262E+01	2.503E+01
22.	1.000E+00	1.724E+01	0.314E+02	7.262E+01	2.503E+01
23.	1.000E+00	1.724E+01	0.314E+02	7.262E+01	2.503E+01
24.	1.000E+00	1.724E+01	0.314E+02	7.262E+01	2.503E+01
25.	1.000E+00	1.724E+01	0.314E+02	7.262E+01	2.503E+01
26.	1.000E+00	1.724E+01	0.314E+02	7.262E+01	2.503E+01
27.	1.000E+00	1.724E+01	0.314E+02	7.262E+01	2.503E+01
28.	1.000E+00	1.724E+01	0.314E+02	7.262E+01	2.503E+01
29.	1.000E+00	1.724E+01	0.314E+02	7.262E+01	2.503E+01
30.	1.000E+00	1.724E+01	0.314E+02	7.262E+01	2.503E+01
31.	1.000E+00	1.724E+01	0.314E+02	7.262E+01	2.503E+01
32.	1.000E+00	1.724E+01	0.314E+02	7.262E+01	2.503E+01
33.	1.000E+00	1.724E+01	0.314E+02	7.262E+01	2.503E+01
34.	1.000E+00	1.724E+01	0.314E+02	7.262E+01	2.503E+01
35.	1.000E+00	1.724E+01	0.314E+02	7.262E+01	2.503E+01
36.	1.000E+00	1.724E+01	0.314E+02	7.262E+01	2.503E+01
37.	1.000E+00	1.724E+01	0.314E+02	7.262E+01	2.503E+01
38.	1.000E+00	1.724E+01	0.314E+02	7.262E+01	2.503E+01
39.	1.000E+00	1.724E+01	0.314E+02	7.262E+01	2.503E+01
40.	1.000E+00	1.724E+01	0.314E+02	7.262E+01	2.503E+01
41.	1.000E+00	1.724E+01	0.314E+02	7.262E+01	2.503E+01
42.	1.000E+00	1.724E+01	0.314E+02	7.262E+01	2.503E+01
43.	1.000E+00	1.724E+01	0.314E+02	7.262E+01	2.503E+01
44.	1.000E+00	1.724E+01	0.314E+02	7.262E+01	2.503E+01
45.	1.000E+00	1.724E+01	0.314E+02	7.262E+01	2.503E+01
46.	1.000E+00	1.724E+01	0.314E+02	7.262E+01	2.503E+01
47.	1.000E+00	1.724E+01	0.314E+02	7.262E+01	2.503E+01
48.	1.000E+00	1.724E+01	0.314E+02	7.262E+01	2.503E+01
49.	1.000E+00	1.724E+01	0.314E+02	7.262E+01	2.503E+01
50.	1.000E+00	1.724E+01	0.314E+02	7.262E+01	2.503E+01
51.	1.000E+00				

wave) and the outer segment.

$$\text{Percent Difference In Strand Segment Length} = \frac{s_{11} - (s_{21} - s_{11})}{s_{11}} \times 100 \quad (\text{III.2})$$

Helix-Angle (Q1)	% Difference
17 degrees	1.4%
45 degrees	3.4%
73 degrees	4.6%

The distribution of local helix angles, Q_0 , for a given nominal Q_1 can also be easily extracted, say, from the right leg of Table 11a and plotted (Figure 26). The distribution of Q_0 at extensive jamming would be essential information for explaining the mechanics of braid tensile strength in some future study.

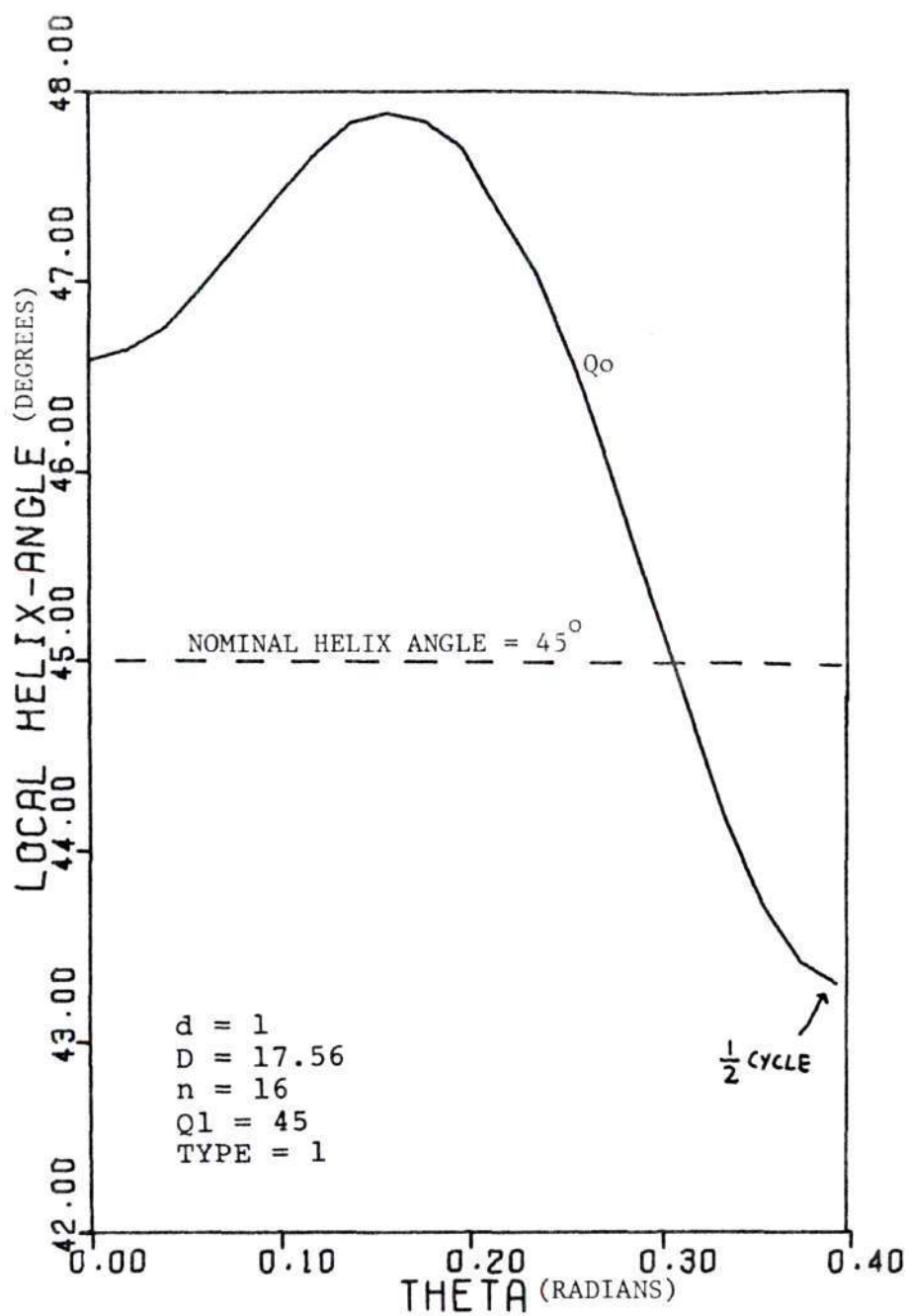


Figure 26. Distribution of Local Helix Angle for an Alternating Right Trellis Leg (TYPE=1, n=16).

CHAPTER IV

EXPERIMENT

Procedure

The tests were designed to measure braid dimensions within, and up to the jamming limits. Although the life of the majority of braids begins after extensive jamming, to be able to design better braid structures it is essential to study the events which precede it. The geometry preceding tensile jam has been traced back to its compressive jamming limit. Though compressive jamming is an integral part of the unique properties which characterize braid structure, it has hardly been mentioned in the previous literature. Its understanding is quite important for sheath-core composite structures especially braid covered elastic shock cord. In shock cord a braid is formed around a tensioned highly elastic core. When the cord is in its relaxed state the sleeve resides in its compressive jamming position. Its configuration influences the shock cord's extensibility and ultimate performance. In any composite structure the maximum diameter of the sheath which governs the amount of core which can be inserted within it, is an important specification.

Since we have been dealing with the relationship

between idealized strands and braid structure, the appropriate choice of test material is one which approaches meeting the initial assumption of circular strand cross-section with no flattening. Accordingly, regular and diamond braided polyester monofilament was selected as the test material. The braids were made specially with a "tracer" strand of a different color to facilitate the measurement of pitch. Monofilaments of .006 and .010 inches were used on 24, 48, 96, and 120 carrier* braiding machines. To obtain a range of geometries from a single machine, braids of different L_0 were made by varying the take-up speed.

The experiment measured the pitch of deformed braids at a variety of known diameters. The helix angle was then calculated from the two quantities using the helix-triangle relationship.

The diameter of the braid was both created and measured by the insertion of metal rods of predetermined diameter. From the inside diameter (I.D.) and strand diameter (d) the nominal diameter D , necessary to calculate Q_1 , is obtained. In theory, $2d + \text{I.D.} = D$ and $4d + \text{I.D.} = \text{O.D.}$.

*A carrier is a device which moves a bobbin holding the yarn for one strand around the machine. The cam design on conventional braiders is fixed to braid a "regular" pattern. Diamond braids are produced by removing every other bobbin. Thus a 96 carrier machine can make a $n=48$ regular braid or a $n=24$ diamond braid.

However, careful measurement often showed the outside diameter (O.D.) to be greater than the insert by $5d$ or $6d$. The inaccuracy was probably due to the imperfect seating of the braid on its core and the difficulties involved in measuring an uneven braid surface. In those cases D was taken to be the midpoint between the inside and outside diameters.

Measurement of inside diameters of less than one-half inch were made by a set of fractional drill blanks graduated in sixty-fourths of an inch. Larger inside diameters were measured by a set of aluminium rods graduated in sixteenths of an inch. A vernier caliper was used to measure outside braid diameter. Length measurements (pitch) were made with a metal ruler graduated in hundredths of an inch with the aid of a magnifying glass.

Each specimen with insert was placed in a lengthwise groove on an examination stage which could be moved in any direction with precision. The magnifying glass and ruler were mounted on separate stands. Each measurement was made three times and the average recorded.

The full range of deformation was achieved by inserting a series of cores of incremented size. Compressive jamming was declared when a larger insert could not be squeezed into the braid without disturbing the integrity of the structure. It was usually a clearly definable event; tensile jamming was more subtle. A tensile

jam was determined by decreasing the insert size until further decrease produced no change in braid pitch length.

In order to obtain accurate measurements the proper seating of the braid on its core was important. In most cases the natural springiness of the monofilament braid caused it to cling to the insert. Its configuration of lowest strain energy was the one with the smallest diameter. In certain size specimens where this was not so, the braid had to be smoothed against the core by hand.

Between one and thirteen measurements of pitch and diameter were made on each of 17 braid samples. After a set of jam-to-jam diameters and corresponding helix angles were obtained for a braid, two bench marks on the "tracer" strand were made one pitch apart with a felt-tipped pen. The braid was then cut apart, the marked strand removed, weighted with .2 grams/denier, and L_0 measured.

Experimental Results

With the aid of computer a plot has been made for each braid tested (Figures 27-35). Each displays the various measurement points against a background of the predicted deformation and jamming curve that the computerized model generates on the basis of L_0 , n , d , and TYPE. Each (D , Q_1) data point is associated by the model with a predicted L_0 . Measures of agreement between the predicted L_0 's and the measured L_0 are given in Table 12 by

average percent difference (G), standard deviation (H), and coefficient of variation (I). Also given is the average calculated Lo (F) which represents the computerized model's best estimation of the sample's real Lo. A measure of the proper shape of the model's predicted curve or the model's ability to fit a curve to the experimental points is given by their standard deviation (J) from the mean calculated Lo. Table 12 provides a summary of tests carried out and references each test to its corresponding graph. The raw data which is the basis for these graphs can be found in Appendix B. The table is separated into diamond and "regular" categories and ordered from greatest to least Lo.

Discussion Of Results

The experiments in general showed good agreement between measured and predicted geometries. In the review of the experimental results attention should be focused on: first, the proximity of the measurement points to the predicted deformation curve; second, the distance of the end points from the jam envelope; and third, whether there is intrusion into the predicted region of impossible braid formation.

The calculated Lo of the experimental points generally fell within three percent of the predicted Lo (see Table 12, column H). Based on the previous discussion of the similarity of arc-length predictions for different

Table 12. Summary Of Experiments

A	B	C	D	E	F	G	H	I	J	K	L	M	N
15	1	24	.006	8	400	392	2.0	9.99	2.5	4.74	1.2	.22	27
11	1	24	.010	12	390	384	1.5	6.74	1.7	2.85	0.7	.23	28
7	1	24	.006	10	298	288	3.3	10.06	3.4	3.58	1.2	.40	29
13	1	24	.010	9	377	372	3.8	6.34	1.7	3.90	1.0	.25	30
12	1	24	.010	11	315	310	1.5	5.04	1.6	1.73	0.6	.36	31
14	1	24	.006	11	290	292	0.6	12.19	4.2	11.5	3.9	.42	32
9	1	6	.010	1	--	64	--	--	--	--	--	.59	33
8	1	6	.010	1	--	25	--	--	--	--	--	3.9	34
22	1	6	.010	1	--	25	--	--	--	--	--	3.8	35
18	2	60	.010	9	460	453	1.5	9.88	2.1	5.78	1.3	.52	36
17	2	24	.006	7	230	225	2.2	5.40	2.4	1.49	0.7	.34	37
5	2	24	.010	13	165	163	1.2	1.82	1.1	0.70	0.4	.65	38
3	2	24	.010	9	164	161	1.8	3.26	2.0	0.97	0.6	.66	39
4	2	24	.010	12	163	158	3.1	5.27	3.2	1.35	0.9	.67	40
6	2	24	.006	8	150	147	2.0	4.52	3.0	0.81	0.6	.78	41
16	2	24	.006	3	123	119	3.2	5.99	4.9	2.05	1.7	1.2	42
10	2	12	.010	3	74	72	2.7	5.00	6.8	3.94	5.4	.83	43

A- braid sample identification number

B- braid TYPE

C- number of strands per set, n

D- strand diameter (inches)

E- number of measurements made

F- measured Lo' (dimensionless)G- average calculated Lo H- percent difference between Lo' and Lo ; $(Lo' - Lo) / Lo' \times 100 = H$ I- standard deviation from Lo' J- Lo' coefficient of variation (percent)K- standard deviation from Lo L- Lo coefficient of variation (percent)M- Crimp-Effect at $Q1 = 45$ degrees (percent)

N- Figure #

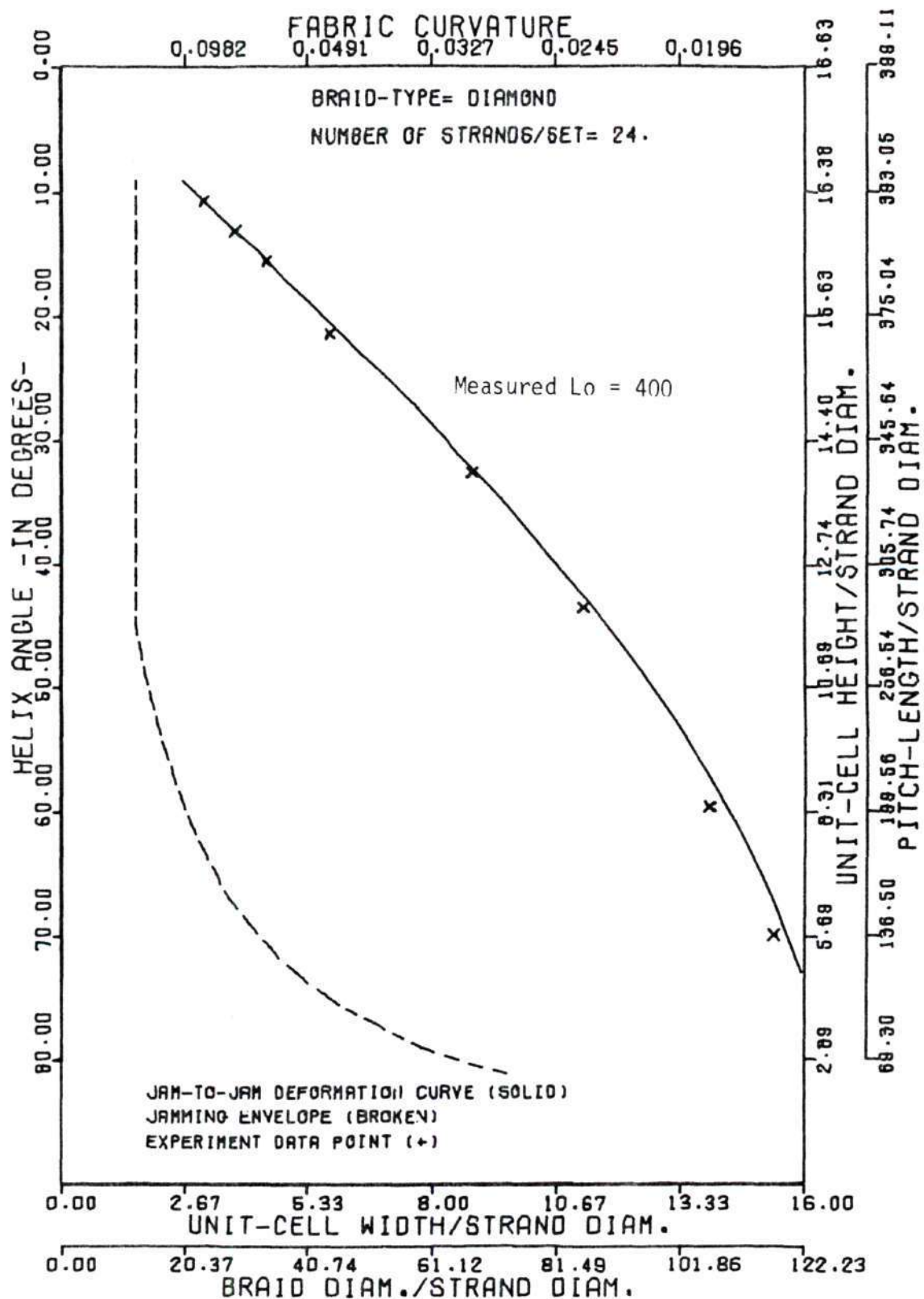


Figure 27. Test Data for Braid Sample #15 (TYPE=1, n=24).

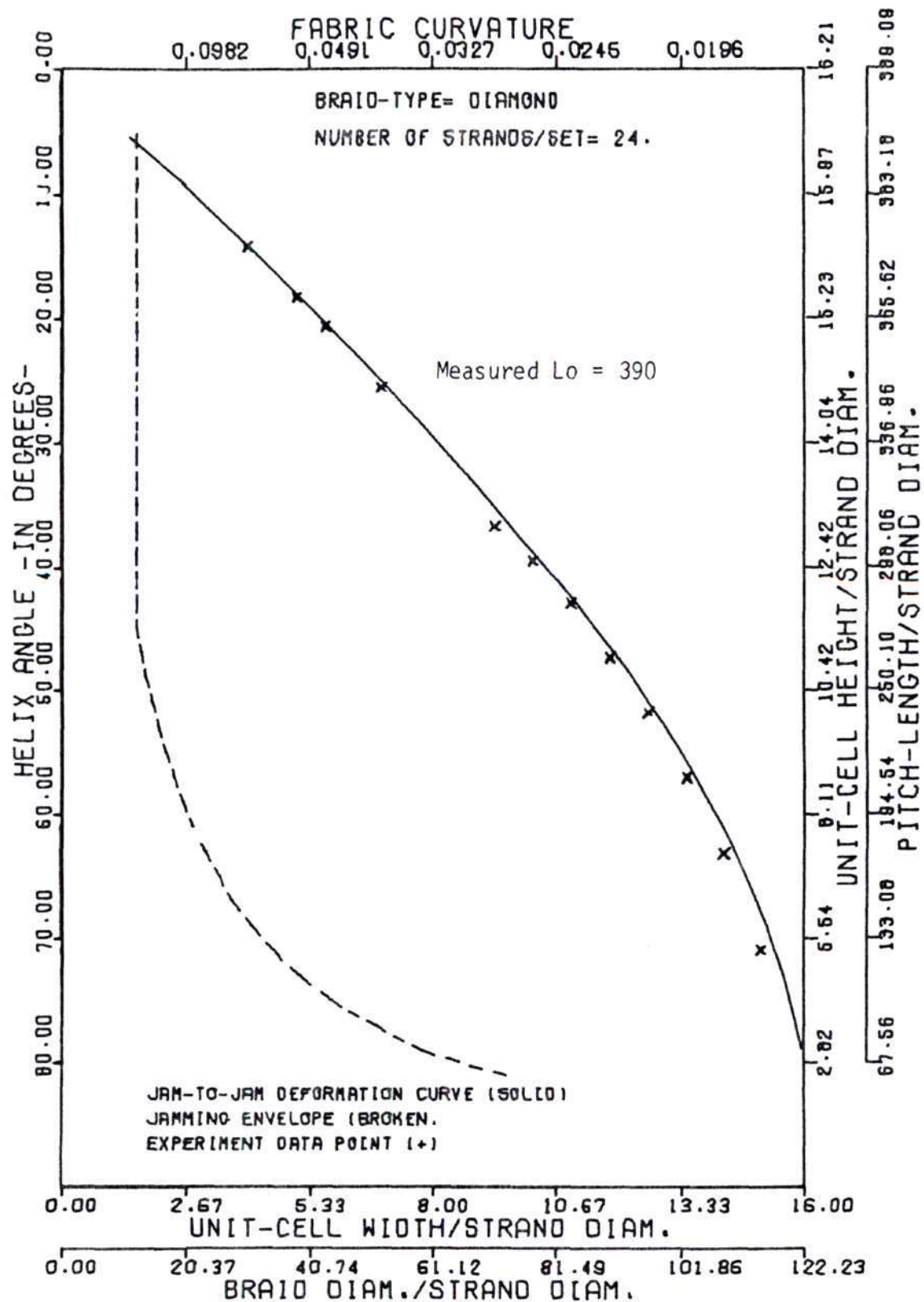


Figure 28. Test Data for Braid Sample #11 (TYPE=1, n=24).

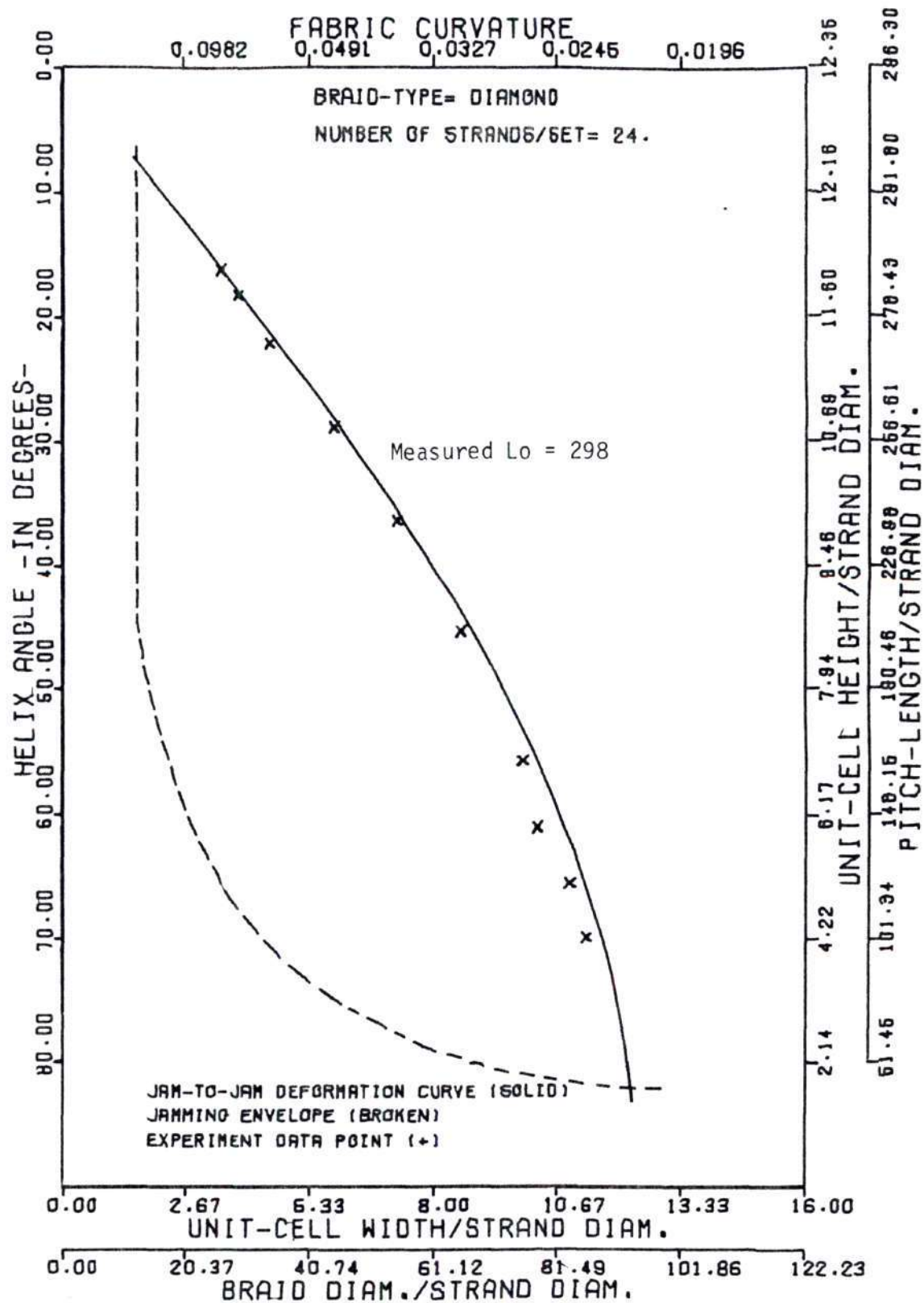


Figure 29. Test Data for Braid Sample #7 (TYPE=1, n=24).

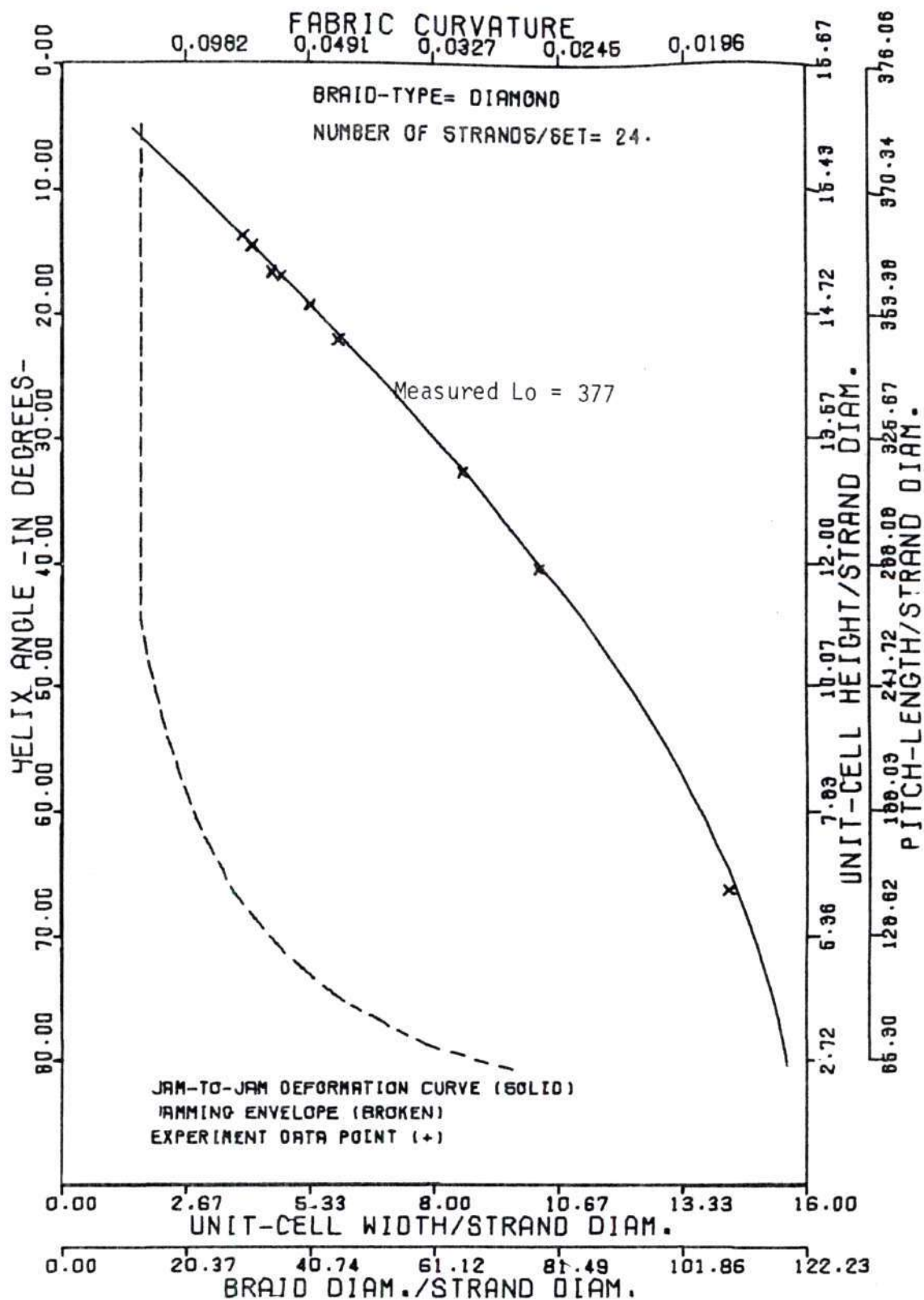


Figure 30. Test Data for Braid Sample #13 (TYPE=1, n=24).

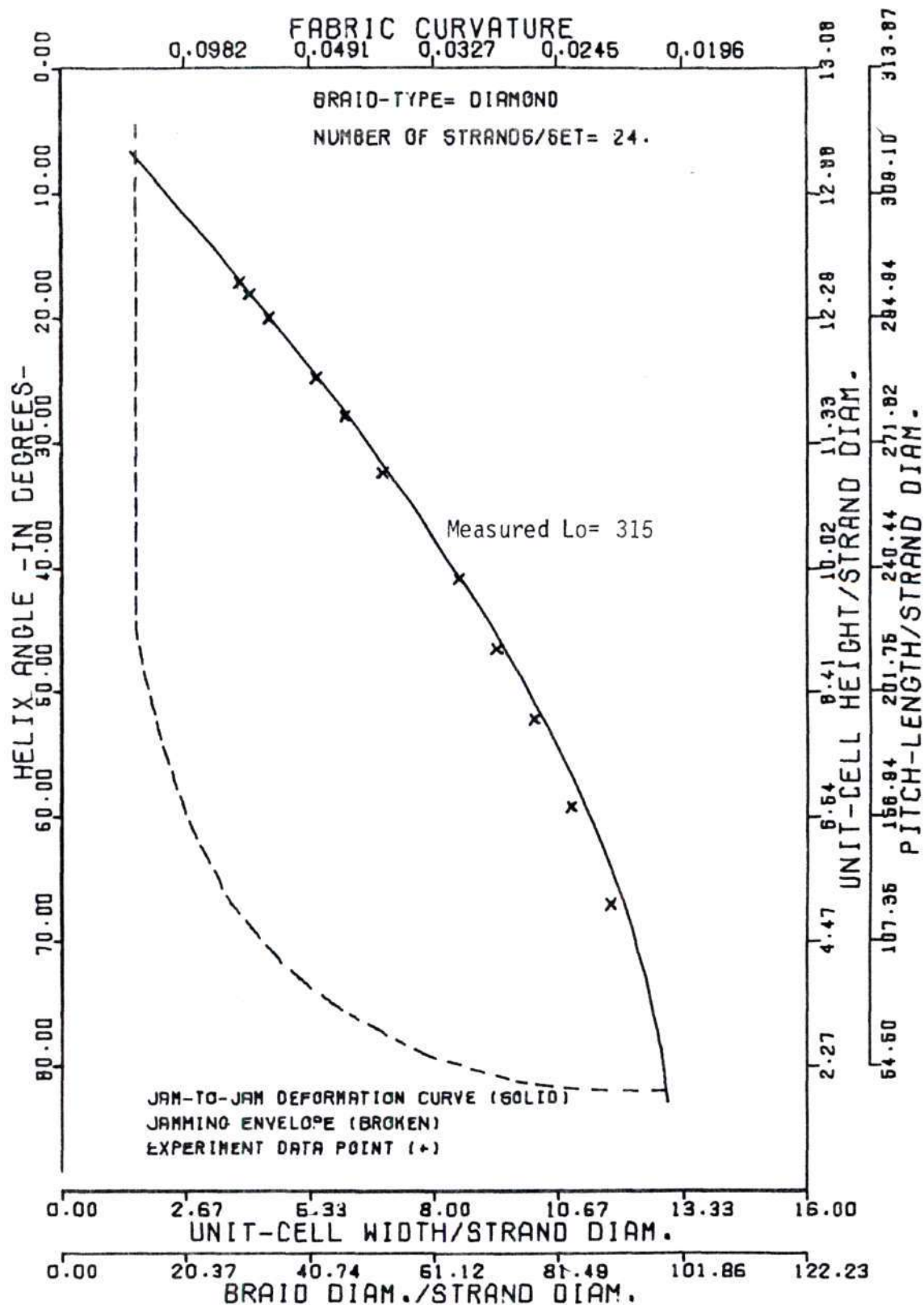


Figure 31. Test Data for Braid Sample #12 (TYPE=1, n=24).

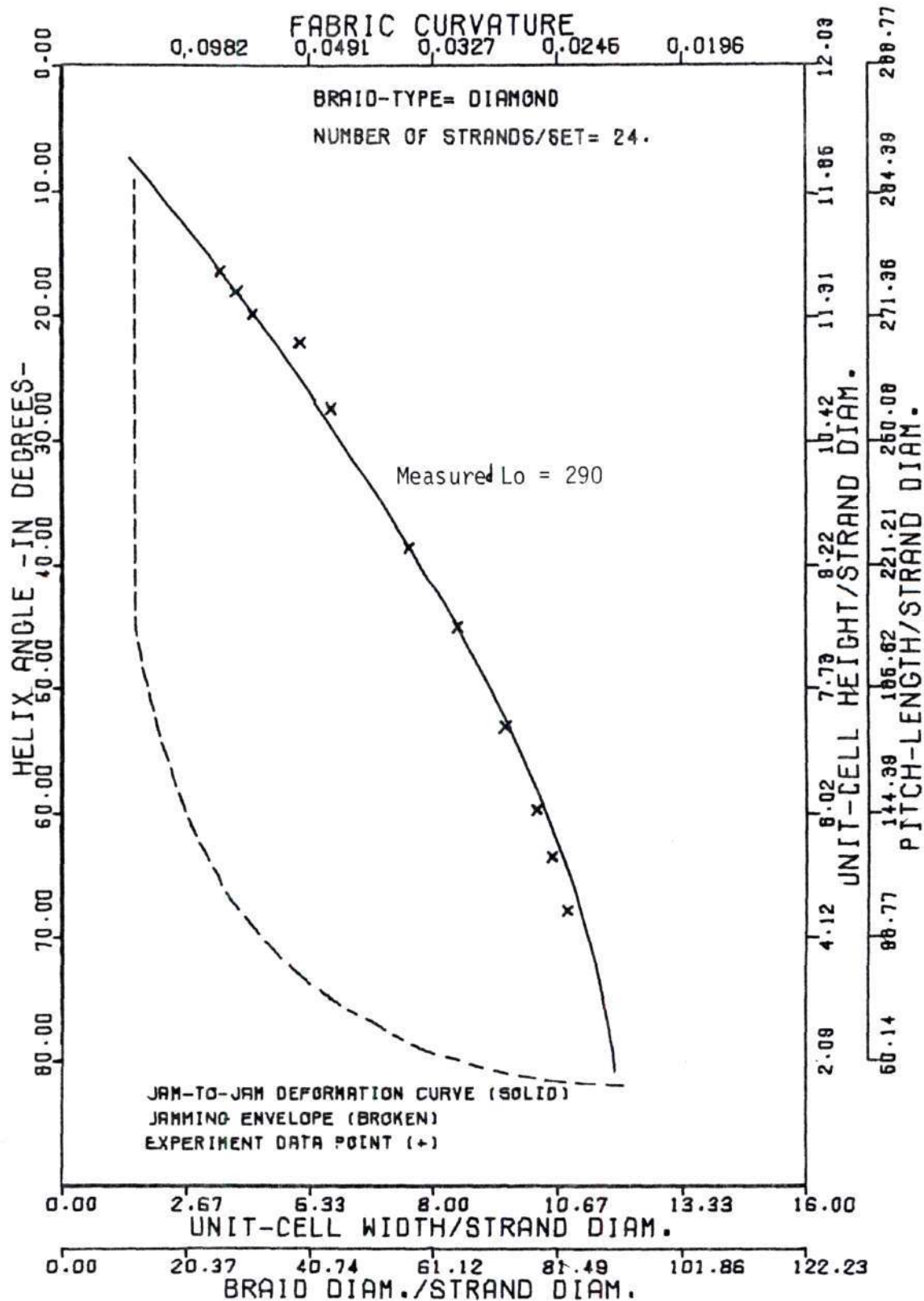


Figure 32. Test Data for Braid Sample #14 (TYPE=1, n=24).

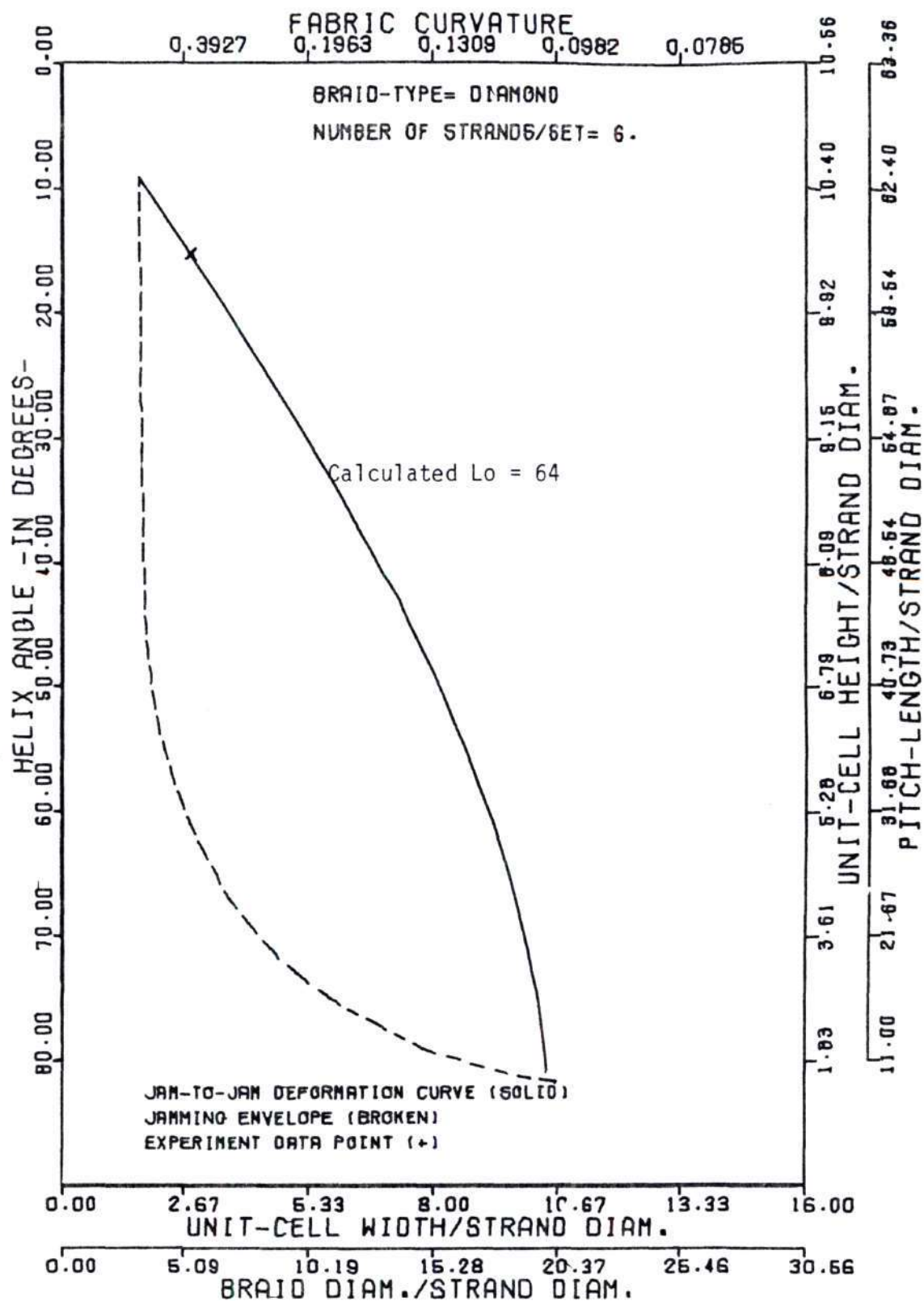


Figure 33. Test Data for Braid Sample #9 (TYPE=1, n=6).

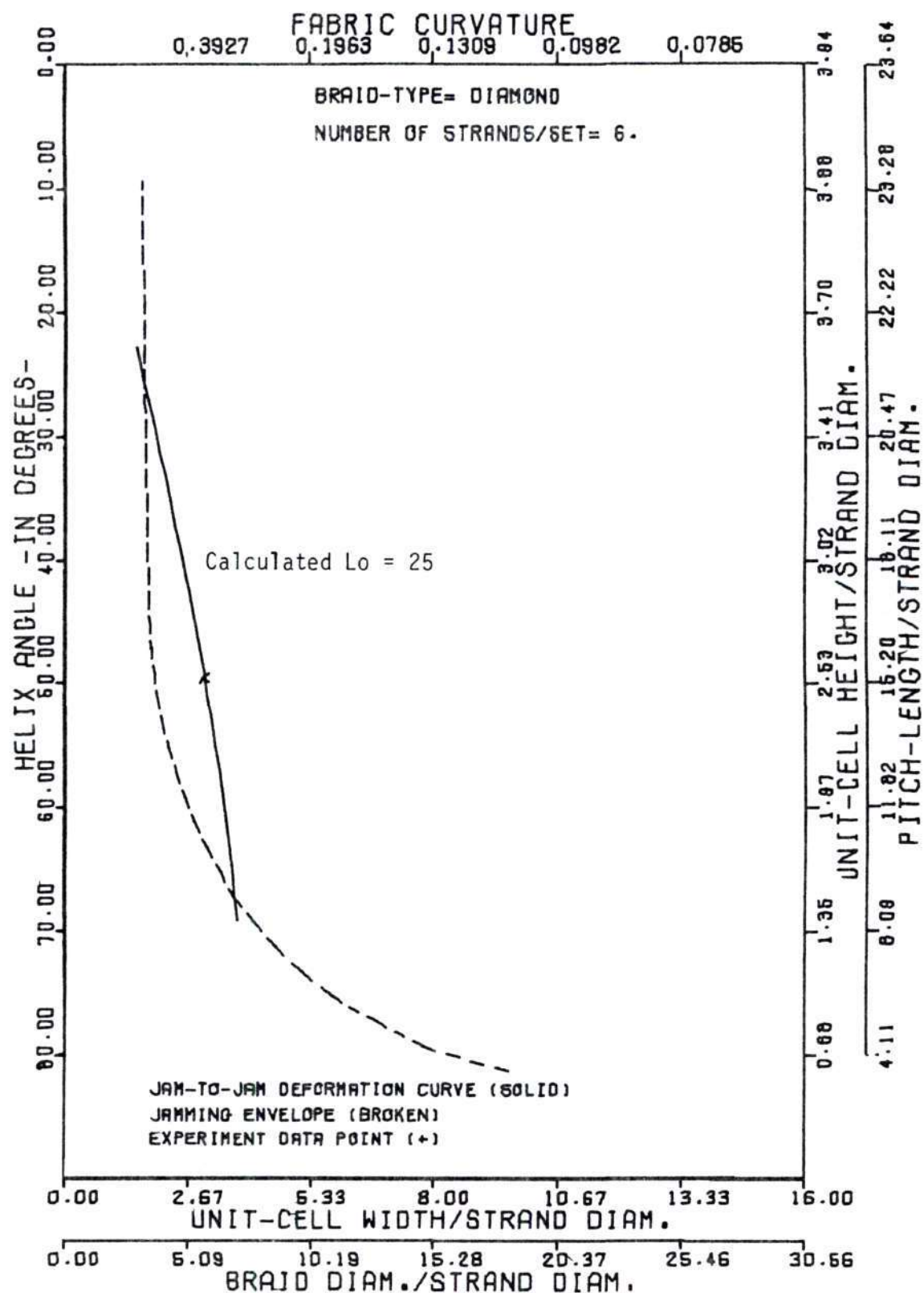


Figure 34. Test Data for Braid Sample #8 (TYPE=1, n=6).

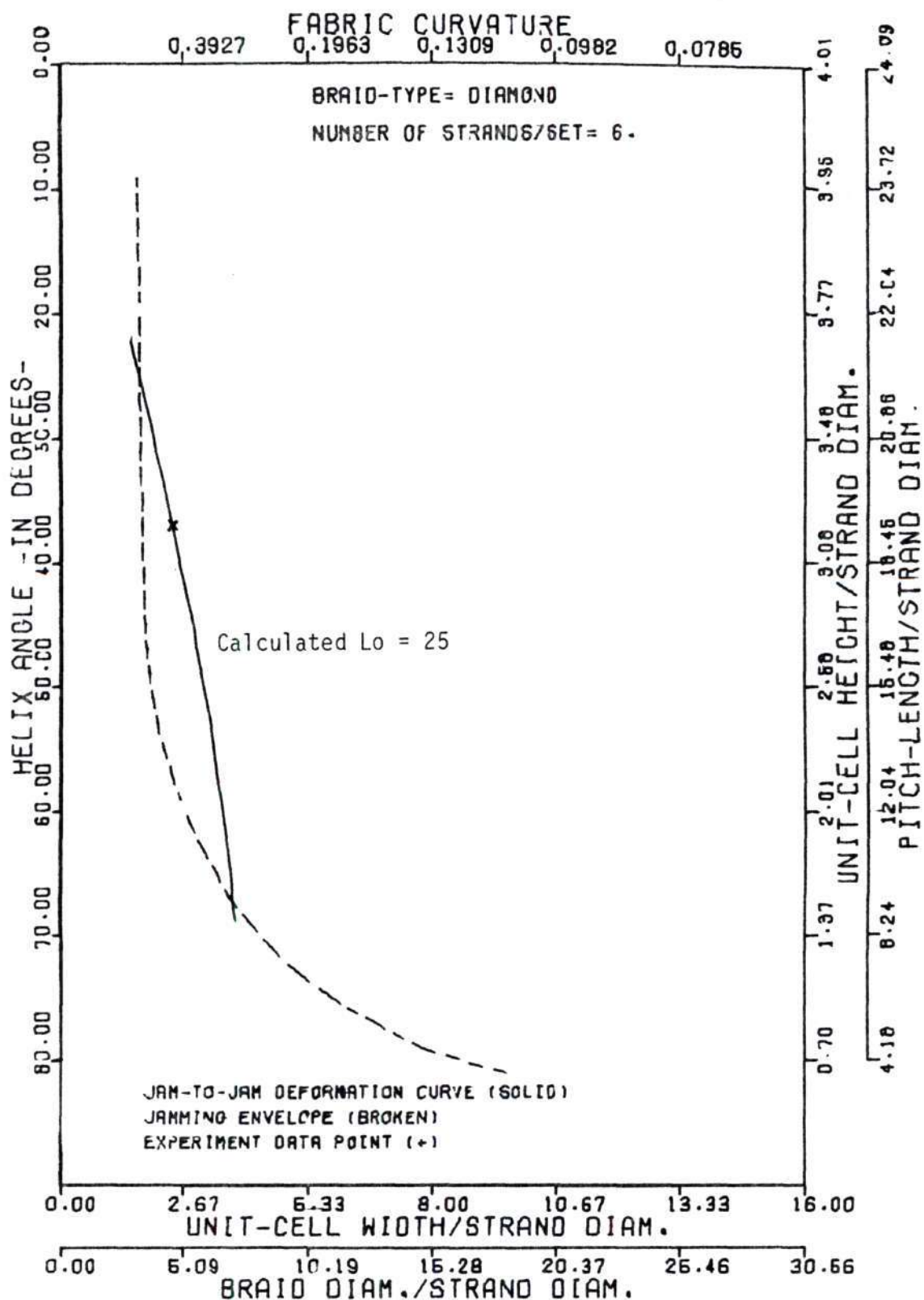


Figure 35. Test Data for Braid Sample #22 (TYPE=1, n=6).

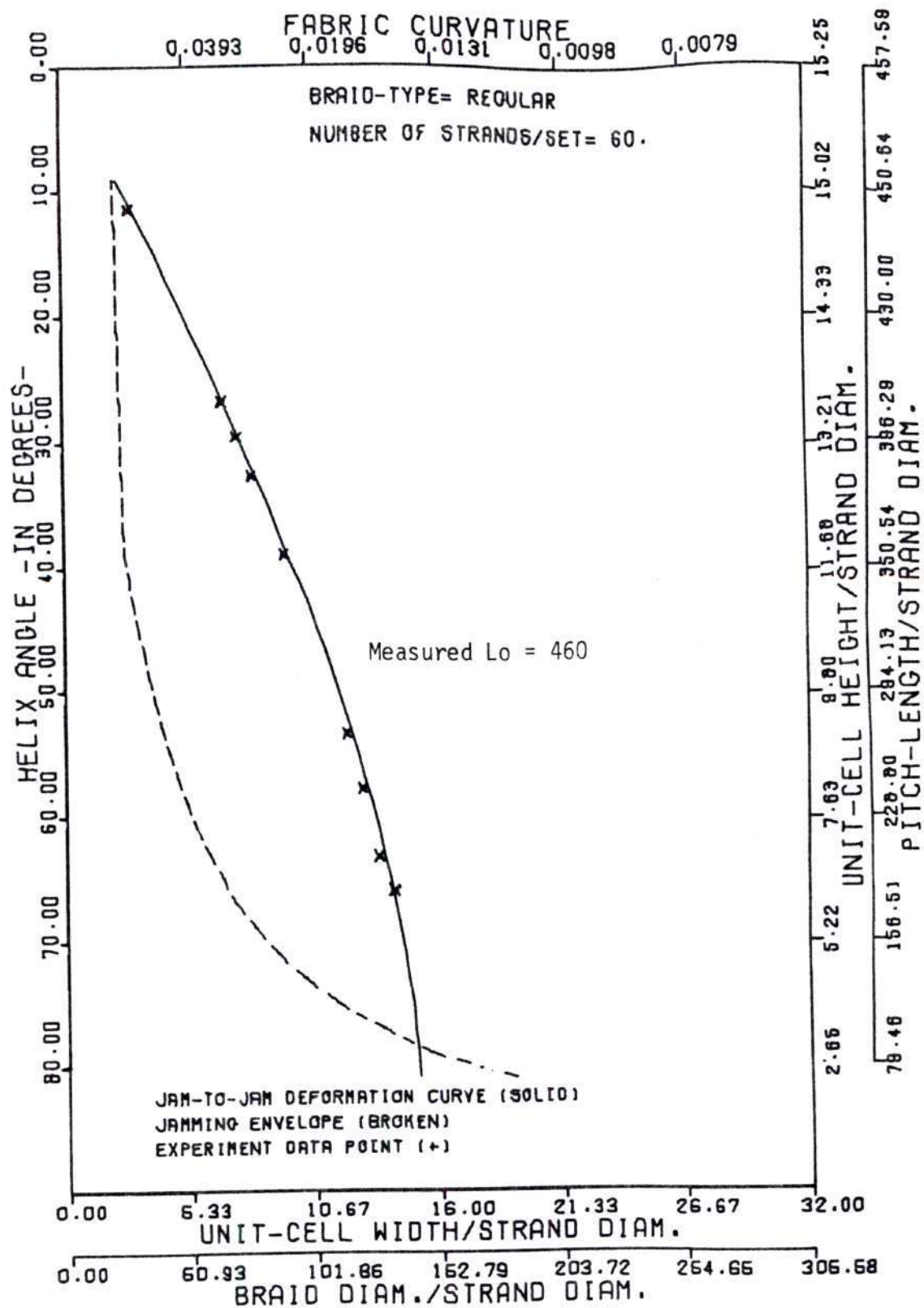


Figure 36. Test Data for Braid Sample #18 (TYPE=2, n=60).

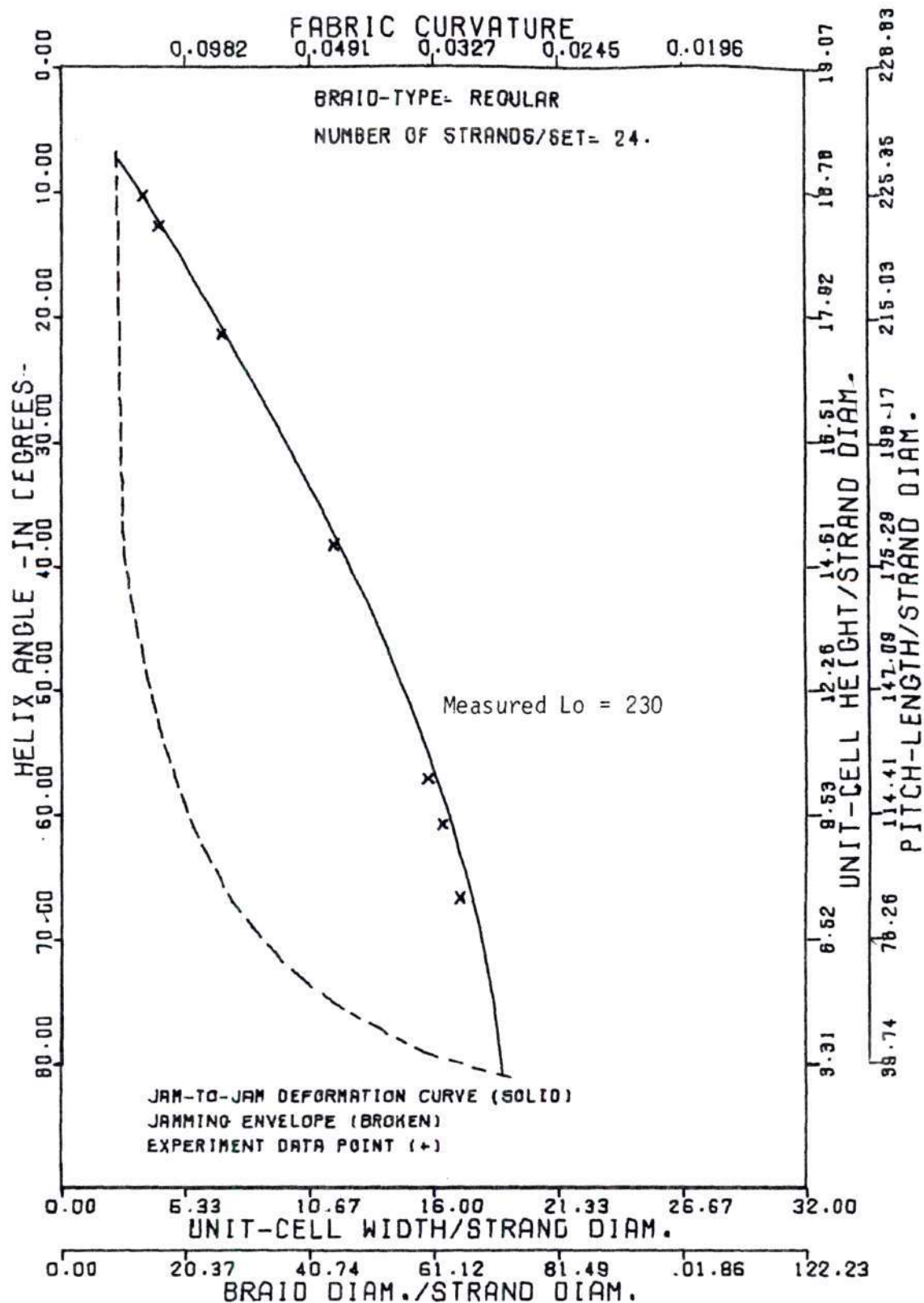


Figure 37. Test Data for Braid Sample #17 (TYPE=2, n=24).

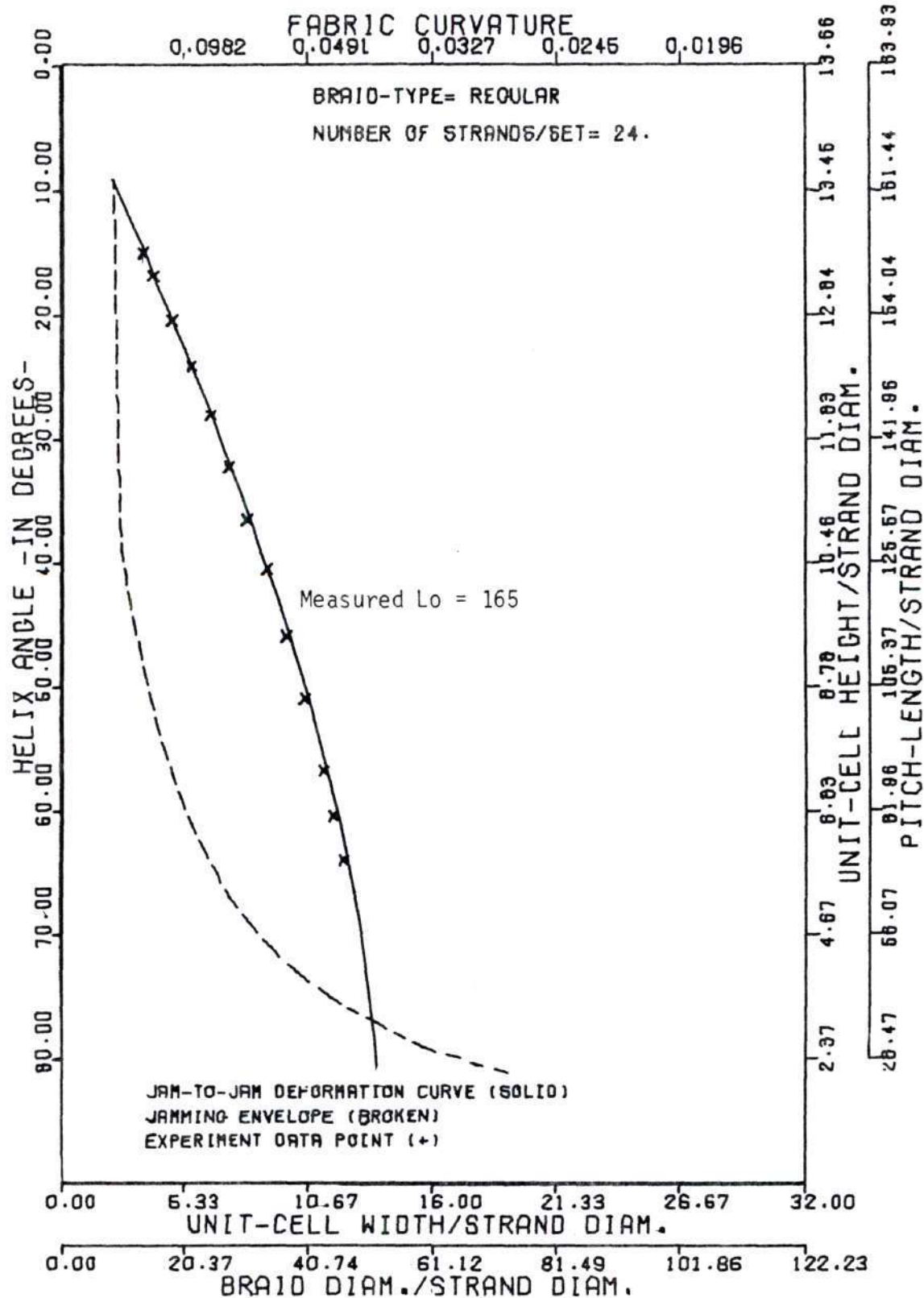


Figure 38. Test Data for Braid Sample #5 (TYPE=2, n=24).

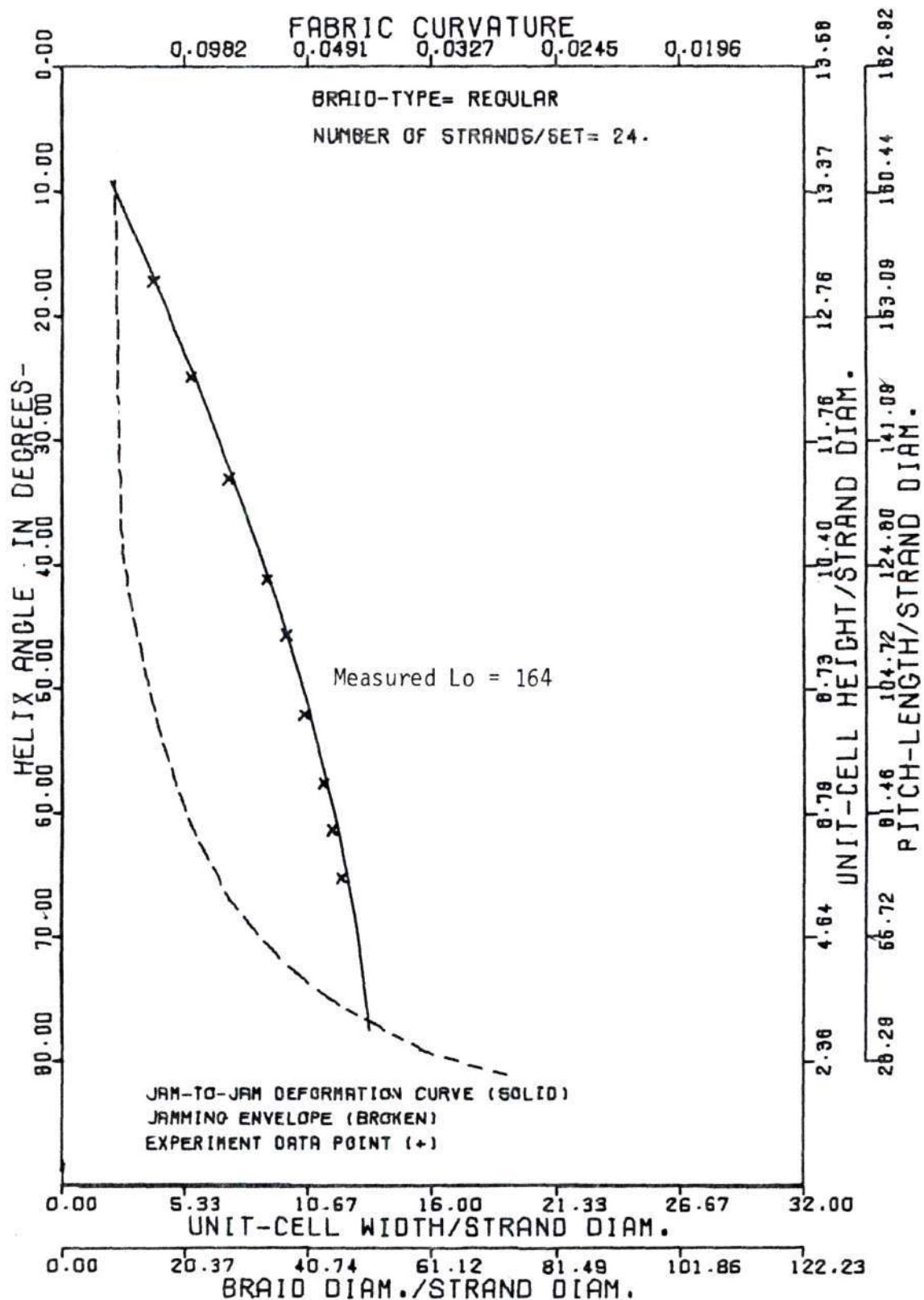


Figure 39. Test Data for Braid Sample #3 (TYPE=2, n=24).

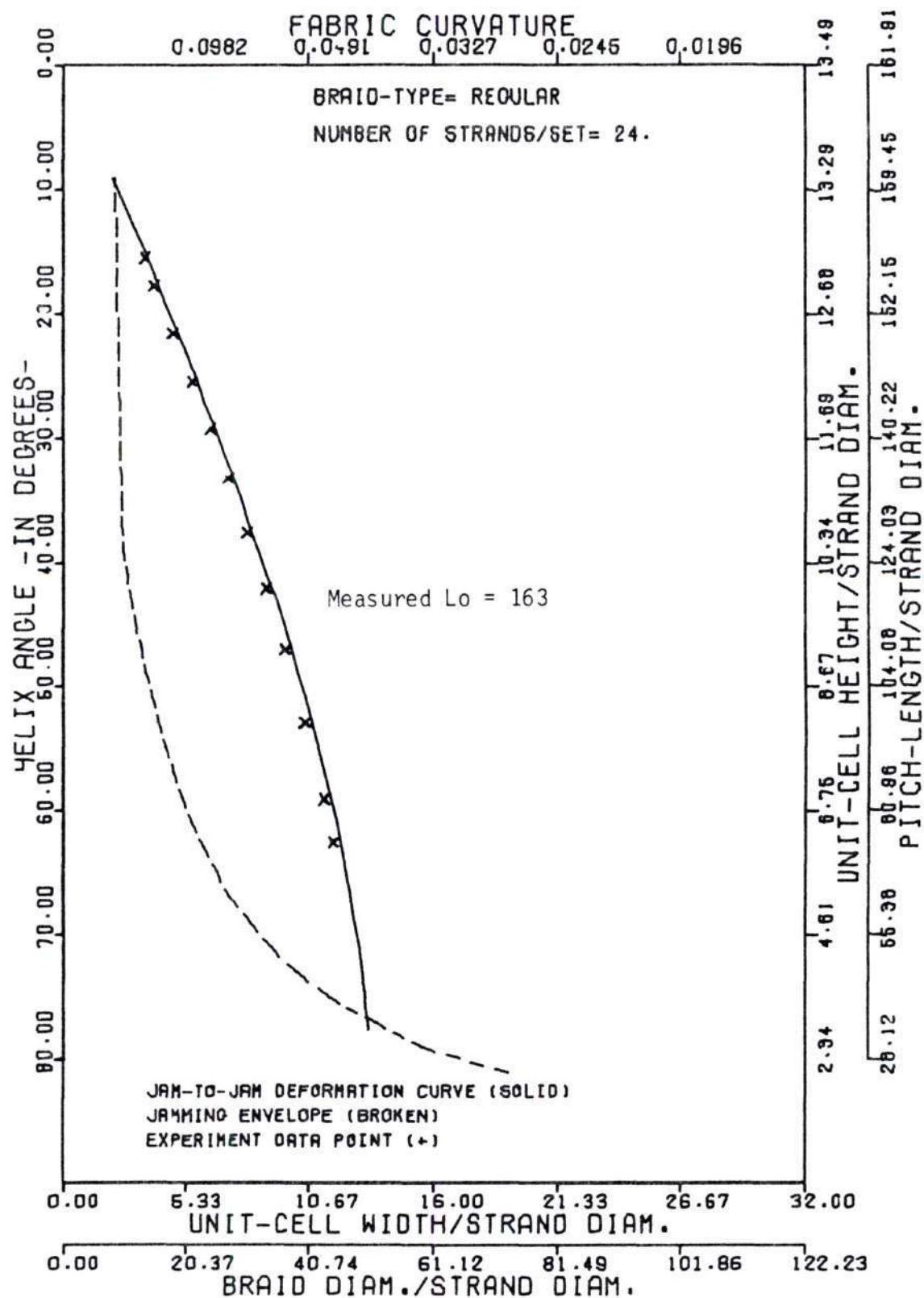


Figure 40. Test Data for Braid Sample #4 (TYPE=2, n=24).

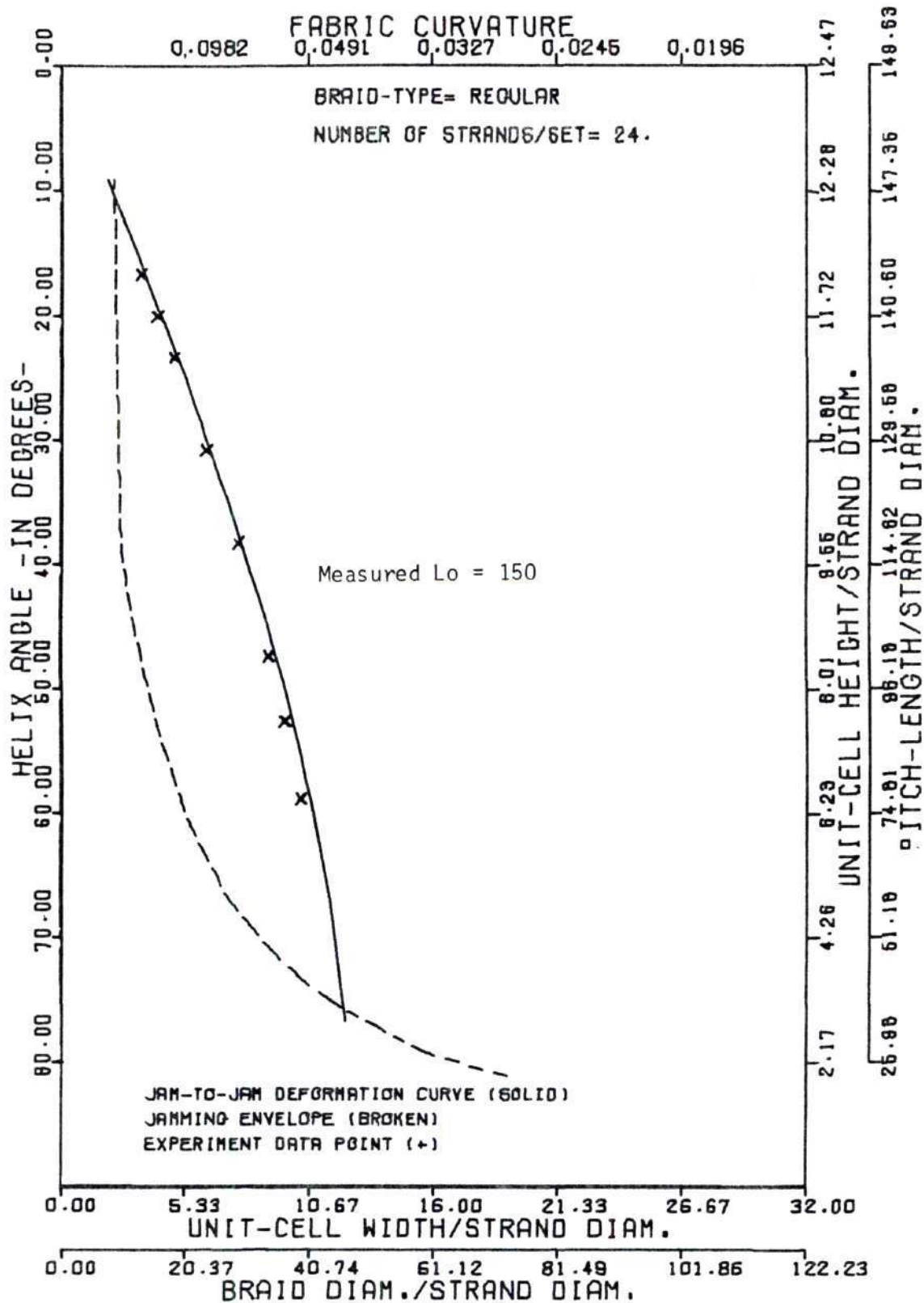


Figure 41. Test Data for Braid Sample #6 (TYPE=2, n=24).

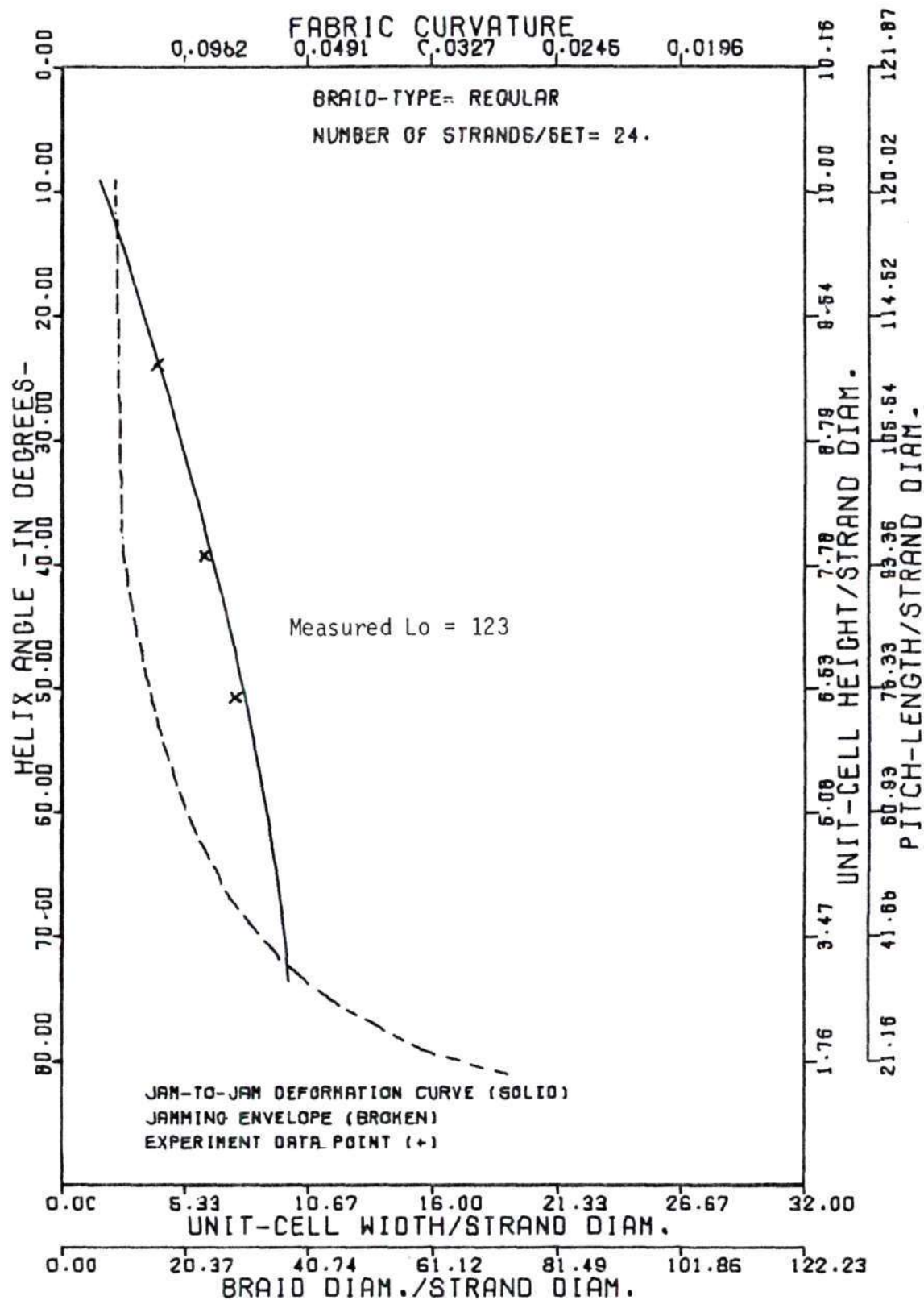


Figure 42. Test Data for Braid Sample #16 (TYPE=2, n=24).

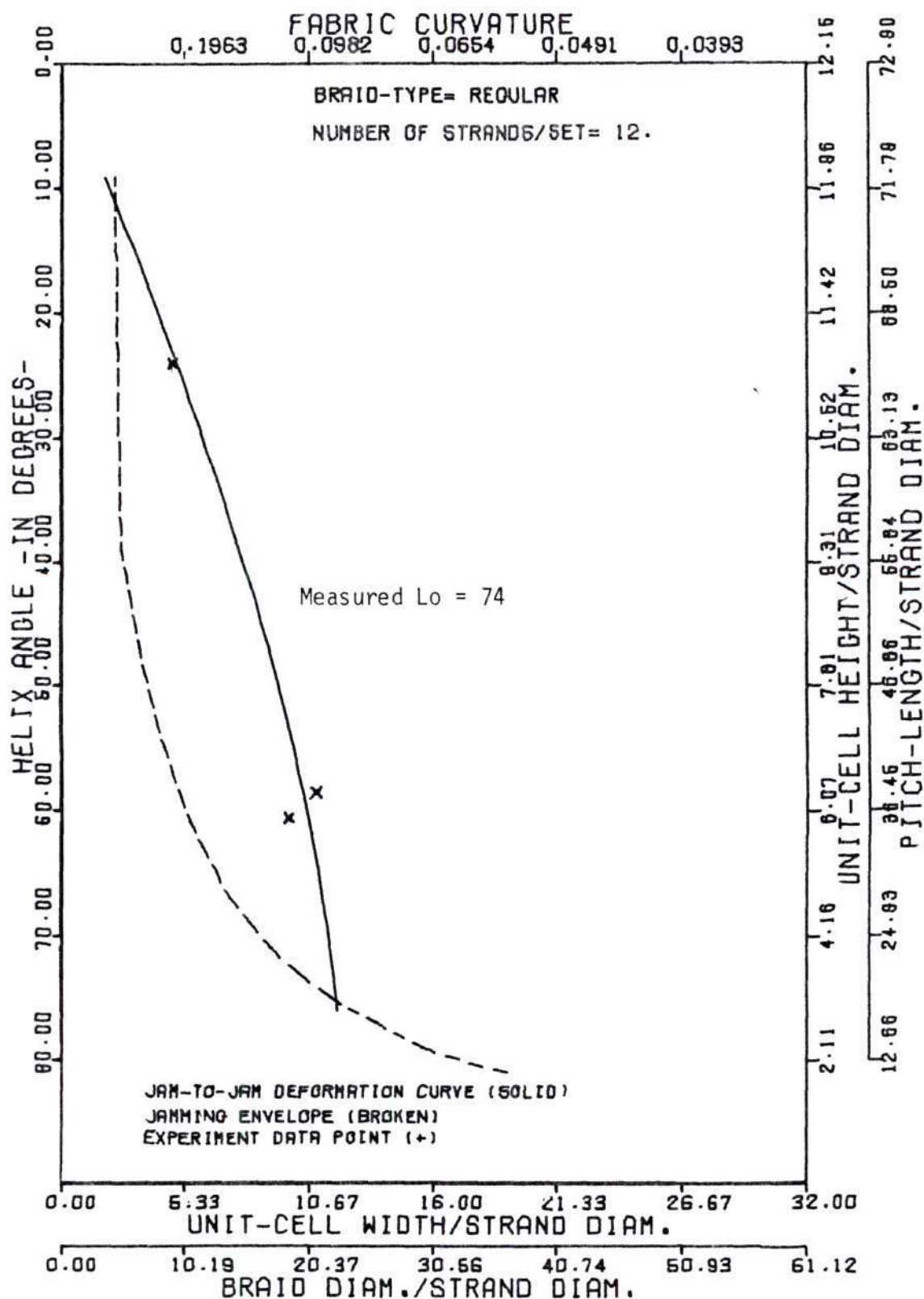


Figure 43. Test Data for Braid Sample #10 (TYPE=2, n=12).

models, it is doubtful that the present model offers significant improvement in that respect. Had crimp not been considered the separation between theory and experiment would have been greater by the percentage of crimp-effect (see Table 12, column M).

The key to interpreting the experimental results and the nature of the specimens tested is the regular recurring distance between measured and predicted jam points. Although the .006 and .010 inch diameter plastic monofilaments were easy to measure and manipulate experimentally, they also had a high bending rigidity which caused premature jamming. The stiffness did not allow the strands to conform to the high curvature required of a deforming braid approaching its theoretical jamming limit. The comparison of distances between predicted and measured jam points in the regular and diamond braid samples reveals the systematic character of the early jamming. The R.H. regular braid with its "longitudinal 1-pair" that does not make large bending demands on its jamming interlaced strands, approaches its theoretical tensile jamming limit more closely than its compressive limit. Diamond braid measurements show equidistance between theory and experiment for tensile and compressive geometries.

The stiffness of the monofilament limited the range of geometries available for test samples. Samples with high strand number and small L_0 which would have provided

experimentally tractable specimens with high crimp were unable to be manufactured. A tightly woven braid (i.e. one with Q_1 close to 45 degrees) with coarse strands on a large braider requires high thread-line tension which interferes with the smoothness of braiding in the braiding zone and produces an improperly formed braid. On a machine with less carriers the braiding process for a high crimp, monofilament braid could be controlled. However the end result was a small diameter braid so locked together that it could not be cut apart to measure L_0 . Braid samples #9, #8, and #22 fall into this category. These samples are important in that they give the magnitude of the crimp-effect attainable for a diamond braid of this material. Their deformation curves fall to the right of the jam envelope as they should.

The problem of achieving a tight braid with a monofilament strand is compounded by the fact that the cross-section does not flatten like that of multifilament yarn. The higher amplitude crimp wave which must interlace with the unflattened cross-sections is subject to even greater bending curvature.

To obtain an estimate of the crimp-effect which is common in a tightly woven braid with multifilament strands, an isolated measurement of braided mountain-climbing rope was made. The $3/8$ inch (O.D.) specimen (TYPE=1, $n=8$) exhibited a two percent crimp-effect. Since no effort was

made to adjust the model for flattening the deformation properties of the multifilament sample listed in Table 13 is only a crude estimate. The table was generated on the basis of measured pitch, L_0 , and nominal braid diameter. The effective (flattened) strand diameter was estimated by dividing the difference in the inside and outside braid diameter by four.

The final discussion topic concerning the experiments is the accuracy of the predicted jam envelope. Since the jamming theory takes fabric curvature into account, it enables the envelope to be placed further to the right than would the flat-cell model. It is important to note that there were still no violations of the "impossible formation zone" to the left of the jam envelope.

Table 13. Between-Jam Deformation of Braid with Multifilament Strands.

JAM-TO-JAM BRAID DEFORMATION CURVE										JAM ENVELOPE		CRIMP-EFFECT
CONVICTION	DI	H	J	FK	(Lo)	ARC-LENGTH/PITCH=	43.750	MODE=	1	U	W	1-L1/L0
JAMMED	9.0	42.2592	2.1305	5367	5.4000	5.2424	.0367			4.0090	1.6060	.022035
JAMMED	11.0	42.2592	2.5397	7630	5.4000	5.2501	1.0205			4.0090	1.6100	.022020
JAMMED	13.0	41.9995	3.0038	6528	5.4000	5.2114	1.2331			4.1220	1.6107	.022001
JAMMED	15.0	41.3304	3.5251	5674	5.4688	5.1603	1.3843			4.1220	1.6187	.021980
JAMMED	17.0	40.9197	3.9422	5022	5.4688	5.1150	1.5038			4.1220	1.6187	.021956
	19.0	40.6043	4.3465	4510	5.4000	5.0574	1.7114			4.1220	1.6187	.021923
	21.0	39.9437	4.8314	4097	5.4688	4.9337	1.9169			4.1549	1.6316	.021900
	23.0	39.3914	5.3224	3750	5.4688	4.9239	2.0301			4.1549	1.6316	.021868
	25.0	38.7352	5.7569	3474	5.4688	4.8481	2.2007			4.1549	1.6316	.021835
	27.0	38.1313	6.1845	3234	5.4688	4.7605	2.4266			4.1549	1.6316	.021793
	29.0	37.4319	6.5046	3028	5.4688	4.6790	2.5936			4.1863	1.6447	.021761
	31.0	36.6055	7.0160	2650	5.4688	4.5858	2.7354			4.1863	1.6447	.021722
	33.0	35.8953	7.4202	2695	5.4688	4.4870	2.9139			4.1863	1.6447	.021681
	35.0	35.3524	7.4148	2559	5.4688	4.3328	3.0039			4.2222	1.6581	.021639
	37.0	34.1957	8.1959	2439	5.4688	4.2732	3.2201			4.2222	1.6581	.021590
	39.0	33.2674	8.5751	2332	5.4688	4.1384	3.3674			4.2567	1.6716	.021551
	41.0	32.3034	8.1398	2237	5.4688	4.0386	3.5167			4.2567	1.6716	.021507
	43.0	31.3103	9.2937	2152	5.4688	3.9138	3.6490			4.2318	1.6854	.021461
	45.0	30.2734	9.5363	2075	5.4688	3.7842	3.7842			4.2318	1.6854	.021410
	47.0	29.1938	9.7072	2007	5.4688	3.6500	3.9141			4.2318	1.6854	.021371
	49.0	28.0905	10.2360	1944	5.4688	3.5113	4.0393			4.5045	1.7086	.021325
	51.0	26.9469	10.5923	1888	5.4688	3.3684	4.1330			4.9471	1.9231	.021281
	53.0	25.7763	10.8857	1837	5.4688	3.2213	4.2748			5.2421	2.0586	.021237
	55.0	24.5022	11.1058	1791	5.4688	3.0703	4.3848			5.6393	2.2146	.021193
	57.0	23.3040	11.4323	1749	5.4688	2.9155	4.4395			6.1013	2.3962	.021151
	59.0	22.0572	11.0590	1712	5.4688	2.7572	4.5087			6.5631	2.5773	.021110
	61.0	20.7635	11.9234	1677	5.4688	2.5954	4.6323			7.0998	2.7881	.021070
	63.0	19.4443	12.1472	1646	5.4688	2.4305	4.7702			7.7322	3.0364	.021033
	65.0	18.1013	12.3563	1619	5.4688	2.2627	4.8323			8.4883	3.3333	.020997
	67.0	16.7361	12.5203	1594	5.4688	2.0920	4.9235			9.2413	3.6290	.020963
	69.0	15.3564	12.7240	1571	5.4688	1.9188	4.9987			10.3422	4.0614	.020931
	71.0	13.9459	12.8321	1551	5.4688	1.7432	5.0627			11.4321	4.5090	.020902
	73.0	12.5242	13.0336	1534	5.4688	1.5655	5.1206			12.9345	5.0676	.020875
JAMMED	75.0	11.6472	13.1711	1518	5.4688	1.3859	5.1723			14.7290	5.7841	.020851
JAMMED	77.0	9.6300	13.2365	1509	5.4688	1.2040	5.2176			17.1544	6.7365	.020829
JAMMED	79.0	8.1742	13.3457	1494	5.4688	1.0218	5.2366			19.7572	7.7586	.020811
JAMMED	81.0	6.7017	13.4086	1485	5.4688	.8377	5.2891			24.3612	9.5745	.020795

ALL LENGTH DIMENSIONS ARE DIVIDED BY STRAND DIAMETER (=) TO MAKE THEM DIMENSIONLESS.
 ABBREVIATIONS USED ARE EXPLAINED IN THE LIST OF SYMBOLS IN CHAPTER 2.

CHAPTER V

CONCLUSIONS AND RECOMMENDATIONS

The more sophisticated treatment of jamming geometry represents a significant step beyond the planar model of Brunnschweiller and Popper. The greater accuracy which comes from considering a circular structure as circular should provide a solid foundation for future studies on the mechanical behavior of braids. The geometry of extensive jamming with its distribution of local helix angles provides a good starting point for the theoretical analysis of post-jamming tensile strength.

Jamming can either occur naturally, adjacent strands in the tubular fabric crowding together as studied, or it can be artificially induced by the insertion of a core. The latter type of jamming, the crowding of strands between sheath and core components before the onset of natural jamming, requires no special model. The pertinent relationships between braid parameters and changing dimensions of the structure are the same and available in the tables and graphs presented. The coordination of the two types of jamming is the key to designing a braid for maximum strength, extensibility, abrasion resistance, and cover. From the relationships and information already

compiled it is a simple matter to choose a particular strand jamming geometry by choosing the diameter of its core. This ability greatly facilitates the task of optimizing a composite braid structure, begun by Hamburger. The logical extension of experiments already performed would be a valuable contribution in this area. Instead of measuring the dimensional aspects of a braided sleeve on a metallic core, its breaking strength should be determined in order to correlate known jam geometries with tensile strength.

Exact knowledge of the arc-length of braided strands is crucial for the design of high performance braids, especially for high modulus materials with low extensibility where a fraction of one percent strain is significant. Although there was no discernible difference in the overall strand-length predictions among the crimped-helical, the flat-cell, and even the helix-triangle (at large C_w) models, it does not mean that the taking into account of increased strand length due to crimp is unimportant. On the contrary, the crimp-effect is quite pronounced (as great as ten percent, see Theoretical Results Group 2) in tightly braided structures.

The geometrical model that has been constructed is general and highly idealized. However it can be adapted to specific strand materials like continuous filament yarn that does not meet its initial assumptions. An approach would be to introduce a flattening factor in the form of a

coefficient which relates the effective (flattened) strand diameter to a hypothetical original diameter (if the cross-section was circular). Then the jamming distance criterion (JD) is to be redefined by allowing a certain percent inter-strand penetration which corresponds to the amount of flattening.

One final recommendation stems from the little known fact that a large proportion of braids find their end use in electrical, mechanical, and thermal insulation. In addition to the work in mechanics, further geometrical work could be done to correlate "ability to cover" with braid parameters and dimensions.

APPENDIX

APPENDIX A

TORSION AND CURVATURE EQUATIONS

All derivatives (') are with respect to θ .

$$\text{Curvature} = \frac{\sqrt{\{(x'^2 + y'^2 + z'^2)(x''^2 + y''^2 + z''^2)(x'x'' + y'y'' + z'z'')\}}}{\{\sqrt{(x'^2 + y'^2 + z'^2)}\}^3} \quad (\text{A.1})$$

$$\text{Geometric Torsion} = \frac{\begin{vmatrix} x' & y' & z' \\ x'' & y'' & z'' \\ x''' & y''' & z''' \end{vmatrix}}{A^2 + B^2 + C^2} \quad (\text{A.2})$$

$$A = \begin{vmatrix} y' & z' \\ y'' & z'' \end{vmatrix} \quad B = \begin{vmatrix} z' & x' \\ z'' & x'' \end{vmatrix} \quad C = \begin{vmatrix} x' & y' \\ x'' & y'' \end{vmatrix}$$

APPENDIX B

Table 14a. Array of Experimental Data (Diamond).

SAMPLE #	BRAID CONSTANTS				MEASURED (INCHES)			CALCULATED		
	TYPE	N	SD(IN.)		D	H	L0'	Q1	LO(IN.)	
7.	1.	24.	.006		.157	1.69	1.79	16.3	1.77	
7.	1.	24.	.006		.173	1.64	1.79	18.3	1.74	
7.	1.	24.	.006		.204	1.57	1.79	22.2	1.70	
7.	1.	24.	.006		.267	1.52	1.79	28.9	1.74	
7.	1.	24.	.006		.329	1.40	1.79	36.4	1.75	
7.	1.	24.	.006		.392	1.21	1.79	45.5	1.73	
7.	1.	24.	.006		.454	.97	1.79	55.8	1.73	
7.	1.	24.	.006		.468	.81	1.79	61.1	1.69	
7.	1.	24.	.006		.501	.71	1.79	65.7	1.73	
7.	1.	24.	.006		.517	.59	1.79	70.0	1.74	
8.	1.	6.	.010		.057	.15	0.00	49.3	.25	
9.	1.	6.	.010		.053	.61	0.00	15.2	.64	
11.	1.	24.	.010		.302	3.76	3.90	14.2	3.89	
11.	1.	24.	.010		.384	3.65	3.90	18.3	3.85	
11.	1.	24.	.010		.431	3.58	3.90	20.7	3.84	
11.	1.	24.	.010		.525	3.45	3.90	25.6	3.83	
11.	1.	24.	.010		.713	3.01	3.90	36.7	3.76	
11.	1.	24.	.010		.775	2.96	3.90	39.4	3.84	
11.	1.	24.	.010		.837	2.82	3.90	43.0	3.86	
11.	1.	24.	.010		.900	2.60	3.90	47.4	3.85	
11.	1.	24.	.010		.963	2.38	3.90	51.8	3.86	
11.	1.	24.	.010		1.025	2.09	3.90	57.0	3.85	
11.	1.	24.	.010		1.087	1.73	3.90	63.1	3.84	
11.	1.	24.	.010		1.150	1.25	3.90	70.9	3.83	
12.	1.	24.	.010		.290	2.96	3.15	17.1	3.11	
12.	1.	24.	.010		.306	2.95	3.15	18.0	3.11	
12.	1.	24.	.010		.337	2.91	3.15	20.0	3.11	
12.	1.	24.	.010		.415	2.83	3.15	24.7	3.13	
12.	1.	24.	.010		.462	2.75	3.15	27.8	3.12	
12.	1.	24.	.010		.525	2.61	3.15	32.3	3.10	
12.	1.	24.	.010		.650	2.36	3.15	40.9	3.13	
12.	1.	24.	.010		.713	2.12	3.15	46.6	3.10	
12.	1.	24.	.010		.775	1.89	3.15	52.2	3.09	
12.	1.	24.	.010		.837	1.57	3.15	59.2	3.07	
12.	1.	24.	.010		.900	1.20	3.15	67.0	3.08	

Table 14b. Array of Experimental Data (Diamond).

SAMPLE #	BRAID CONSTANTS			MEASURED (INCHES)			CALCULATED	
	TYPE	N	SD (IN.)	D	H	L0'	Q1	LO (IN.)
13.	1.	24.	.010	.337	3.46	3.77	17.0	3.63
13.	1.	24.	.010	.306	3.62	3.77	14.9	3.76
13.	1.	24.	.010	.290	3.63	3.77	14.1	3.75
13.	1.	24.	.010	.353	3.56	3.77	17.3	3.74
13.	1.	24.	.010	.400	3.51	3.77	19.7	3.74
13.	1.	24.	.010	.448	3.40	3.77	22.5	3.69
13.	1.	24.	.010	.650	3.14	3.77	33.0	3.76
13.	1.	24.	.010	.775	2.82	3.77	40.8	3.74
13.	1.	24.	.010	1.087	1.48	3.77	66.6	3.73
14.	1.	24.	.006	.234	1.80	1.74	22.2	1.95
14.	1.	24.	.006	.265	1.60	1.74	27.5	1.81
14.	1.	24.	.006	.187	1.62	1.74	19.9	1.73
14.	1.	24.	.006	.171	1.64	1.74	18.1	1.73
14.	1.	24.	.006	.155	1.65	1.74	16.4	1.73
14.	1.	24.	.006	.343	1.35	1.74	38.6	1.73
14.	1.	24.	.006	.390	1.22	1.74	45.1	1.74
14.	1.	24.	.006	.437	1.03	1.74	53.1	1.72
14.	1.	24.	.006	.468	.86	1.74	59.7	1.71
14.	1.	24.	.006	.484	.76	1.74	63.4	1.71
14.	1.	24.	.006	.499	.64	1.74	67.8	1.70
15.	1.	24.	.006	.140	2.33	2.40	10.7	2.38
15.	1.	24.	.006	.171	2.30	2.40	13.1	2.37
15.	1.	24.	.006	.202	2.28	2.40	15.6	2.37
15.	1.	24.	.006	.265	2.12	2.40	21.4	2.28
15.	1.	24.	.006	.405	1.99	2.40	32.6	2.37
15.	1.	24.	.006	.515	1.70	2.40	43.6	2.35
15.	1.	24.	.006	.640	1.18	2.40	59.6	2.34
15.	1.	24.	.006	.703	.81	2.40	69.9	2.36
21.	1.	6.	.010	.028	.25	0.00	19.5	.27
22.	1.	6.	.010	.046	.19	0.00	37.0	.25
23.	1.	8.	.032	.312	.76	1.40	52.2	1.27
23.	1.	8.	.032	.281	.90	1.40	44.4	1.29
23.	1.	8.	.032	.252	.97	1.40	39.2	1.28
23.	1.	8.	.032	.224	1.03	1.40	34.3	1.28

Table 15a. Array of Experimental Data (Regular).

SAMPLE #	BRAID CONSTANTS				MEASURED (INCHES)			CALCULATED	
	TYPE	N	SD (IN.)		D	H	L0'	Q1	LO (IN.)
3.	2.	24.	.010		.150	1.53	1.64	17.1	1.61
3.	2.	24.	.010		.212	1.44	1.64	24.8	1.60
3.	2.	24.	.010		.275	1.33	1.64	33.0	1.60
3.	2.	24.	.010		.337	1.21	1.64	41.2	1.62
3.	2.	24.	.010		.369	1.13	1.64	45.7	1.63
3.	2.	24.	.010		.400	.98	1.64	52.1	1.60
3.	2.	24.	.010		.431	.86	1.64	57.6	1.62
3.	2.	24.	.010		.447	.77	1.64	61.3	1.61
3.	2.	24.	.010		.462	.67	1.64	65.2	1.61
4.	2.	24.	.010		.134	1.52	1.63	15.5	1.59
4.	2.	24.	.010		.150	1.47	1.63	17.8	1.56
4.	2.	24.	.010		.181	1.44	1.63	21.5	1.56
4.	2.	24.	.010		.212	1.40	1.63	25.4	1.56
4.	2.	24.	.010		.244	1.37	1.63	29.2	1.58
4.	2.	24.	.010		.275	1.32	1.63	33.2	1.59
4.	2.	24.	.010		.306	1.25	1.63	37.6	1.59
4.	2.	24.	.010		.337	1.17	1.63	42.1	1.59
4.	2.	24.	.010		.369	1.08	1.63	47.0	1.60
4.	2.	24.	.010		.400	.95	1.63	52.9	1.59
4.	2.	24.	.010		.431	.81	1.63	59.1	1.59
4.	2.	24.	.010		.447	.73	1.63	62.5	1.59
5.	2.	24.	.010		.134	1.57	1.65	15.0	1.64
5.	2.	24.	.010		.150	1.56	1.65	16.8	1.64
5.	2.	24.	.010		.181	1.53	1.65	20.4	1.64
5.	2.	24.	.010		.212	1.49	1.65	24.1	1.64
5.	2.	24.	.010		.244	1.44	1.65	28.0	1.64
5.	2.	24.	.010		.275	1.37	1.65	32.2	1.63
5.	2.	24.	.010		.306	1.30	1.65	36.5	1.63
5.	2.	24.	.010		.337	1.24	1.65	40.5	1.64
5.	2.	24.	.010		.369	1.12	1.65	46.0	1.62
5.	2.	24.	.010		.400	1.02	1.65	50.9	1.63
5.	2.	24.	.010		.431	.89	1.65	56.7	1.63
5.	2.	24.	.010		.447	.80	1.65	60.3	1.63
5.	2.	24.	.010		.462	.71	1.65	63.9	1.63

Table 15b. Array of Experimental Data (Regular).

SAMPLE #	BRAID CONSTANTS			MEASURED (INCHES)			CALCULATED	
	TYPE	N	SD(IN.)	D	H	L0'	Q1	LO(IN.)
6.	2.	24.	.006	.079	.83	.91	16.6	.87
6.	2.	24.	.006	.095	.82	.91	20.0	.88
6.	2.	24.	.006	.111	.81	.91	23.3	.89
6.	2.	24.	.006	.142	.75	.91	30.7	.88
6.	2.	24.	.006	.173	.69	.91	38.2	.89
6.	2.	24.	.006	.204	.59	.91	47.4	.88
6.	2.	24.	.006	.220	.53	.91	52.5	.88
6.	2.	24.	.006	.236	.45	.91	58.7	.87
10.	2.	12.	.010	.092	.64	.74	24.2	.71
10.	2.	12.	.010	.210	.40	.74	58.8	.78
10.	2.	12.	.010	.188	.33	.74	60.8	.68
16.	2.	24.	.006	.093	.66	.74	23.9	.73
16.	2.	24.	.006	.140	.54	.74	39.2	.71
16.	2.	24.	.006	.171	.44	.74	50.7	.70
17.	2.	24.	.006	.077	1.34	1.38	10.2	1.37
17.	2.	24.	.006	.093	1.30	1.38	12.7	1.34
17.	2.	24.	.006	.155	1.25	1.38	21.3	1.35
17.	2.	24.	.006	.265	1.06	1.38	38.1	1.35
17.	2.	24.	.006	.359	.73	1.38	57.1	1.35
17.	2.	24.	.006	.374	.66	1.38	60.7	1.35
17.	2.	24.	.006	.390	.53	1.38	66.6	1.34
18.	2.	60.	.010	1.150	2.68	4.60	53.4	4.52
18.	2.	60.	.010	1.212	2.40	4.60	57.8	4.53
18.	2.	60.	.010	1.275	2.02	4.60	63.2	4.51
18.	2.	60.	.010	1.338	1.87	4.60	66.0	4.62
18.	2.	60.	.010	.900	3.50	4.60	38.9	4.52
18.	2.	60.	.010	.650	4.05	4.60	26.8	4.56
18.	2.	60.	.010	.712	3.94	4.60	29.6	4.55
18.	2.	60.	.010	.775	3.79	4.60	32.7	4.53
18.	2.	60.	.010	.275	4.28	4.60	11.4	4.39

APPENDIX C

COMPUTER PROGRAM FOR BRAID CALCULATIONS

Input/Output

A general, multi-purpose computer program was written to perform the necessary theoretical calculations using the FORTRAN IV programming language. Input to the program is provided from a separate data file consisting of ranges of braid parameters and four coded program instructions. The program produces output in both tabular and graphical (Calcomp Plotter) form. The input set is arranged as follows

```

RNPTS,RMAX,RMIN
NSTRA,N1,N2,N3...
XLENG,YLENG,XMAX,YMAX
HQMIN,HQMIN,HQINC
ARCMIN,ARCMAX,ARCINC
OUTP,TYPE,MODE,KEY

```

The FORTRAN variable names are defined as follows:

```

RNPTS- the number of points in the array of braid
diameters
RMAX- maximum value in braid diameter array
(dimensionless,D/d)
RMIN- minimum value in braid diameter array

```


(dimensionless, D/d)

NSTRA- number of braids with different n to be considered

N1,N2...- enumeration of the n of NSTRA different braids

XLENG- length of the x-axis for the Calcomp plot (in inches)

YLENG- length of the y-axis for the Calcomp plot (in inches)

XMAX- maximum value of array to be plotted on the x-axis (for scaling purposes)

YMAX- maximum value of array to be plotted on the y-axis

HQMIN- minimum helix angle to be considered (in degrees)

HQMIN- maximum helix angle to be considered (in degrees)

HQINC- size of increment to be used in generating array of helix angles (in degrees)

ARCMIN- minimum strand arc-length/pitch to be used in arc-length array (dimensionless, L_0/d)

ARCMAX- maximum strand arc-length/pitch, L_0/d

ARCINC- arc-length increment for generating array of arc-lengths

OUTP- designates graphical and/or tabular output

OUTP=2.- tables and Calcomp plotter

OUTP=4.- Calcomp plotter

OUTP=5.- tables

TYPE- type of braid construction

TYPE=1.- diamond braid

TYPE=2.- right-handed regular braid

TYPE=3.- left-handed regular braid

MODE- method used to calculate arc-length

MODE=1 - Equation II.11 of the crimped helical model is used

MODE=3 - arc-length from an uncrimped simple helix is used

MODE=4 - flat-cell Equation I.2 is used

KEY- designates which set of basic operations is to be performed on the input set which result in the following functional relations

KEY=0 - amount of interlacing crimp versus braid diameter

KEY=1 - strand arc-length/pitch versus braid diameter

KEY=2 - helix angle versus braid diameter for a given L_0 or family of L_0 , (braid deformation curves)

KEY=3 - limiting helix angle due to jamming, vs. braid diameter (jam envelope) and braid deformation curves

KEY=4 - idealized projection, of braid geometry of given dimensions and TYPE onto the x-y plane

KEY=5 - gives coordinates, direction cosines, jamming distances, and other vectorial information for 21 points along l_0 , it calls subroutine DIRCOS to generate vector analysis tables

Main Program And Subroutines

An overview of the main program with its various subroutines is shown in Figure 44. The main program consists of four major DO-LOOPS. The first generates an array of braid diameters to be used as the independent variable in most of the different KEYS. The others cycle through sets of n , Lo , and Ql depending on KEY. A description of the basic purpose of each subroutine and function subroutine follow:

READIN- reads the input data file into the program

LISTPAR- immediately prints a list of the input parameters for job identification

DPREP- if experimental data is included in the input, it performs preliminary editing and calculation before it loads the data into an array preliminary editing and calculations before it loads the data into arrays to be plotted with the appropriate theoretical predictions

ARCL- is a function subroutine which calculates $Lo = fnc(Ql, d/d, n)$ according to the values of MODE and TYPE

FCELL- is a subroutine subservient to ARCL, it calculates Lo for the flat-cell model when $MODE=4$

RRATIO- uses the false-position method to calculate D as an implicit function of Ql , Lo , and n .

TABLES- formats and provides tabular output

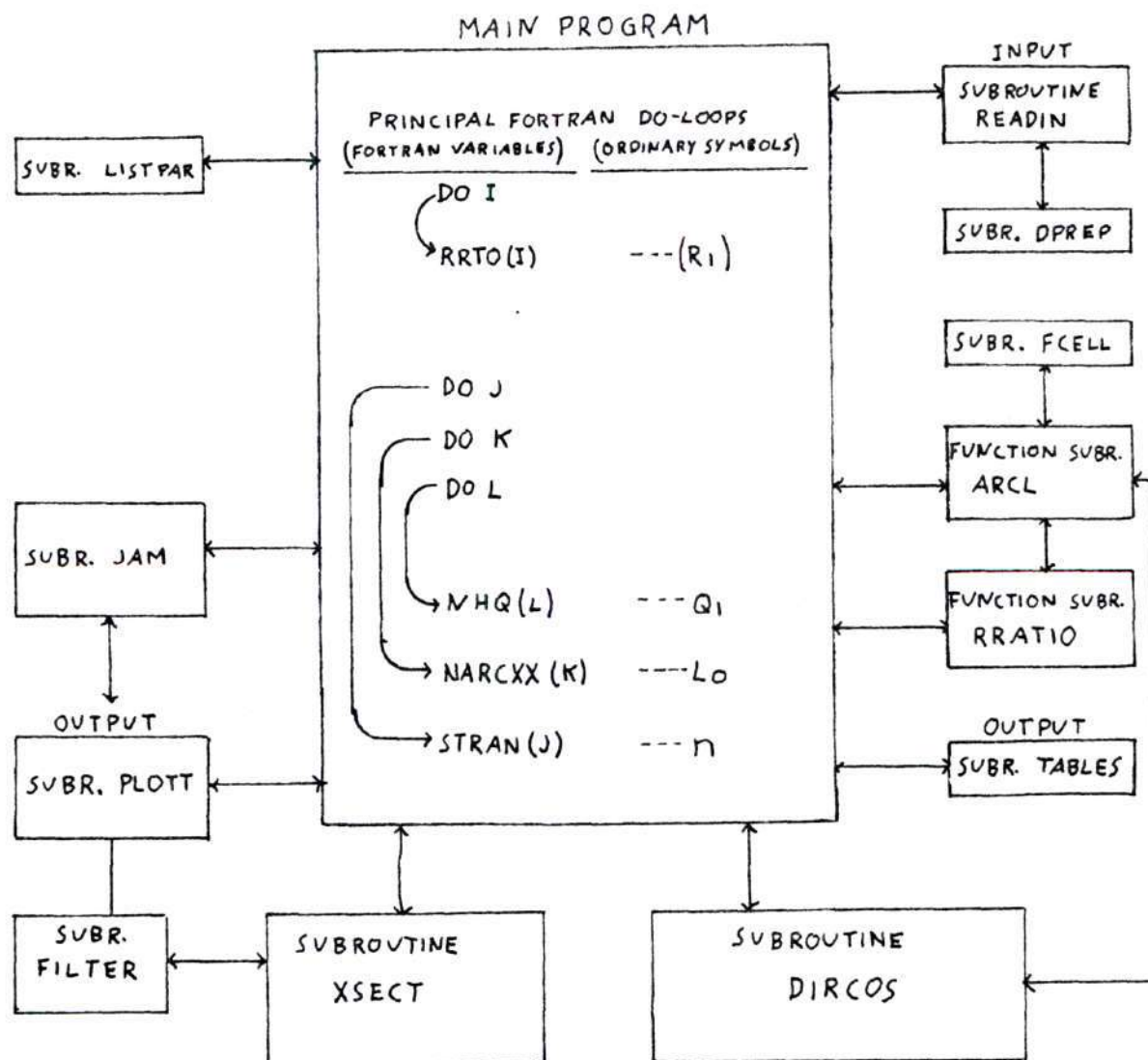


FIGURE 44. STRUCTURE OF MULTI-PURPOSE BRAIDS COMPUTER PROGRAM.

PLOTT- calls the appropriate Calcomp library subroutines that produce the curves, axes, and labeling for the graphs

FILTER- is used by PLOTT to remove values in excess of XMAX and YMAX from the arrays to be plotted

JAM- a principal subroutine which starts with an array of helix angles and determines a corresponding array of limiting braid diameters using an iterative procedure explained in Chapter II and displayed in Figure 12.

XSECT- employs the x and y coordinates of position vector (Eq.II.10) and the parametric equations for ellipse and circle to form the array for the plotted cross-sectional projection of the idealized braid structure

DIRCOS- it generates the tables of vector analysis for 21 points along l_0 as a function of D, d, Q_1 , and TYPE.

BIBLIOGRAPHY

LITERATURE CITED

1. Hamburger, W, J, Effect of Yarn Elongations on Parachute Fabric Strength, Rayon Textile Monthly, March p.51, May p.85, June p.50, (1942).
2. Brunnschweiler, D., Braids and Braiding, Journal of the Textile Institute, 44, P666, (1953).
3. Brunnschweiler, D., The Structure and Tensile Properties of Braids, J. Text. Inst., 45, T55, (1954).
4. Popper, Peter, Braided Structures, MIT Summer Session, unpublished, (1970).
5. Peirce, F. T., The Geometry of Cloth Structure, J. Text. Inst., 28, T45, (1937).
6. Konopasek, M. and Hearle, J.W.S., Computational Theory of Bending Curves Part I, Fibre Science And Technology, 5, p.1, (1972).
7. Konopasek, M. and Shanahan, W.J., Mechanical Model of the 2/2 Twill Weave, J. Text. Inst., 66, p.361, (1975).